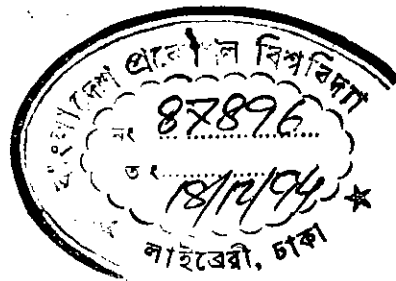


**ANALYSIS OF DELTA MODULATED  
SWITCH MODE POWER SUPPLY**

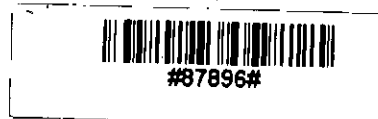
*MINHAZ UDDIN AHMED*

A thesis  
submitted to the Department of Electrical and  
Electronic Engineering in partial fulfilment  
of the requirements for the  
degree of  
Master of Science in Engineering (EEE)



DEPARTMENT OF ELECTRICAL AND ELECTRONIC ENGINEERING  
BANGLADESH UNIVERSITY OF ENGINEERING AND TECHNOLOGY  
DHAKA, BANGLADESH. NOVEMBER, 1994.

(ii)



623.81536  
1994  
MIN

The thesis titled, "Analysis of Delta Modulated Switch Mode Power Supply" submitted by Minhaz Uddin Ahmed, Roll No. 901341P, Registration No. 88308 of M. Sc. Engg. (EEE) has been accepted as satisfactory in partial fulfilment of the requirements for the degree of Master of Science in Engineering (Electrical and Electronic). Date of examination November 27, 1994.

#### BOARD OF EXAMINERS

1. *machondhr* 27.11.94  
Dr. Mohammad Ali Choudhury  
Associate Professor  
Department of Electrical and  
Electronic Engineering  
BUET, Dhaka.  
Chairman  
(Supervisor)
2. *ABM Siddique* 27/11/94  
Dr. A. B. M. Siddique Hossain  
Professor & Head  
Department of Electrical and  
Electronic Engineering  
BUET, Dhaka.  
Member  
(Ex-officio)
3. *Saifur Rahman* 27.11.94  
Dr. Saifur Rahman  
Assistant Professor  
Department of Electrical and  
Electronic Engineering  
BUET, Dhaka.  
Member  
(Internal)
4. *Kazi Khairul Islam* 27-11-94  
Dr. Kazi Khairul Islam  
Associate Professor and Head of  
the Department of EEE, BIT, Rajshahi.  
P. O. Kazla, Rajshahi.  
Member  
(External)

## Declaration

This is certified that this work has been done by me and has not been submitted elsewhere for the award of any degree or diploma.



Dr. Mohammad Ali Choudhury

Supervisor



Minhaz Uddin Ahmed

Candidate and the student

Dated, Dhaka

November 27, 1994

Dated, Dhaka

November 27, 1994

## **Acknowledgement**

It is a great pleasure of the author to acknowledge his heartiest gratitude to his supervisor, Dr. Mohammad Ali Choudhury, Associate Professor, Department of Electrical and Electronic Engineering, BUET, Dhaka, for his sincere guidance, kind co-operation, constant encouragement and valuable suggestions.

The author also wishes to express his thanks and sincerest gratitude to Dr. Syed Fazl-i-Rahman, Professor and former Head of the Department and Dr. A.B.M. Siddique Hossain, Professor and Head of the Department of Electrical and Electronic Engineering, BUET, Dhaka for his help and co-operation.

The author also acknowledges his profound indebtedness and respect to his mother and other close relatives specially his elder brother Fakhruddin Ahmed, ACA, ACMA, Deputy General Manager, Reliance Insurance Co., Dhaka and Md. Abul Kalam, Assistant Divisional Engineer, BTTB, Gazipur for their encouragements, valuable advices and co-operation in preparing the thesis. Finally, the author would like to offer his sincere thanks to his friends, colleagues, well wishers specially all teachers and staff of the Electrical and Electronic Engineering Department BUET, Dhaka.

## **Abstract**

High frequency switching power supplies are becoming part of electronic equipments to provide regulated dc of desired voltages at a low cost and efficient manner. These power supplies have three distinct advantages over their counterpart the linear power supplies. The advantages are smaller compact size due to elimination of step down transformer and small filters due to high frequency operation. They are more efficient because the regulating switches work in switching (ON/OFF) mode ensuring minimum device loss. The other advantages are their output voltage are isolated and can be controlled for a wide range of input voltage fluctuation by ON/OFF ratio (duty cycle) control.

Four common types of switch mode dc to dc converters are BUCK (step down), BOOST (step up), BUCK-BOOST (step up/down) and CŪk converters. At present these converters use high frequency multiple pulse or sine triangular modulation to generate the controlling signal/s of switching devices. Recently delta modulation technique has been adopted in many power converters for easy implementation and versatile control. In this research possible use of rectangular wave delta modulation to control a BUCK type switch mode power supply has been investigated. It is known that in rectangular wave delta modulators several parameters like magnitude of reference wave, window width, frequency and slope of modulating wave can be varied to change the shape of modulated wave. In this work it has been shown that of these parameters frequency variation of the modulating signal can usefully be used in controlling a BUCK type switch mode power supply. To investigate further a BUCK type delta modulated switch mode power supply has been designed, constructed and tested. From theoretical and practical investigation it is clear that controlling a switching power supply by delta modulated wave is possible and may be advantageous. The advantages may be easy implementation of control circuit and possible on line harmonic control. Further investigation is necessary to find the applicability of delta modulation to control switch mode power supply in future.

# CONTENTS

Acknowledgement	v
Abstract	vi
Contents	vii
List of Figures	ix
Chapter - 1 : INTRODUCTION	1
1.1 Introduction	1
1.2 Review of switchmode power supplies	4
1.2.1 Principle of operation	4
1.2.2 Types of converters	8
1.2.3 Switching	21
1.2.4 Review of magnetic circuit as applied to an smps	24
1.3 Advantages and applications of a smps	33
1.4 Review of pwm techniques as used in power converters	36
1.5 Delta modulation and its advantages	42
1.6 Proposed research and objectives	46
1.7 Organization of the thesis	47
Chapter - 2 : ANALYSIS OF DELTA MODULATION FOR AN SMPS	48
2.1 Delta modulator description	48
2.2 Characteristics of delta modulated wave	52
2.3 Switching point determination of dm	57
2.4 Change of modulator parameters	61
2.4.1 Change of modulator parameter to find effect on modulated smps wave	61
2.4.2 Discussion	63

Chapter - 3 : Practical Implementation	84
3.1 Implementation of delta modulation control circuit for pulse width modulated smps	84
3.2 Experimental delta modulation for static converters	87
3.2.1 Implementation of the logic circuits	87
3.2.2 Effect of change of frequency of the input sine wave to the DM	89
3.2.3 Effect of change of band width of the Hysteresis band of the DM	94
3.2.4 Effect of change of slope (Volt/Sec) of the carrier wave	97
3.2.5 Discussion	100
3.3. Practical SMPS requirements	100
3.3.1 Voltage controlled oscillator, ICL 8038	108
3.3.2 Amplification of the sine wave generated by VCO	110
3.3.3 Rectification of sine wave	110
3.3.4 Necessity of Hex inverting buffer	110
3.4 Filter design : voltage ripple	111
3.5 Semiconductor implementation of the switching action	115
3.6 Results	117
Chapter - 4 : Conclusions	122
References	126
Appendix	130

## List of Figures

1 :	Block diagram of an SMPS.	3
2 :	Linear(dissipative) power conversion circuit.	7
3 :	Switchmode(nondissipative) power conversion circuit.	7
4 :	General switchmode power conversion.	7
5 :	Simple generalized dc-to-dc converter topology (buck, boost and buck-boost realization by rearrangement of components).	9
6 :	Controlled dc-to-dc power conversion in a basic buck converter through pulse width modulation.	9
7 :	Equivalent circuit and quantitative evaluation of the output voltage switching ripple.	11
8 :	Process of bilateral inversion to create step-up converter from step-down converter.	11
9 :	Circuit diagram of boost converter.	14
10 :	Equivalent circuit, voltage and current waveform of boost converter.	14
11 :	Circuit diagram of buck-boost converter.	17
12 :	Converter efficiency in presence of switch nonidealities(non zero transistor and diode voltage drops.)	17
13 :	C $\dot{u}$ k converter circuit diagram :implemented by a transistor and a diode.	20
14 :	Equivalent circuits and waveforms of C $\dot{u}$ k converter.	20
15 :	Frequency view point reveals that for low output switching ripple filter corner frequency must be well below switching frequency.	23
16 :	Switching losses.	23



17 : Ampere's circuital law to a single conductor in free space.	29
18 : Orientation of magnetic domains (a) Random orientation of magnetic domains in demagnetized materials (b) orientation in the direction of external field H generated by coil current I.	29
19 : (a) High permeability $\mu$ (steep slope on a B-H curve) (b) saturation.	29
20 : B-H Curves of magnetic materials (a) Square-loop ferromagnetic materials exhibit high saturation flux density (b) linear ferromagnetic materials have lower saturation flux density.	31
21 : B-H Curves of magnetic materials (a) Non-linear, double valued B-H loop characteristic of square material (b) linear materials.	31
22 : Storage components and switches for efficient SMPS.	35
23 : Isolation in an SMPS by transformers (a) Simple bifilar winding step for dc isolation in SMPS (b) through breaking electrical connections.	35
24 : Isolated multiple output SMPS with polarity inversion.	35
25 : Single pulse-width modulation.	38
26 : Multiple pulse-width modulation.	38
27 : Sinusoidal pulse-width modulation.	38
28 : Optimized pulse-width modulation.	41
29 : Delta pulse-width modulation.	41
30 : Trapezoidal pulse-width modulation.	41
31 : Graphical illustration of delta modulation technique (a) Without hysteresis, (b) With hysteresis	50

32	: Block diagram of two basic DM encoder.	50
33	: Expected waveforms of encoder of Fig.-32.	51
34	: Delta modulator block diagram used to explain one of the characteristics ( $V/f = \text{constant}$ ) of modulated wave.	53
35	: Delta modulator output waveform : PWM signal tends to square wave signal with increasing slope of the carrier signal.	54
36	: Graphical representation of $V/f$ with respect to frequency. Frequency at $V/f = \text{constant}$ is the base frequency.	56
37	: Normal integrator of a DM.	56
38	: Multiplier integrator of a DM.	56
39	: Simulated waveform of delta modulator and SMPS voltage waveform (a) modulator waveforms (b) modulated output of modulator (c) SMPS output (d) spectrum of SMPS output. $f_m=1,000 \text{ Hz.}, V_m=7V, \Delta V=1.5V, S=200,000V/Sec.$	64
40	: Simulated waveform of delta modulator and SMPS voltage waveform (a) modulator waveforms (b) modulated output of modulator (c) SMPS output (d) spectrum of SMPS output. $f_m=2,000 \text{ Hz.}, V_m=7V, \Delta V=1.5V, S=200,000V/Sec.$	65
41	: Simulated waveform of delta modulator and SMPS voltage waveform (a) modulator waveforms (b) modulated output of modulator (c) SMPS output (d) spectrum of SMPS output. $f_m=3,000 \text{ Hz.}, V_m=7V, \Delta V=1.5V, S=200,000V/Sec.$	66

- 42 : Simulated waveform of delta modulator and SMPS  
voltage waveform (a) modulator waveforms  
(b) modulated output of modulator (c) SMPS output  
(d) spectrum of SMPS output.  
 $f_m=4,000$  Hz.,  $V_m=7V$ ,  $\Delta V=1.5V$ ,  $S=200,000V/Sec.$  67
- 43 : Simulated waveform of delta modulator and SMPS  
voltage waveform (a) modulator waveforms  
(b) modulated output of modulator (c) SMPS output  
(d) spectrum of SMPS output.  
 $f_m=3,000$  Hz.,  $V_m=7V$ ,  $\Delta V=1.5V$ ,  $S=200,000V/Sec.$  68
- 44 : Simulated waveform of delta modulator and SMPS  
voltage waveform (a) modulator waveforms  
(b) modulated output of modulator (c) SMPS output  
(d) spectrum of SMPS output.  
 $f_m=3,000$  Hz.,  $V_m=7V$ ,  $\Delta V=3V$ ,  $S=200,000V/Sec.$  69
- 45 : Simulated waveform of delta modulator and SMPS  
voltage waveform (a) modulator waveforms  
(b) modulated output of modulator (c) SMPS output  
(d) spectrum of SMPS output.  
 $f_m=3,000$  Hz.,  $V_m=7V$ ,  $\Delta V=4V$ ,  $S=200,000V/Sec.$  70
- 46 : Simulated waveform of delta modulator and SMPS  
voltage waveform (a) modulator waveforms  
(b) modulated output of modulator (c) SMPS output  
(d) spectrum of SMPS output.  
 $f_m=3,000$  Hz.,  $V_m=7V$ ,  $\Delta V=5V$ ,  $S=200,000V/Sec.$  71

- 47 : Simulated waveform of delta modulator and SMPS  
voltage waveform (a) modulator waveforms  
(b) modulated output of modulator (c) SMPS output  
(d) spectrum of SMPS output.  
 $f_m=3,000$  Hz.,  $V_m=7V$ ,  $\Delta V=5.5V$ ,  $S=200,000V/Sec.$  72
- 48 : Simulated waveform of delta modulator and SMPS  
voltage waveform (a) modulator waveforms  
(b) modulated output of modulator (c) SMPS output  
(d) spectrum of SMPS output.  
 $f_m=3,000$  Hz.,  $V_m=7V$ ,  $\Delta V=6V$ ,  $S=200,000V/Sec.$  73
- 49 : Simulated waveform of delta modulator and SMPS  
voltage waveform (a) modulator waveforms  
(b) modulated output of modulator (c) SMPS output  
(d) spectrum of SMPS output.  
 $f_m=3,000$  Hz.,  $V_m=7V$ ,  $\Delta V=3V$ ,  $S=150,000V/Sec.$  74
- 50 : Simulated waveform of delta modulator and SMPS  
voltage waveform (a) modulator waveforms  
(b) modulated output of modulator (c) SMPS output  
(d) spectrum of SMPS output.  
 $f_m=3,000$  Hz.,  $V_m=7V$ ,  $\Delta V=3V$ ,  $S=200,000V/Sec.$  75
- 51 : Simulated waveform of delta modulator and SMPS  
voltage waveform (a) modulator waveforms  
(b) modulated output of modulator (c) SMPS output  
(d) spectrum of SMPS output.  
 $f_m=3,000$  Hz.,  $V_m=7V$ ,  $\Delta V=3V$ ,  $S=300,000V/Sec.$  76

- 52 : Simulated waveform of delta modulator and SMPS  
voltage waveform (a) modulator waveforms  
(b) modulated output of modulator (c) SMPS output  
(d) spectrum of SMPS output.  
 $f_m=3,000$  Hz.,  $V_m=7V$ ,  $\Delta V=3V$ ,  $S=400,000V/Sec.$  77
- 53 : Simulated waveform of delta modulator and SMPS  
voltage waveform (a) modulator waveforms  
(b) modulated output of modulator (c) SMPS output  
(d) spectrum of SMPS output.  
 $f_m=3,000$  Hz.,  $V_m=7V$ ,  $\Delta V=3V$ ,  $S=500,000V/Sec.$  78
- 54 : Simulated waveform of delta modulator and SMPS  
voltage waveform (a) modulator waveforms  
(b) modulated output of modulator (c) SMPS output  
(d) spectrum of SMPS output.  
 $f_m=3,000$  Hz.,  $V_m=5V$ ,  $\Delta V=3V$ ,  $S=200,000V/Sec.$  79
- 55 : Simulated waveform of delta modulator and SMPS  
voltage waveform (a) modulator waveforms  
(b) modulated output of modulator (c) SMPS output  
(d) spectrum of SMPS output.  
 $f_m=3,000$  Hz.,  $V_m=6V$ ,  $\Delta V=4V$ ,  $S=200,000V/Sec.$  80
- 56 : Simulated waveform of delta modulator and SMPS  
voltage waveform (a) modulator waveforms  
(b) modulated output of modulator (c) SMPS output  
(d) spectrum of SMPS output.  
 $f_m=3,000$  Hz.,  $V_m=7V$ ,  $\Delta V=4V$ ,  $S=200,000V/Sec.$  81

57	: Simulated waveform of delta modulator and SMPS voltage waveform (a) modulator waveforms (b) modulated output of modulator (c) SMPS output (d) spectrum of SMPS output. $f_m=3,000$ Hz., $V_m=8V$ , $\Delta V=4V$ , $S=200,000V/Sec.$	82
58	: Simulated waveform of delta modulator and SMPS voltage waveform (a) modulator waveforms (b) modulated output of modulator (c) SMPS output (d) spectrum of SMPS output. $f_m=3,000$ Hz., $V_m=8.5V$ , $\Delta V=4V$ , $S=200,000V/Sec.$	83
59	: A practical circuit for producing switching waveform of delta modulated inverters.	85
60	: Graphical illustration of DM technique for the SMPS.	86
61	: Illustration of practical waveforms of delta modulation circuit. $f=40$ Hz.	88
62	: Carrier and modulated output of a DM circuit for $f=40$ Hz., $\Delta V=4$ Volt, $S=5,405$ V/Sec.	90
63	: Carrier and modulated output of a DM circuit for $f=40$ Hz. and $60$ Hz., $\Delta V=4$ Volt, $S=5,405$ V/Sec.	91
64	: Carrier and modulated output of a DM circuit for $f=60$ Hz. and $80$ Hz., $\Delta V=4$ Volt, $S=5,405$ V/Sec.	92
65	: Carrier and modulated output of a DM circuit for $f=80$ Hz. and $100$ Hz., $\Delta V=4$ Volt, $S=5,405$ V/Sec.	93
66	: Carrier and modulated output of a DM circuit for $f=40$ Hz., $\Delta V=4$ Volt and $7$ Volt, $S=5,405$ and $9,459$ V/Sec.	95
67	: Carrier and modulated output of a DM circuit for $f=100$ Hz., $\Delta V=4$ Volt and $7$ Volt, $S=5,405$ and $9,459$ V/Sec.	96

68 : Effect of change of slope of the carrier wave with constant frequency (f=40 Hz.).	98
69 : Effect of change of slope of the carrier wave with constant frequency (f=100 Hz.).	99
70 : Transistor acting as a switch in an SMPS.	103
71 : Conventional switching regulator.	106
72 : Circuit diagram of a delta modulated SMPS.	109
73 : (a) Original circuit (b) when switch is ON (c) when switch is OFF (d) voltage waveform (e) inductor current waveform neglecting voltage ripple.	112
74 : Semiconductor implementation of SMPS circuit.	116
75 : Output of the SMPS without feedback (a) without any filter (b) Inductive filter only.	118
76 : Output of the SMPS without feedback (a) Capacitor (22 $\mu$ F) & inductor (0.125 mh) filter (b) increased capacitor value (3300 $\mu$ F) and same inductor value.	119
77 : Output of the SMPS with feedback : input (a) increased from 40 to 50 volt A.C. (b) decreased from 50 to 35 volt A.C. and (c) increased from 35 to 40 volt A.C.	121

ANALYSIS OF DELTA MODULATED SWITCHMODE  
POWER SUPPLY

## Chapter - 1

### Introduction

#### 1.1 INTRODUCTION :

A switch mode power supply (SMPS) is a dc to dc static power converter switched at a very high frequency. Conversion of both step down and step up dc with insignificant filter size having facility of feed back regulation by ON/OFF high frequency switching is possible in an SMPS. These power supply units are light weight and more efficient than their counterpart linear power supplies. Various features like isolated multiple outputs and self protection of power units and loads can be incorporated in an SMPS. As a result, use of SMPSs are on increase in space power applications, computers, TV and industrial units. SMPSs have advantages of being low cost, light weight, efficient, compact, self regulating and self protected. Diverse types of SMPS are investigated to meet users requirements and research is still continuing to find newer ways of switching, increased switching frequencies, modified topologies and enhanced performance of filters to reduce ripples and EMI.



A simple SMPS consists of a rectifier fed by line voltage (transformerless), a filter (to obtain pure dc), an static switch (BJT, MOSFET etc. switched by control circuitry at a very high frequency to step down or step up dc voltage by ON/OFF ratio control), the filter (electrolytic capacitor and ferrite core inductor) and feedback the circuit (for voltage regulation). Fig.-1 shows the block diagram of an SMPS.

Switch mode power conversion requires fundamental knowledge in three areas :

1. Power circuit configurations
2. Control system and
3. Magnetic circuits.

Principles of magnetic circuit analysis require better understanding of power inductor and power transformer design requirements. Closing the feedback loops in PWM systems requires basic understanding of dc-to-dc converter dynamics and understanding of transfer functions and frequency response methods [1].

The control circuit of an SMPS basically generates high frequency gating pulses for the switching device to control the dc. Switching is performed in multiple pulse width modulation (pwm) fashion according to feedback error signal from the load to serve two purposes

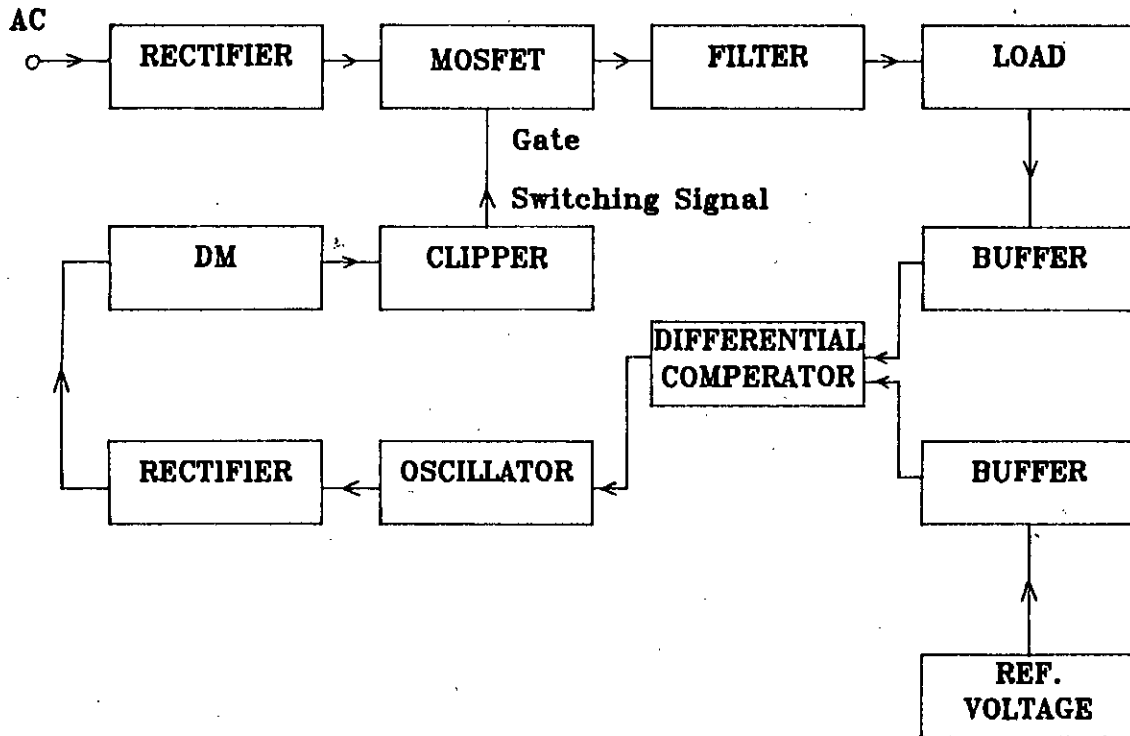


Fig.-1 : Block diagram of an SMPS.

- a) Produce high frequency switching signal
- b) Control ON/OFF period of switching signal to maintain constant voltage across load.

High frequency pwm switching also reduce filter requirements at the INPUT/OUTPUT side(s) of the converter. Simplest pwm control uses multiple pulse modulation generated by comparing a dc with a high frequency carrier triangular wave. However, energy efficient SMPS use more advanced sine pwm waves generated by comparison of sine wave with triangular wave. In this thesis focus is given on analysis and implementation of delta modulated pwm switching of a step down SMPS. Delta modulation is the simplest known modulation technique, easily implementable and easy to control process and would give an edge over other modulation process in use for switching SMPSs these days.

## 1.2 REVIEW OF SWITCHMODE POWER SUPPLIES :

### 1.2.1 PRINCIPLE OF OPERATION :[1]

Fig.-2 illustrates the circuit for classical linear power conversion. Here power is controlled by a series linear element, either a resistor (mechanical control) or a transistor is used in the linear mode (electronic control). The total load current is passed through the series linear element. Thus greater the difference between input and output

voltage (the higher the controlling power range of the linear element) more power is lost in the controlling device. Linear power conversion is dissipative (even in the ideal case of the element) and hence inefficient. The efficiency range is typically 30 to 60%.

The circuit of Fig.-3, describes basic principle of a switch mode power conversion. The controlling device is a switch. By controlling the ratio of the time intervals spent in the ON and OFF position (defined as duty ratio), the power flow to the load can be controlled in a very efficient way. Ideally this method is 100% efficient. In practice, the efficiency is reduced as the switch is non-ideal and losses occur in power circuits.

The semiconductor devices can be used as a switch in an efficient way (for example, bipolar transistor). When the switch is a transistor it is driven by a pulse width modulator (PWM). The dc load voltage is controlled by controlling the duty cycle of the rectangular waveform supplied to the base of the switching transistor. When the switch is fully ON, it has only a small saturation voltage drop across it (typically 0.3 Volt to 1 Volt). In the OFF condition, the power loss is negligible.

The output of the switch mode power conversion control (Fig.-3) is not dc as in the linear power supplies (Fig.-2). This type of output is applicable in some cases such as oven heating without proper filtration. If constant dc is required, then output of SMPS has to be smoothed out by the addition of a low-pass LC filter.

*Switches are required as basic components for efficient electric power conversion and control. Ideally lossless storage components, inductors and capacitors are required to generate dc output voltage. Inductors and capacitors are used to smooth the pulsating dc originating from the switching action.*

Although the conversion would be 100% efficient in the ideal case of lossless components (Fig.-4), in practice each of the components is lossy. Thus, efficiency is reduced. Hence, one of the prime objectives in switch mode power conversion is to realize conversion (such as dc-to-dc conversion) with the least number of components having better efficiency and reliability.

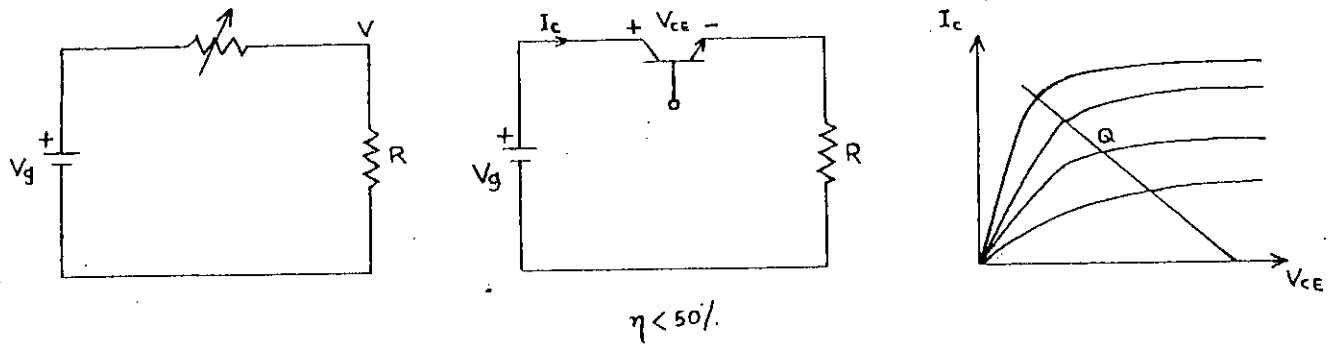


Fig.-2 : Linear (dissipative) power conversion circuit.

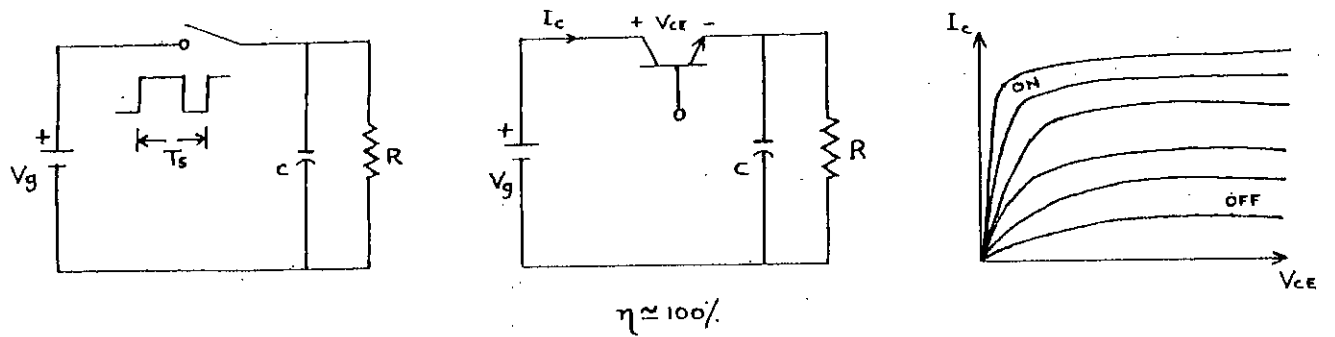


Fig.-3 : Switchmode (nondissipative) power conversion circuit.

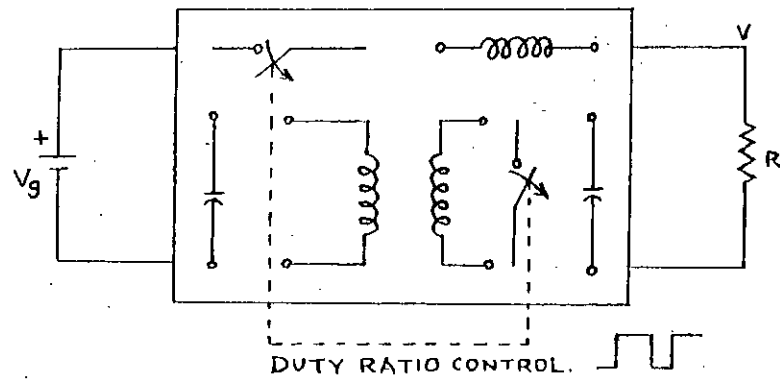


Fig.-4 : General switchmode power conversion.

### 1.2.2 TYPES OF CONVERTERS :

The simplest dc-to-dc SMPS converter topology consist of a single switch (Single-Pole double throw ideal switch S in Fig.-5), a single inductor and a single capacitor.

By different arrangement of these limited number of components, four type of converter have been developed in the past [references] , these are,

- a. Buck (step down) converter
- b. Boost (step up) converter
- c. Buck-Boost converter and
4. CŪk converter.

#### Buck Converter : [1,2]

The simplest configuration of Buck converter is shown in Fig.-6. The input dc voltage  $V_g$  is chopped by the switch S. Hence, this converter is also called Chopper. Due to the chopping, an intermediate pulsed waveform  $V_1$  is produced. This voltage  $V_1$  is filtered by a low-pass filter.

When the switch is ON ( $t=T_{on}$ ) input current rises through filter inductor L, capacitor C and load resistor R. As the switch is turned OFF ( $t=T_{off}$ ) the freewheeling diode  $D_m$  conducts due to energy stored in the inductor and the inductor

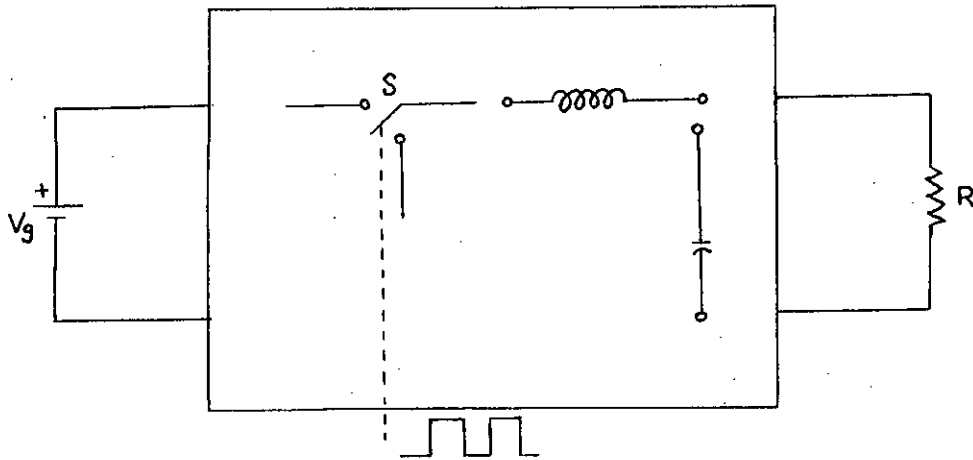


Fig.-5 : Simple generalized dc-to-dc converter topology (buck, boost and buck-boost can be realized by rearrangement of components).

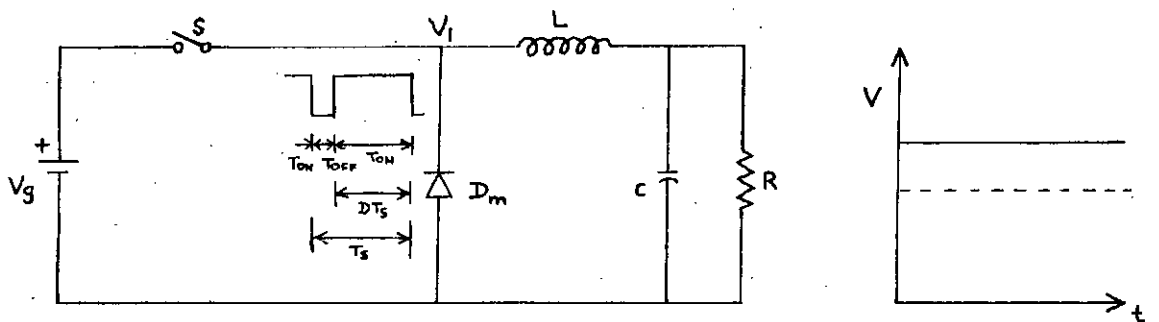


Fig.-6 : Controlled dc-to-dc power conversion in a basic buck converter through pulse width modulation.



current continuous to flow through L, C, load and diode  $D_0$ . The inductor current falls until the switch is again turned ON in the next cycle.

Let,

$D$  = Duty ratio

By definition,

$$D = (\text{On time interval}) / (\text{Total switching interval})$$

$$= T_{\text{on}} / T_s$$

$$\therefore T_{\text{on}} = DT_s \quad \dots\dots\dots(1)$$

Let,

$$T_{\text{off}} = D' T_s \quad \dots\dots\dots(2)$$

$$V_{\text{av}} = 1/T_s \int_0^{T_s} v \cdot dt$$

$$= 1/T_s \left[ \int_0^{DT_s} V_g \cdot dt + \int_{DT_s}^{T_s} 0 \cdot dt \right]$$

$$= 1/T_s [V_g(DT_s - 0) + 0(T_s - DT_s)]$$

$$= 1/T_s (V_g \cdot DT_s)$$

$$= DV_g$$

$\therefore$  output dc voltage,

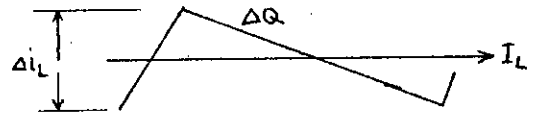
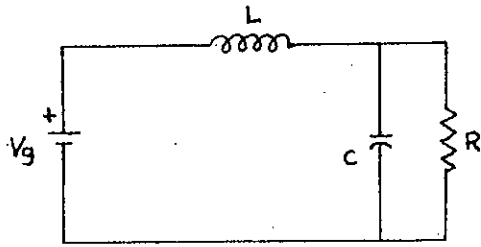
$$V_{\text{dc}} = V_{\text{av}}$$

$$\Rightarrow V = DV_g \quad \dots\dots\dots(3)$$

*Thus, by controlling the duty ratio of the switch, the output dc voltage can be controlled.*

Equivalent circuit, current and voltage waveforms of BUCKTYPE SMPS are shown in Fig.-7.

at  $t=T_{on}$ ,



at  $t=T_{off}$ ,

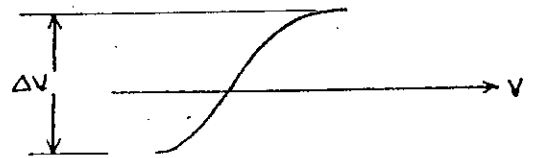
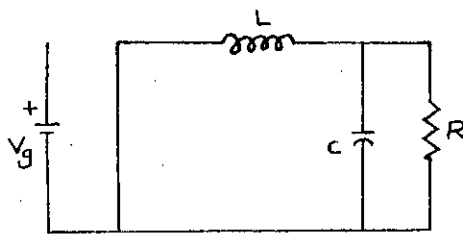


Fig.-7 : Equivalent circuit and quantitative evaluation of the output voltage switching ripple.

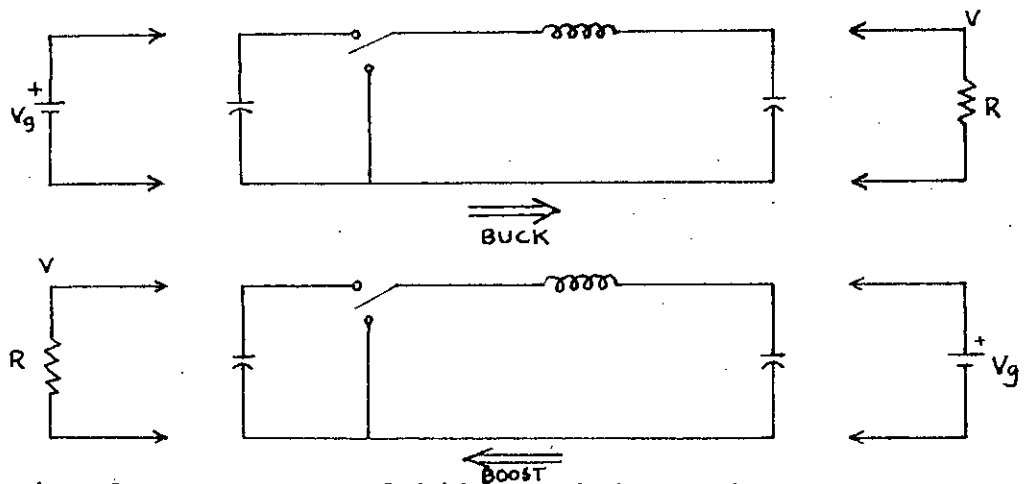


Fig.-8 : Process of bilateral inversion to create step-up converter from step-down converter.

The buck converter pulsating input current, often requires an input filter to smooth out large current variations. Hence the buck converter of Fig. 8(a) has an input capacitance to reduce current ripple returned to the source.

Boost Converter :[1,2]

A simple interchange of the source and load of the BUCK CONVERTER (bilateral inversion) generates a boost converter from the original buck converter as shown in Fig.-8

Operation of boost converter can be explained from Fig.-9. When the switch is ON ( $t=T_{on}$ ) the input current rises through filter inductor L and the switch. When the switch is OFF ( $t=T_{off}$ ) the current that was flowing through the switch would now flow through L, C, load and diode  $D_m$ . The inductor current falls until the switch is again turned ON in the next cycle.

The dc gain of the new boost configuration, due to the nature of the source and load interchange, is equal to the reciprocal of the buck converter gain, i.e,

The boost converter gain is,

$$V/V_g = 1/D \geq 1 \quad \text{for } D[0.1] \quad \dots\dots\dots(4)$$

In the Practical implementation of boost converter as shown in Fig.-9, the input capacitance is also omitted as non essential for basic operation of the converter. Hence, again, conversion

is realized by the least number of components : a single switch, an inductor and a capacitor.

Equivalent circuit, current and voltage waveforms of an SMPS operated in BOOST type topology are shown in Fig.-10.

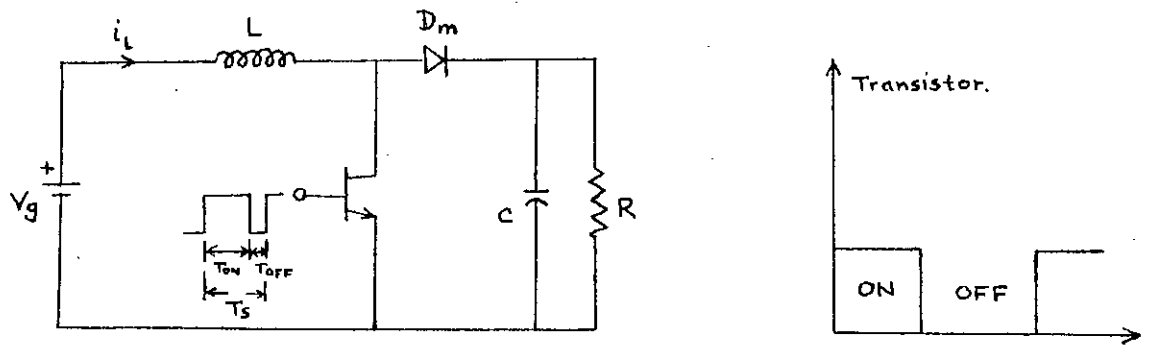
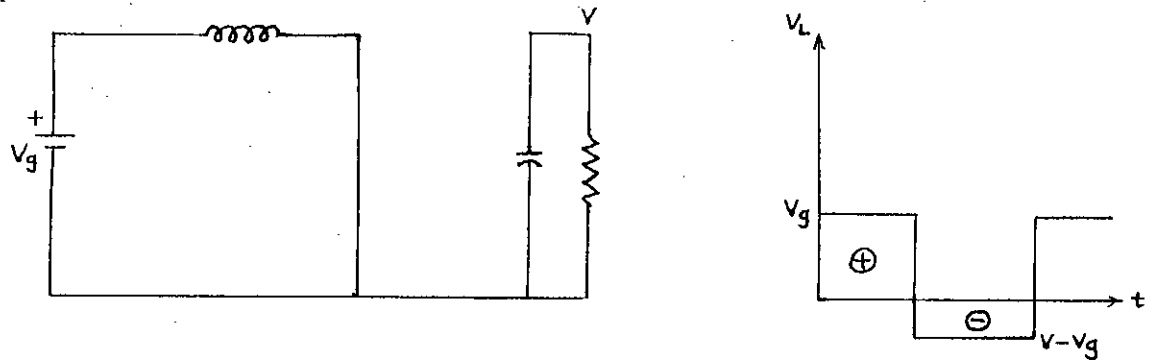


Fig.-9 : Circuit diagram of boost converter.

at  $t=T_{on}$ ,



at  $t=T_{off}$ ,

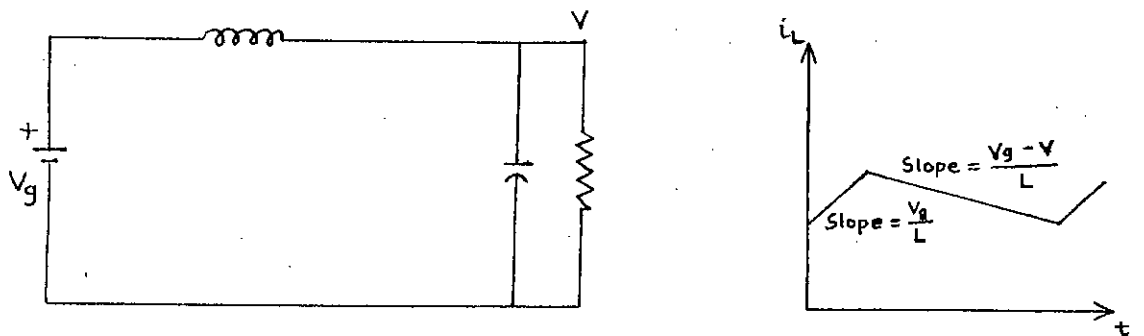
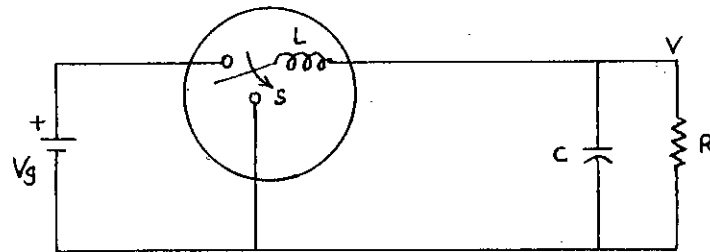


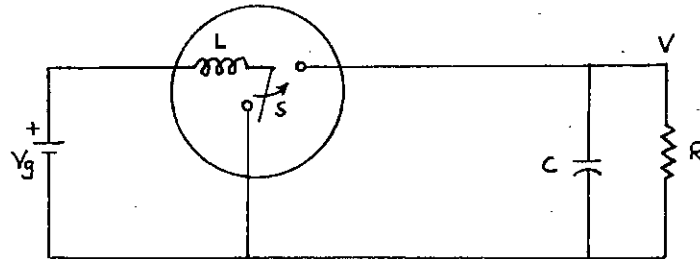
Fig.-10 : Equivalent circuit, voltage and current waveform of boost converter.

BUCK-BOOST CONVERTER : [1,2]

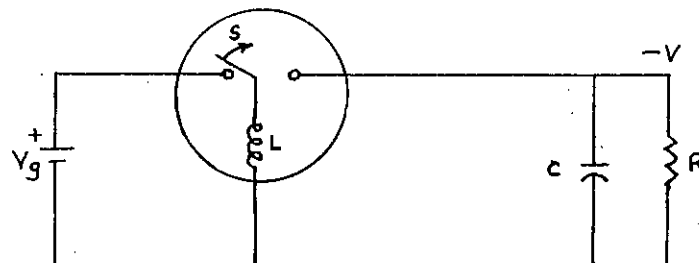
Buck converters can step-down and boost converters can step-up dc voltages separately. The buck-boost converter in which the inductor is grounded can perform either of these two conversions. The output voltage polarity is opposite and as a result the converter is also known as an *inverting* converter.



Buck converter



Boost converter



Conventional buck-boost converter

To explain the operation of buck-boost converter, let us consider Fig.-11. When the switch is turned ON, the diode  $D_m$  is reversed biased. The input current rises through inductor L and the switch. When the switch is turned OFF ( $t=t_{off}$ ) the current which was flowing through inductor L, would flow through L, C,  $D_m$  and the load. The energy stored in inductor L would be transferred to the load and the inductor current would fall until the switch is again turned ON in the next cycle.

From the usual volt-sec balance in steady state, the dc voltage gain is obtained as,

$$V/V_g = D/(1-D) \quad \dots\dots\dots(4)$$

Thus either a step-up ( $D>0.5$ ) or a step-down ( $D<0.5$ ) conversion can be achieved with the same converter. For  $D=1.0$ , the gain becomes infinite, but practically a finite voltage gain results due to the inclusion of inductor's parasitic resistance.

Equivalent circuit of a BUCK-BOOST converter, current and voltage waveforms are shown in Fig.-12.

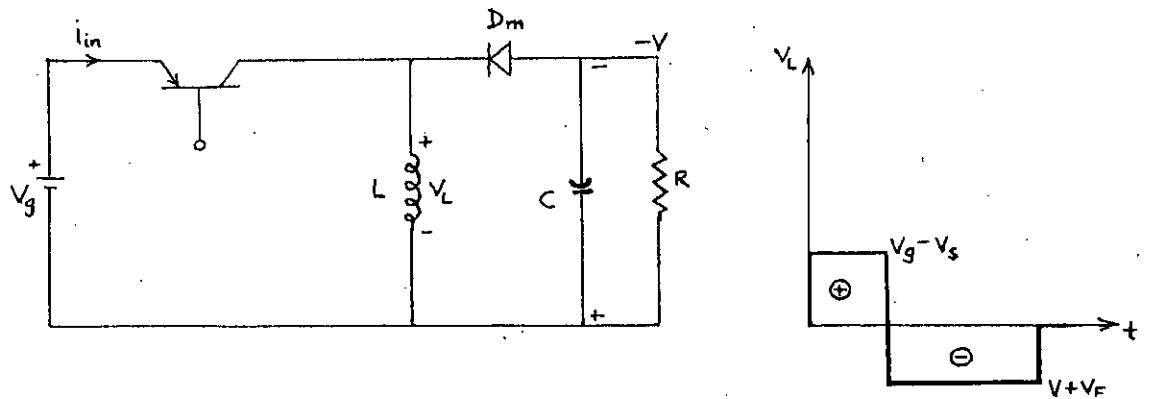
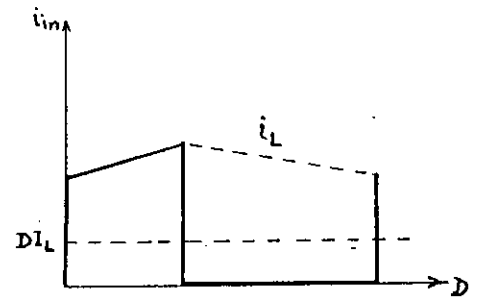
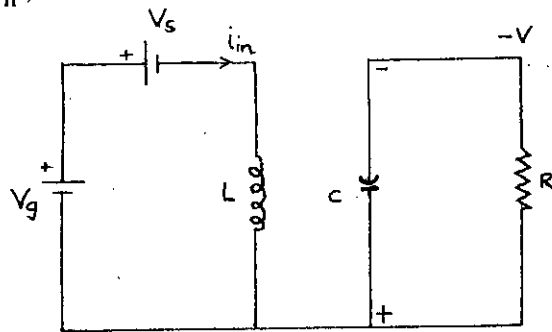


Fig.-11 : Circuit diagram of buck-boost converter.

at  $t=T_{on}$ ,



at  $t=T_{off}$ ,

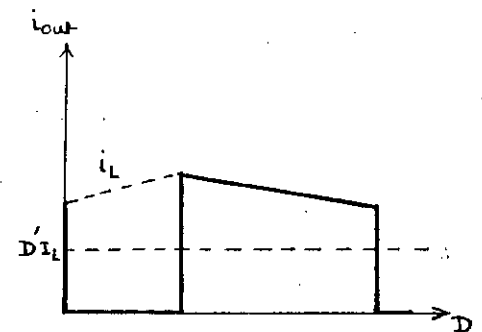
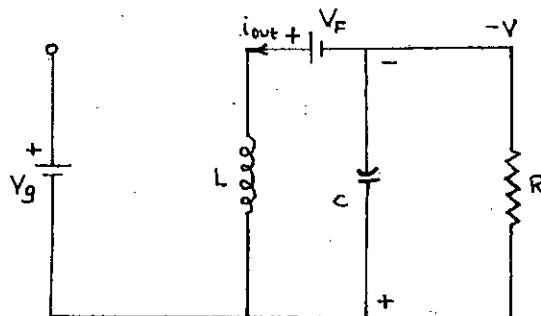


Fig.-12 : Converter efficiency in presence of switch nonidealities (non zero transistor and diode voltage drops.)



Cûk Converter :[1,2]

Similar to the buck-boost converter, Cûk converter provides an output voltage which is less than or greater than the input voltage but the output voltage polarity is opposite to that of the input voltage. The cûk converter is based on *capacitive energy transfer*. Thus its dc current gain may be easily deduced from the capacitor current waveform using a charge balance method in steady-state (Fig.-13)

$$I_1 D' T_s = I_2 D T_s \quad \dots\dots\dots(6)$$

or, from the 100% efficiency argument, dc voltage gain is,

$$V/V_g = D/(1-D) \quad \dots\dots\dots(7)$$

For simplicity of argument, the inductors were assumed to be large enough such that the slope is negligible and results in rectangular current wave form.

When the switch is turned ON ( $t=T_{on}$ ) current rises through inductor  $L_1$  . At the same time voltage of capacitor  $C_1$  reverse biases diode  $D_m$  and turns it OFF. Capacitor  $C_1$  discharges to the circuit formed by  $C_1$ ,  $C_2$ , load and  $L_2$ . When the switch is turned OFF ( $t=t_{off}$ ) the capacitor  $C_1$  is charged from the input supply and the energy stored in the inductor  $L_2$  is transferred to the load. The diode  $D_m$  and the switch provides a

synchronous switching action. The capacitor  $C_1$  is the medium for transferring energy from the source to the load.

Equivalent circuit, current and voltage waveforms are shown in Fig.-14.

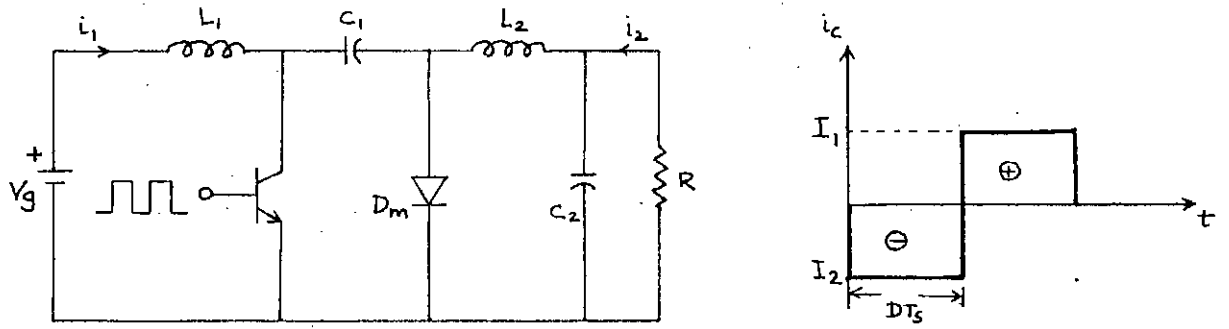
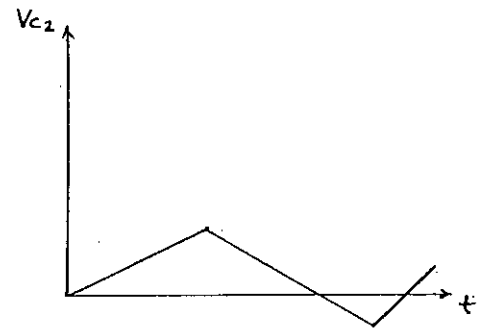
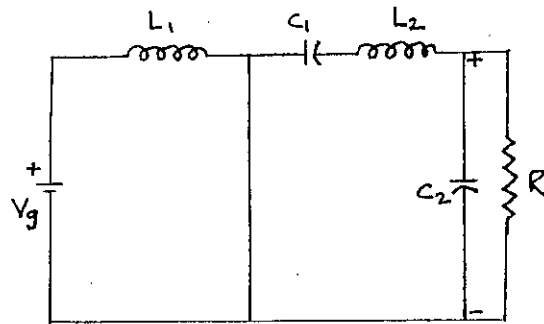


Fig.-13 : Cûk converter circuit diagram :implemented by a transistor and a diode.

at  $t=T_{on}$ ,



at  $t=T_{off}$ ,

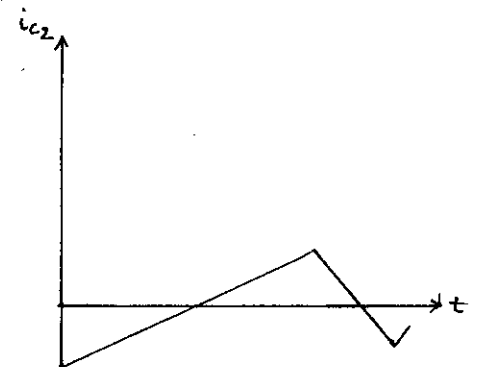
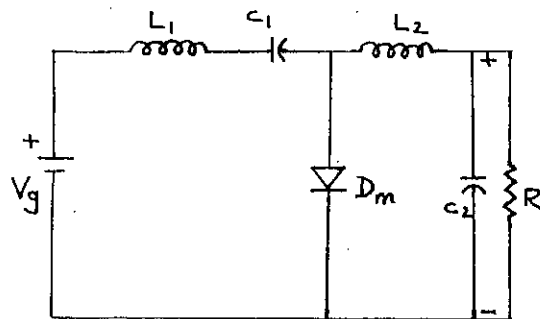


Fig.-14 : Equivalent circuits and waveforms of cûk converter.

### 1.2.3 SWITCHING :

The output voltage is not an ideal dc. In addition to a dc component it consists of ripple voltage component at switching frequency  $f_s \leq 1/T_s$ , as shown in Fig.-15. The pulse width modulated (pwm) voltage waveform at the input of the low-pass LC filter may be split into its dc component and harmonics at the switching frequency  $f_s$  and integer multiples by use of sampling frequency of the Fourier series. The dc component passes unattenuated through the filter to generate desirable dc output  $V = DV_g$ .

Provided that the filter corner frequency  $f_c = 1/2\pi \sqrt{LC}$  is significantly lower than the switching frequency (typically at least a decade below  $f_s$ ) the first and higher order harmonics are substantially attenuated by the LC filter, resulting in an acceptably low switching ripple voltage at the output.

#### Switching losses :

Efficiency of an SMPS is ideally 100%. But due to nonideal elements (stray resistances in inductances and capacitors) and switching of devices, losses take place in an SMPS. Losses due to nonideal elements accounts negligibly towards total loss. However, the losses associated with switching device is substantial and it changes with regulation and switching. Switching device losses are of two types

1. Product of device drop (0.3 to 0.7 V) and current through the device during ON time
2. Product of voltage and current in the device during turn ON or OFF period.

Usually no loss occurs during OFF period. The second loss depends largely on the frequency of switching and time required to turn ON and OFF. Switching loss is illustrated in Fig.-16

ON/OFF switching per second gives rise to losses in SMPS and dissipates as heat.

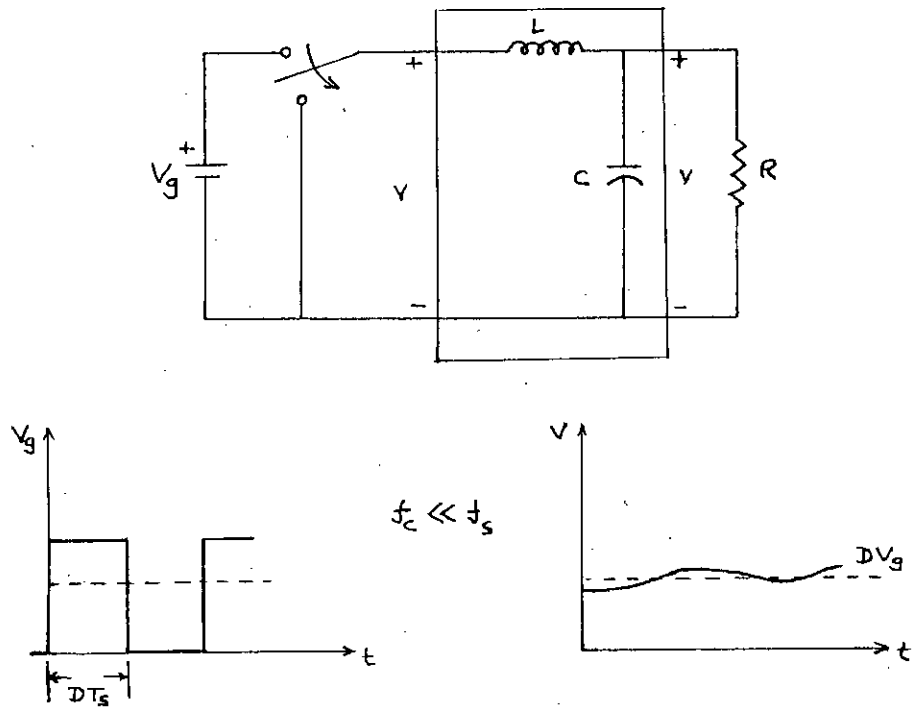


Fig.-15 : Frequency view point reveals that for low output switching ripple filter corner frequency must be well below switching frequency.

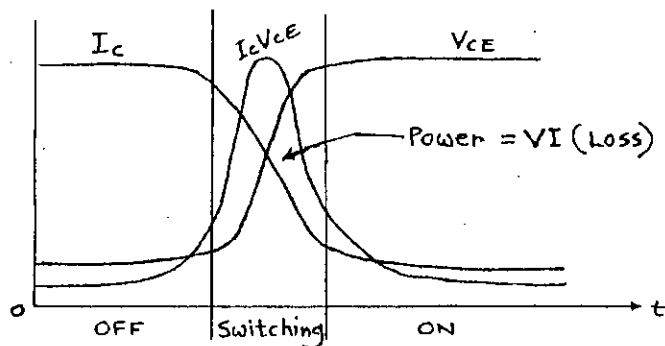


Fig.-16 : Switching losses.

#### 1.2.4 REVIEW OF MAGNETIC CIRCUIT AS APPLIED TO AN SMPS :

Design of filter circuit comprising inductor and capacitors of an SMPS require special attention to magnetic materials and properties because they have to work under very high frequencies. Since eddy current and hysteresis losses in the magnetic circuits are dependent on frequency, these losses would be large if iron core inductors were used. Special grade ferrite cores are used in the construction of filter inductors of SMPS. Emphasis is given to the selection of B-H curve of the core material of the inductors and isolation transformers (if used any). Following is the preview of magnetic concept applied to ferrites used in SMPS.

Two vector field quantities are associated with the magnetic field,

- 1) field intensity
- 2) flux density.

The electric current produces the magnetic field and hence the field intensity vector H (also known as field strength) is directly related to the electric current as given by the Ampere's law in the integral form,

$$\oint H \cdot dl = \iiint_s J \cdot ds \quad \dots\dots\dots(8)$$

The flux density B (also called magnetic induction) is directly related to the effects (mechanical forces, electric voltages) of the field as given by Faraday's law of electromagnetic induction (rate of change of magnetic flux,  $\phi$ )

$$\begin{aligned}
 V &= \frac{d}{dt}(N\phi) \\
 &= \frac{d}{dt}N\int B \cdot ds \quad \dots\dots\dots(9)
 \end{aligned}$$

For the simple case of the infinite straight conductor in free space carrying current I, the field intensity vector H can be easily found using the symmetry argument (equal tangential vector H at distances of radius r) as seen in Fig.-17. Ampere's circuital law then simplifies to

$$H = I/2\pi r \quad \dots\dots\dots(10)$$

In principle, the magnetic field intensity H caused by the conductor carrying current I can be found for any point in free space. Associated with vector H is the flux density vector B, which in free space is always parallel in direction and proportional in magnitude, (as seen in Fig.-17) such that

$$B = \mu_0 H \quad \dots\dots\dots(11)$$

where  $\mu_0$  is the permeability of free space which characterizes this medium for its magnetic properties, just as conductivity  $\sigma_0$  characterizes electrical properties.



Characteristics of ferromagnetic materials :

Ferromagnetic materials are able to produce larger effect (larger B hence larger flux) with smaller H hence smaller current. This can be understood easily by visualizing the presence of a great number of magnetized regions, called magnetic domains, such as shown in Fig.-18.

Each magnetic domain may be conceptually visualized as originating from a magnetic dipole (small loop of current). For demagnetized materials such as shown in Fig.-18(a) (current I reduced to zero), these magnetic dipole has a random orientation in space. Thus the net flux contribution of the elementary magnetic domains on a global scale is zero, although locally it may be fully magnetized. However, even a small current I in the conductor, such as shown in Fig.-18(b), may generate sufficient external field strength H to orient the majority of the small magnetic domains in the direction of the external field H. Thus the flux density in free space  $\mu_0 H$  is augmented many times by the additional intrinsic flux density of the material  $B_i$  as seen in Fig.-17(b). Stating this in equation form,

$$B = \mu_0 H + B_i \quad \dots\dots\dots(12)$$

Further increase of current I results in further increase of external field H, and hence leads to an even greater number of magnetic domains oriented in its direction. For an ideal linear medium ( $B_1$  parallel to H and proportional to its magnitude), mathematically this may be expressed as,

$$B_1 = \mu_0 \chi H \quad \dots\dots\dots(13)$$

where,  $\chi$  is magnetic susceptibility.

combining equation 12 & 13,

$$\begin{aligned} B &= \mu_0 H + B_1 = \mu_0 H + \mu_0 \chi H \\ &= \mu_0 (1 + \chi) H \\ &= \mu_r \mu_0 H \\ &= \mu H \quad \dots\dots\dots(14) \end{aligned}$$

where  $\mu_r$  is the relative permeability of the ferromagnetic material, which can be in range of 100 to 100,000.

Comparison of equation 11 & 14, pictorially represented in Fig.-19 (a), emphasizes the role of the ferromagnetic material in enhancing its magnetic characteristics through greatly increased slope on the B-H characteristic. However, after a certain point, further increase of field strength does not lead to as rapid increase of flux density as before (following the dotted line in Fig.-19(a)), but instead follows the slope of the flux density in free space, as illustrated in

Fig.-19(b). This is due to the finite number of magnetic domains as in Fig.-19. Thus, when the externally applied field strength  $H$  is sufficient to orient all magnetic domains in its direction, further increase of  $H$  will not produce as rapid increase of flux density. In other words, a phenomenon called saturation of magnetic flux density occurs as illustrated in Fig.-20. This saturation flux density  $B_{sat}$  becomes a very important ferromagnetic material parameter since, it has direct bearing on the size and weight of the magnetic components.

Another important classification of the ferromagnetic materials is also readily visible from Fig.-20. In some materials such as silicon iron (3% Si, 9% Fe), Orthonol (50% Ni, 50% Fe), even a very small field strength  $H$  is capable of fully aligning all magnetic domains and results in the square characteristic of Fig.-20(a). These materials are often termed square-loop materials. On the other hand, in materials such as Ferrite (MnZn alloy) the flux density variation is gradual, such that a distinct linear region is visible before the saturation point is reached. These materials are ideally categorized as linear materials. They can be approximated by equation (14) and a constant permeability  $\mu$  designating the slope of the characteristic. Experimentally, either square or linear materials exhibit a nonlinear relationship of  $B$  and  $H$ , such that no align value of permeability can be used to

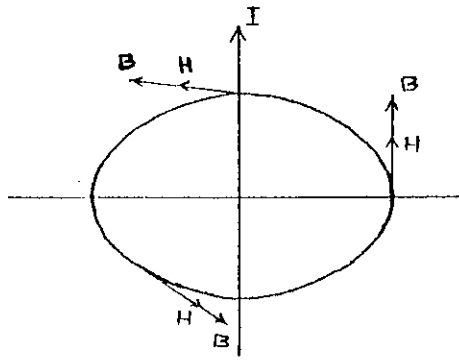


Fig.-17 : Ampere's circuital law to a single conductor in free space.

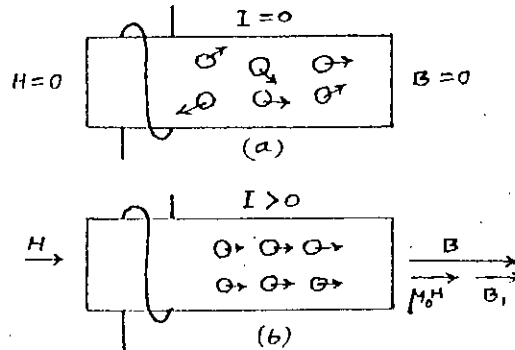


Fig.-18 : Orientation of magnetic domains  
 (a) Random orientation of magnetic domains in demagnetized materials  
 (b) their orientation in the direction of external field  $H$  generated by coil current  $I$ .

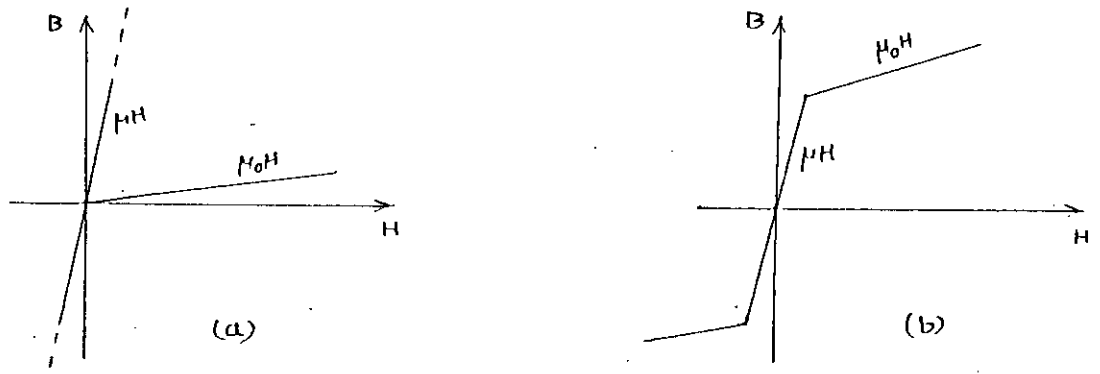


Fig.-19 : (a) High permeability  $\mu$  (steep slope on a B-H curve) (b) saturation.

characterize it, as seen from the experimentally measured B-H characteristic for square and linear materials in Fig.-21.1. Thus, due to the nonlinear magnetization characteristic, the B-H characteristic exhibits hysteresis loop behavior. The static losses are directly associated with the area of the B-H loop at a given frequency, while the dynamic losses characterize additional core losses owing to the winding of the B-H loop at higher frequencies. Although they can also be appropriately modelled (12), we shall limit our discussion to the linear materials characterized by constant  $\mu$  in (14) and the idealized B-H characteristic of Fig.-21(b). This enable us to get a handle on the flux distribution in magnetic circuits, just as easily as finding the current distribution in electric circuits by use of Kirchoff's laws[1].

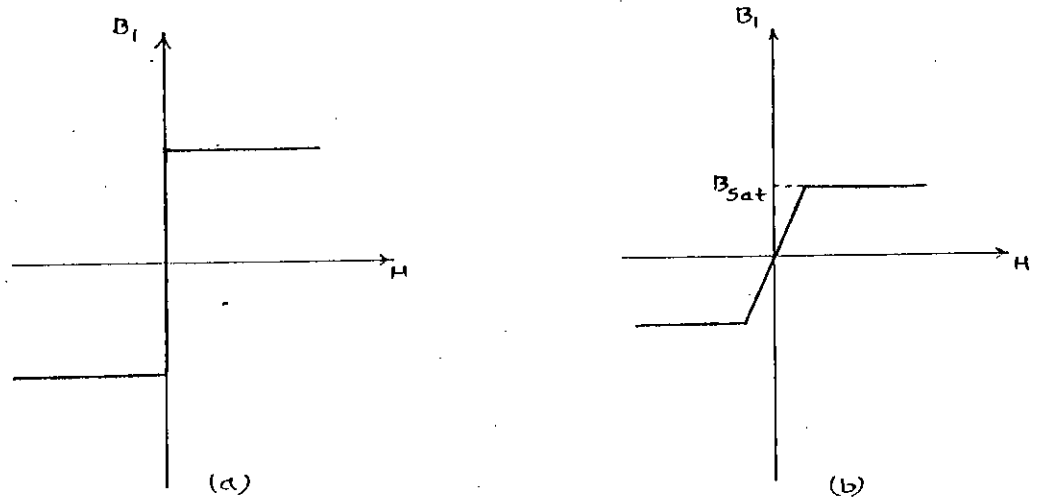


Fig.-20 : B-H Curves of magnetic materials

(a) Square-loop ferromagnetic materials exhibit high saturation flux density (b) linear ferromagnetic materials have lower saturation flux density.

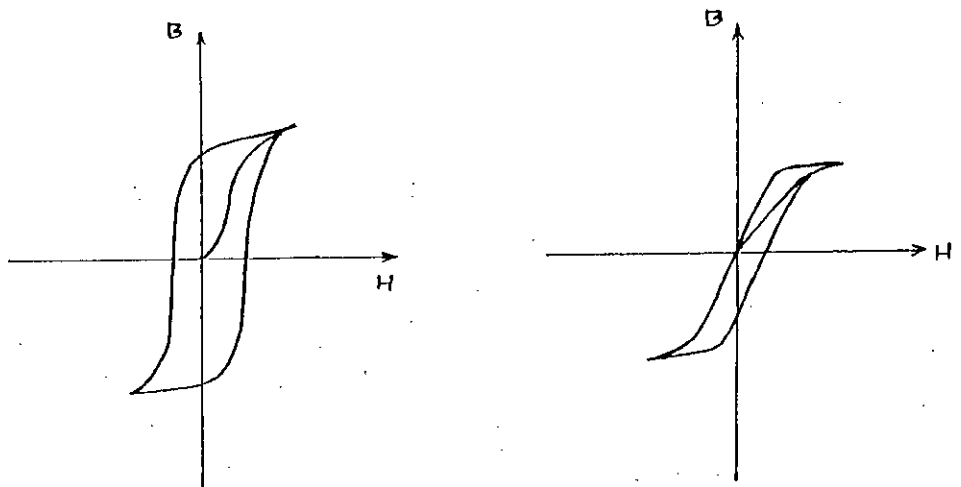


Fig.-21 : B-H Curves of magnetic materials

(a) Non-linear, double valued B-H loop characteristic of square material (b) linear materials.

### Regulation :

Switchmode power supplies are self regulating. The switching schemes (pwm) are incorporated with feedback from the output and ON/OFF periods are controlled according to change in load. As a result a predesigned constant voltage is maintained across load at the output of an SMPS. Usually SMPS are designed with stringent voltage regulation (0.01%) these days. However, this regulation is not unlimited. Normally 20-30% fluctuation of input voltage variation and about 50% load variation are accounted in by feedback control. Beyond specified load or input variation, SMPSSs are provided with overload and under voltage protection. Virtual load is always connected to protect SMPSSs from severe damage that may occur if they are turned ON without load.

### Protection :

Protection of SMPS from over voltage, under voltage, overload and switching transients are problematic. Recent SMPSSs are provided with power on checks or wrong connections, spike voltages and no-load shut down protections. These three protections are not inherent to SMPSSs and must be provided by static relays and sensors. In the occurrence of any of the faults mentioned modern SMPSSs are provided with automatic shut down by static relay connected to the input side of the power supply.

### 1.3 ADVANTAGES AND APPLICATIONS OF AN SMPS :[1,2]

Switchmode power supplies have following advantageous features,

- \* Isolation between the source and the load
- \* High power density for reduction of size and weight
- \* Controlled direction of power flow
- \* High conversion efficiency
- \* Input and output waveforms with a low total harmonic distortion for small filters
- \* Controlled power factor if the source is an ac voltage

For efficient switch mode power conversion, following components are required (Fig.-22).

The transformer shown is an additional unit which is used in practical unit for dc isolation between input and output and ground.

#### Isolated supply :

DC isolation between input and output is required for many reasons such as main protection, requirement for different output grounds. Besides, dc isolation is also required for many practical applications and a number of additional side benefits achieved. As illustrated in Fig.-23,, the dc isolation can be obtained in two simple steps, first two winding inductor is built (Fig.-23(a)), and then electrical



connection between the two windings is broken, thus resulting in the dc isolated version of Fig.-23(b). This process itself suggests that the transformer obtained in such a way must have the same inductive storage capability as the original single inductor. This has a serious drawback since such a transformer has to be designed to withstand a dc bias greater than the average input current and also limit its usefulness for higher power design.

However, for lower power design, the isolation feature brings as a by product some additional benefits. A simple change of the isolation transformer turns ratio contributes an additional step-up (or step-down) factor as illustrated in Fig.-24.

Other advantages of SMPS such as high efficiency, reliable regulation, light weight and self protection etc are obvious from previous discussion. Due to various advantages that can be achieved by an SMPS these dc power supplies are having wide variety of applications at present. The main use of these power supplies are in space, aerospace and computer fields because of their compact nature with reduced weight and high efficiency. Radio, TV transmitters and receivers and mobile telephone and radar equipments are also adopting these power supplies for their better voltage regulation and high efficiency. Industrial control units are also gradually adopting SMPSs for their power supplies.

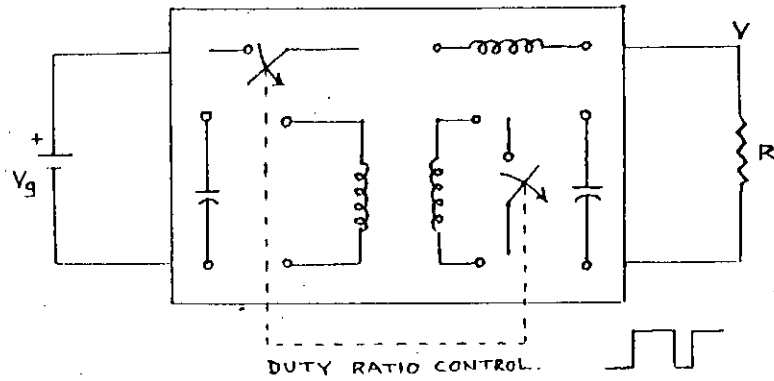


Fig.-22 : Storage components and switches for efficient SMPS.

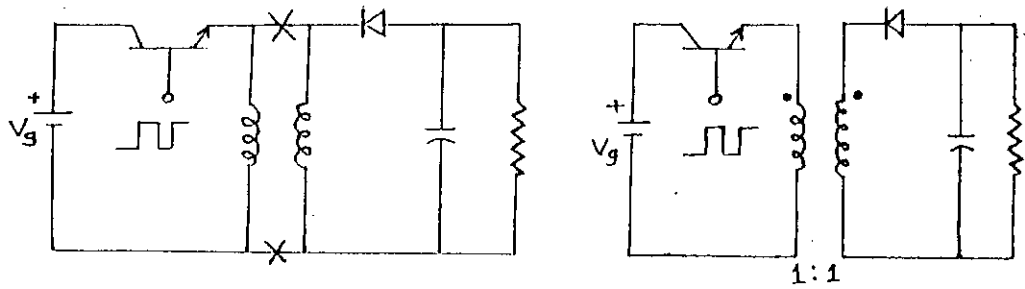


Fig.-23 : Isolation in an SMPS by transformers  
 (a) Simple bifilar winding step for dc isolation in SMPS (b) through breaking electrical connections.

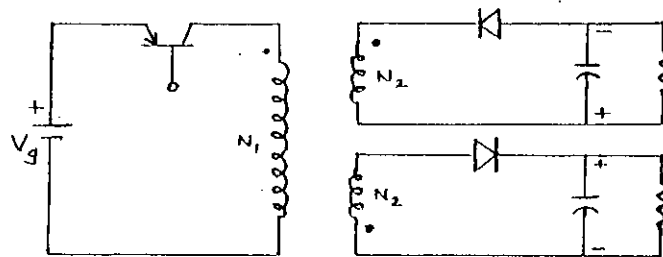


Fig.-24 : Isolated multiple output SMPS with polarity inversion.

#### 1.4 REVIEW OF PWM TECHNIQUES AS USED IN POWER CONVERTERS :

In many industrial applications, it is often required to control the output voltage of the converter. The most efficient method of controlling the gain (and output voltage) is to incorporate pulse-width-modulation (PWM) control within the inverters. The commonly used techniques are :

- 1) Single-pulse-width modulation
- 2) Multiple-pulse-width modulation
- 3) Sinusoidal pulse-width modulation
- 4) Optimized pulse-width modulation
- 5) Delta pulse-width modulation
- 6) Trapezoidal pulse-width modulation

##### Single-pulse-width modulation :[2]

In single-pulse-width modulation control, there is only one pulse per half-cycle and the width of the pulse is varied to control the converter output voltage. The gating signals are generated by comparing a rectangular reference signal of amplitude,  $A_r$ , with a triangular carrier wave of amplitude,  $A_c$ , as shown in Fig.-25. The frequency of the reference signal determines the fundamental frequency of output voltage. By varying  $A_r$  from 0 to  $A_c$ , the pulse width  $\delta$ , can be varied from 0 to  $180^\circ$ .

### Multiple-pulse-width modulation :[2]

In multiple-pulse-width modulation, several pulses in each half cycle of the output voltage is used to reduce the harmonic contents. The gating signals are generated by comparing a reference signal  $A_r$  with a triangular carrier wave  $A_c$  as shown in Fig.-26. The frequency of reference signal sets the output frequency,  $f_o$ , and the carrier frequency,  $f_c$ , determines the number of pulses per half-cycle. The modulation index ( $=A_r/A_c$ ) controls the output voltage.

### Sinusoidal pulse-width modulation :[2]

In sinusoidal pulse-width modulation the width of each pulse is varied in proportion to the amplitude of a sine wave evaluated at the center of the same pulse. The distortion factor and the lower-order harmonics are reduced significantly. The gating signals as shown in Fig.-27 are generated by comparing a sinusoidal reference signal with a triangular carrier wave of frequency,  $f_c$ . The frequency of reference signal,  $f_r$ , determines the converter output frequency,  $f_o$ , and its peak amplitude,  $A_r$ , controls the modulation index,  $M$ , and in turn controls the rms output voltage,  $V_o$ .

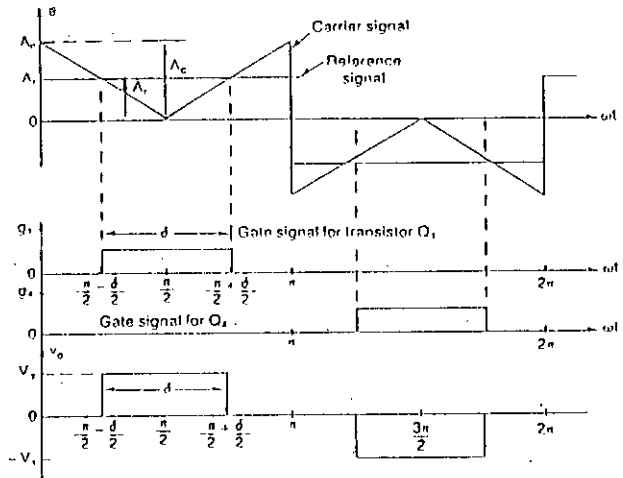


Fig.-25 : Single pulse-width modulation.

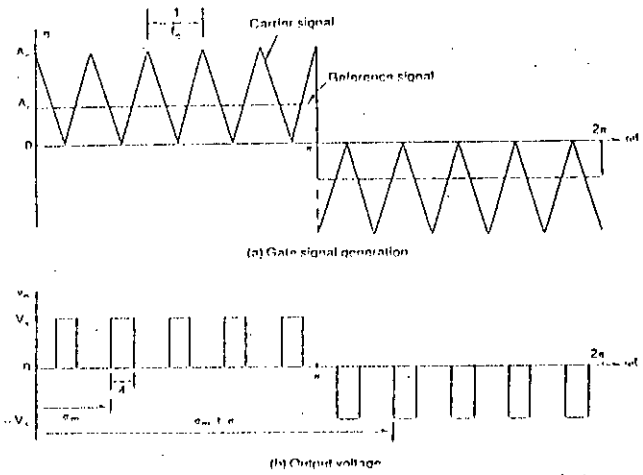


Fig.-26 : Multiple pulse-width modulation.

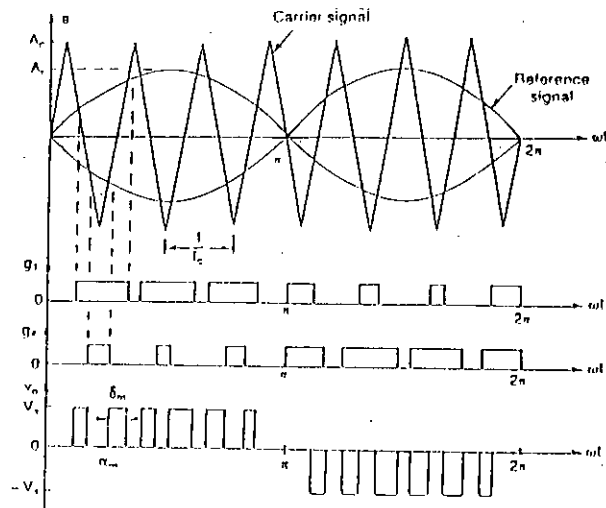


Fig.-27 : Sinusoidal pulse-width modulation.

Optimized pulse-width modulation :[3,4,5]

The pulse width modulation processes generated by OFF line computer computation and micro computer implementation can be made such that selected harmonics can be completely eliminated from the output waveforms of the converters. Such optimization can also include performance enhancement of converter application as well. In selective harmonic elimination, the Fourier series of the output waveform are expressed in terms of arbitrary switching points  $\alpha_1, \alpha_2, \alpha_3, \dots, \alpha_n$  etc. Then by setting Fourier coefficients to desired values ( $a_n =$  some value or 0,  $b_n =$  some value or 0) a set of equations are obtained which are solved simultaneously to have values of  $\alpha_1, \alpha_2, \dots, \alpha_n$  (switching points of the converter). Once the modulation pattern is generated by desired  $\alpha_1, \alpha_2, \dots, \alpha_n$ , the converter output waveform will not contain any harmonics which were set to zero during formulation of equations. Also magnitude of fundamental and other harmonics of the converter waveform can be pre-set as described. Such implementation is still done by OFF line computation of switching points and generating the gating signals of the converter by micro-computer. However, effort is also underway to realize such implementation in micro-computer ON line basis.

Delta pulse-width modulation :[2]

In delta modulation, a triangular wave is allowed to oscillate within a defined window  $\Delta V$  above and below the reference sine wave  $v_r$ . The converter switching function, which is identical to the output voltage  $v_o$  is generated from the vertices of the triangular wave  $v_c$  as shown in Fig.-29. It is also known as hysteresis modulation. If the frequency of the modulating wave is changed keeping the slope of the triangular wave constant, the number of pulse and pulses widths of the modulated wave would change. The fundamental output voltage can be upto  $1.27 V_s$  and is dependent on the peak amplitude  $A_r$  and frequency  $f_r$  of the reference voltage.

Trapezoidal pulse-width modulation :[2]

The gating signals are generated by comparing a triangular carrier wave with a modulating trapezoidal wave as shown in Fig.-30. The trapezoidal wave can be obtained from a triangular wave by limiting its magnitude to  $\pm A_r$ , which is related to the peak value  $A_{r(max)}$  by

$$A_r = \sigma A_{r(max)} \dots\dots\dots(15)$$

where,  $\sigma$  is called the triangular factor, because the waveform becomes a triangular wave when  $\sigma = 1$ .

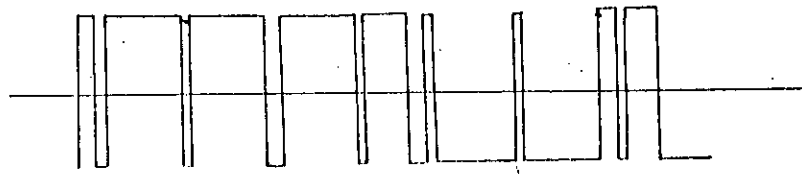


Fig.-28 : Optimized pulse-width modulation.

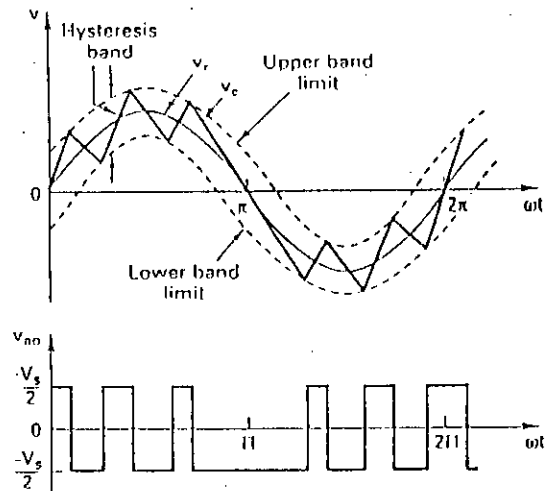


Fig.-29 : Delta pulse-width modulation.

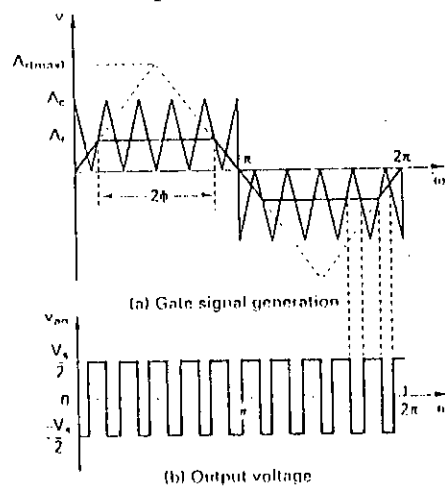


Fig.-30 : Trapezoidal pulse-width modulation.



### 1.5 DELTA MODULATION AND ITS ADVANTAGES :

Linear delta modulation was first reported in 1946 and early description emerged in 1950s [6,7]. In linear delta modulation, an encoder, is accommodated at the transmitter and receives a band limited analog signal and produces a binary output signal. The output pulses are also locally decoded back into an analog waveform by an integrator in feedback loop and subtracted from input signal to form an error which is quantized to one of the two possible levels depending on its polarity. The closed loop arrangement of the delta modulator ensures that the polarity of the pulses are adjusted by the sign of the error signal which causes the locally decoded waveform to track the input signal. Stated another way, the delta modulator produces binary pulses at its output which represent the sign difference between the input and feedback signal. The modulation is known as linear, because the decoder is a linear network. Despite the attractive simplicity of the delta modulation coders, their drawbacks had prevented their wide use initially [8]. Delta modulation remained simply an interesting field for theoretical studies in communication systems for decades. This situation began to change when refinements were suggested [9] and today the development of delta modulation is in full progress. Many communication research laboratories are engaged in exploring in depth the theory and the application of delta modulation [10-12]. The simplicity of delta modulation (DM) has inspired numerous

refinements and variations since its basic invention in 1946 by Deloraine and Derjavictch. Most of these DM systems have been motivated by application to digitization of audio and video signals. The initial DM coder consisted of signal integrator (analog) or a first order predictor (digital implementation) in its feedback path. Subsequently, DM coder with double integrator and multiple integrator or its counterpart, the predictors were used in the feedback path for more precision in digitization [13]. Some investigators replaced the integrator of the feedback loop by RC network [14] giving rise to exponential delta modulation encoders. Both signal integration or the double integration delta modulation were found suitable for coding signals of correlated waveforms. To suit the DM technique for uncorrelated signal, sigma delta modulation was introduced in 1962 [15,16]. Sigma delta modulation uses an integrator to integrate the input prior to DM coding. This preemphasizes the low frequencies in the input and increases the adjacent sample correlations. For using variable step size quantization to compete with pulse width modulation (PWM), adaptive delta modulation (ADM) was suggested by many authors [16,17]. In adaptive DM, the value of the signal at each sample time is predicted to be non-linear function of the past values of the quantized signal. The other two kinds of the delta modulation scheme encountered in literatures are companded delta

modulation scheme and the asynchronous delta modulation [18,19]. Companded DM technique uses compression of large levels as compared to the smaller ones prior to encoding, using compressor circuit. The asynchronous delta modulation systems have digital output quantized in amplitude but not in time. The rectangular wave delta modulation (RWM) is one type of asynchronous DM technique. In RWM DM, the memoryless quantizer of delta modulation scheme is replaced by nonlinear element whose characteristics are that of a hysteresis loop and the sampler is permanently closed. This form of delta modulation was first reported by Sharma and Das [20,21].

In single stage delta modulation scheme, the encoder generates information which is dependent on the polarity of the error signal, where the error signal is the difference between input signal and the reconstructed version of the input signal. The basic problem with any form of single stage DM is that the encoder generates information which is only dependent on the polarity of the error and once the input signal is modulated to pulse waveforms, the error information is lost and no minimization of signal distortion is possible. Multistage delta modulation was introduced in communication networks to overcome this problem by successive approximation of input signals with the help of several coders[22,23,24].

Rectangular wave delta modulation in its single stage and multistage forms have been reported in this thesis for the operation of a switch mode power supply. Detailed mathematical models are developed for this purpose and their theoretical and practical investigations have been done.

## 1.6 PROPOSED RESEARCH AND OBJECTIVES :

Delta modulation is the simplest technique requiring minimum hardware components. Recently its application in power electronics has been reported in switching static inverters and rectifiers. Switch mode power supplies usually use triangular wave carrier modulation of dc to obtain proper switching signals of static devices. In this thesis possible use of delta modulation in switching an SMPS has been investigated. Theoretical study has been made to find out suitable parameter variation of a delta modulator to determine an effective method of voltage regulation of an SMPS by delta modulation. Such parametric study were done by FAST FOURIER transform on modulated switching signals. Practical implementation of a delta modulated SMPS has been carried out to verify theoretical results.

## 1.7 ORGANIZATION OF THE THESIS :

This thesis consists of four chapters. Chapter-1 deals with introduction to SMPS and PWM techniques. It also incorporates various advantages and requirements of the SMPS. Objective of thesis research and discussions on expected results are also included in Chapter-1. Chapter-2 includes detailed parametric study of a delta modulator. Results of parametric study of delta modulator is necessary for proper choice of modulator parameter that can be utilized in voltage regulation of an SMPS. Chapter-3 incorporates practical implemental details of a delta modulated SMPS. Results of the modulator and SMPS performance with theoretical predictions are presented in this thesis. Chapter-4 concludes the thesis with summary, achievements and suggestion on future works.

## Chapter - 2

### **Analysis of delta modulation for an SMPS**

This chapter contains the analytical performances of delta modulator used in the SMPS. Focus is given to optimize the pwm waveform obtained by delta modulation.

#### **2.1 DELTA MODULATOR DESCRIPTION :**

The delta modulation scheme used in operating an SMPS is a single stage type. In single stage delta modulation (DM) scheme, the encoder generates information which is dependent on the polarity of the error signal  $e(t)$  (Fig.-31), where the error signal is the difference between input sine wave signal  $n(t)$  and the locally reconstructed version of the input signal  $\hat{n}(t)$ . The signal  $\hat{n}(t)$  tracks the input signal in steps of specified  $\Delta$ . Many variation of the delta modulation is possible. The block diagram of two basic types of single stage delta modulation schemes are shown in Fig.-32. One is the modulator with hard limiter, comparator and feed forward path, the other is with hysteresis quantizer, comparator and feed forward path. The expected wave forms of the two modulators

are shown in Fig.-33. In the first modulator the error signal is unbounded and as a result the expected signal may not follow the input signal in amplitude. Whereas, in the second modulator, the hysteresis quantizer is limiting the travel of expected signal within a band and thus tracking the input signal both in slope and magnitude. The second type of modulator is known as rectangular wave hysteresis delta modulator. In both the modulators sampler is absent and this results in variable pulse width rectangular modulated wave. In an actual delta modulator used in communication circuits a sampler is provided after the quantizer producing pulsed modulated wave. However, in a static converter switching the rectangular pwm waves are necessary for the switching device of the converter. Hence, for the application in static converter delta modulators' samplers are omitted. The effect of withdrawing sampler from a delta modulator is to produce rectangular pwm and the estimated wave appearing like a triangular wave superimposed on the input signal. Estimated wave in a delta modulator is also called the carrier wave.



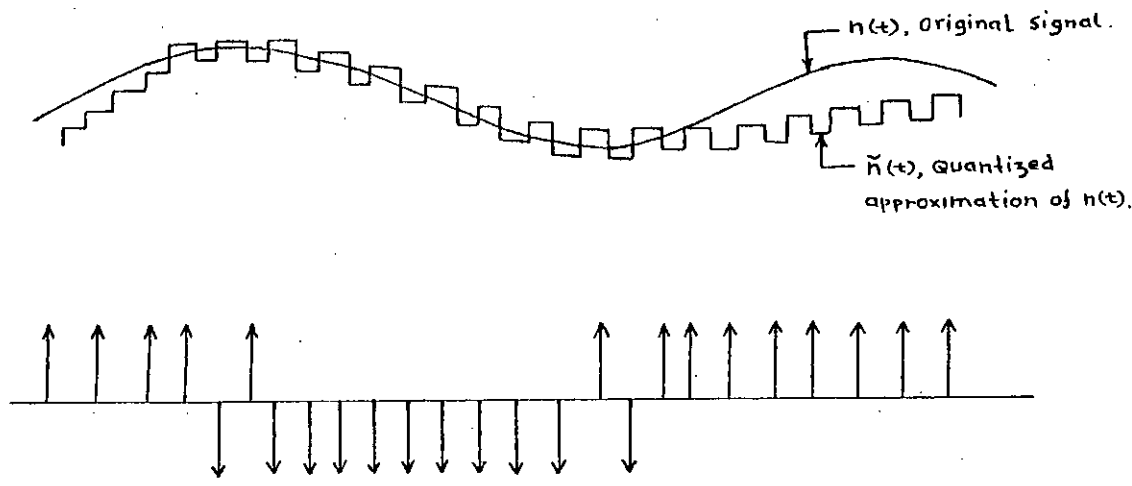
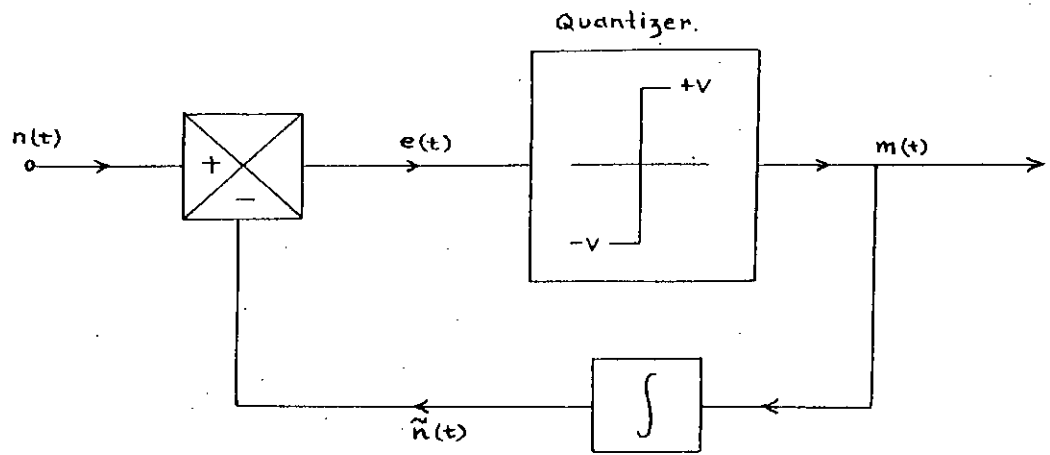
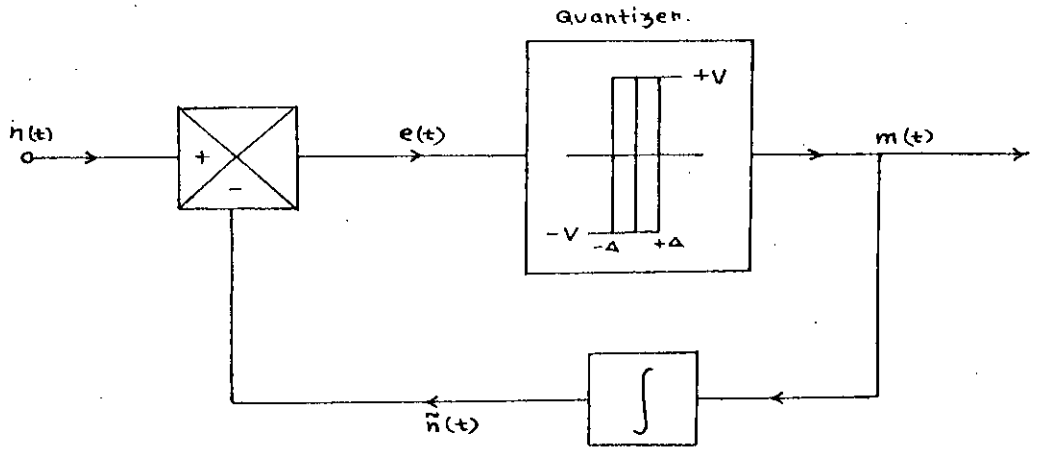


Fig.-31 : Graphical illustration of delta modulation technique.



(a) Without hysteresis



(b) With hysteresis

Fig.-32 : Block diagram of two basic DM encoder.

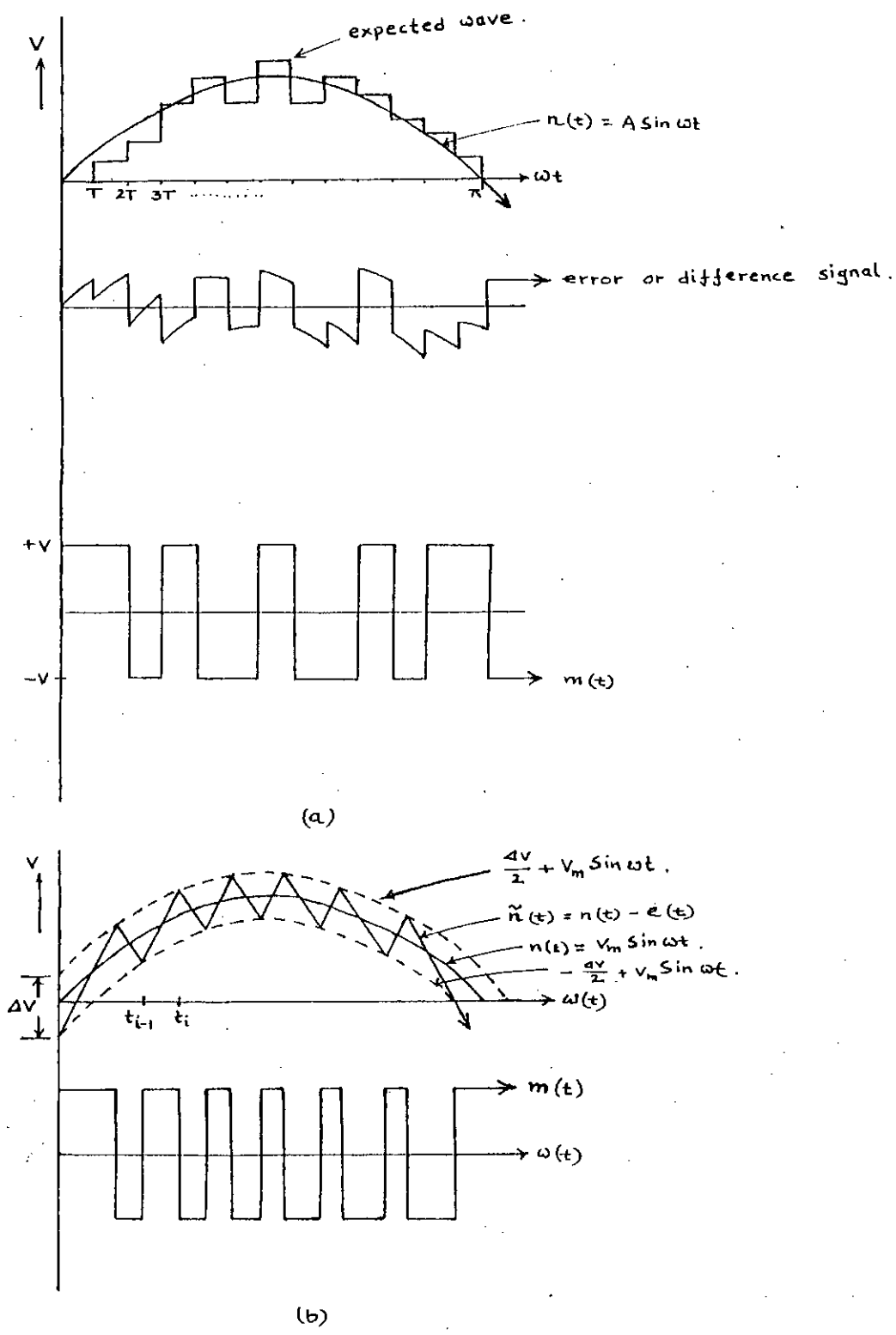


Fig.-33 : Expected waveforms of encoder of Fig.-32.

## 2.2 CHARACTERISTICS OF DELTA MODULATED WAVE :

One of the important characteristics of delta modulator when used in converter application is that the output voltage to frequency ratio of the modulator remains constant, i.e.,

$$V/f = \text{constant.}$$

Above statement can be verified by following [Fig.-34]

$$V_i/V_o = 1/j\omega RC$$

$$V_o/V_i = j\omega RC$$

$$V_o/V_{i1} = V_o/V_R = j\omega RC$$

[where,  $V_{i1}$  is the fundamental component of  $V_i$ .]

$$V_o/\omega = jV_R RC$$

$$V_o/f = j2\pi V_R RC \quad \dots\dots\dots(16)$$

Since  $\pi$ ,  $V_R$  and  $RC$  product of the modulator are all constants,

$$V_o/f = K \quad \dots\dots\dots(17)$$

Another important characteristics of the delta modulated wave is that, with increasing frequency of the input signal and constant hysteresis band, the pwm signal tends to be square wave. This is explained in Fig.-35.

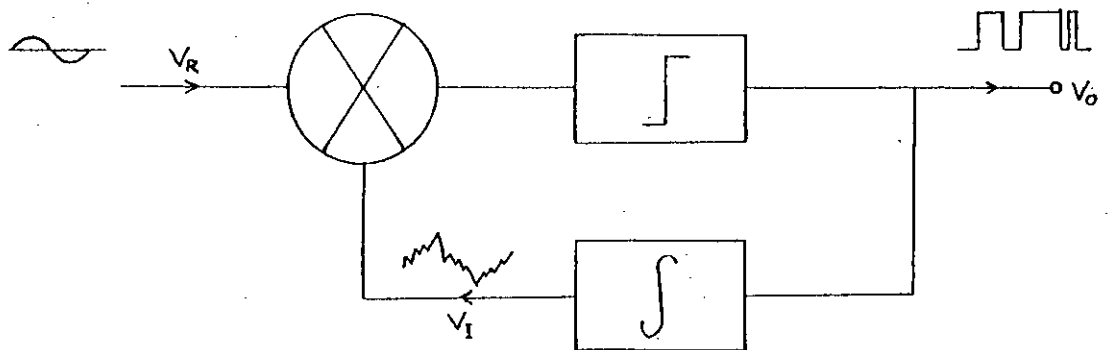


Fig.-34 : Delta modulator block diagram used to explain one of the characteristics ( $V/f = \text{constant}$ ) of modulated wave.

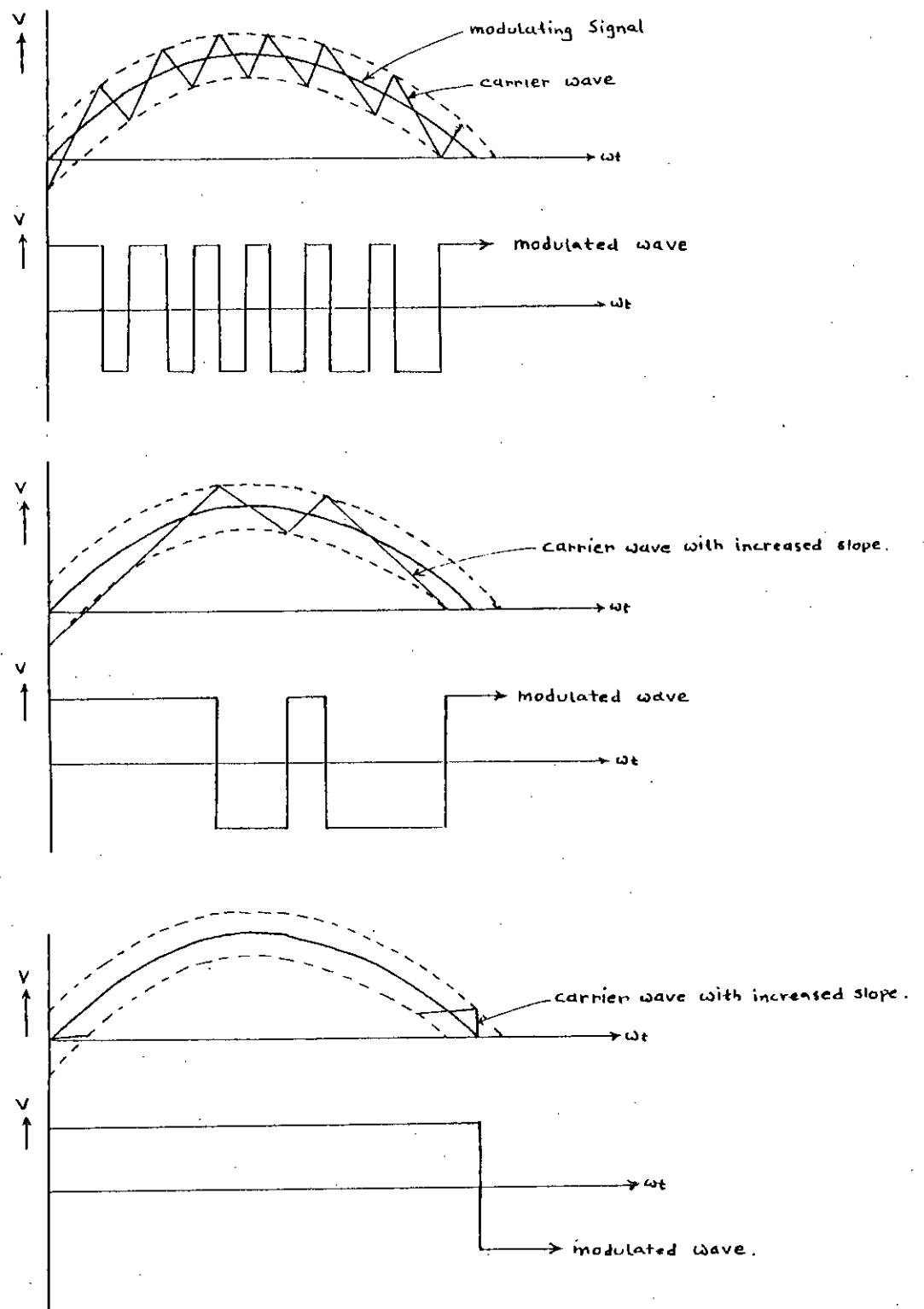


Fig.-35 : Delta modulator output wave form : PWM signal tends to square wave signal with increasing slope of the carrier signal with all other parameters remaining constant.

Third characteristic of the delta modulator is that the slope of the carrier wave and the band width  $\Delta V$  of the hysteresis band can be tuned easily to change the output modulated wave. The integrator of DM as shown in Fig.-37 can be modified as shown in Fig-38. For the normal integrator shown in Fig.-37, the slope is determined by R and C.

$$V_o = (1/j\omega RC) V_i$$

$$\therefore \text{Slope, } S = RC. \quad \dots\dots\dots(18)$$

The modified integrator shown in Fig.-38 includes a multiplier and

$$\begin{aligned} V_o &= (1/j\omega RC)V_{in}E_c \\ &= \{1/j\omega(RC/E_c)\}V_{in} \end{aligned}$$

$$\text{Hence, Slope, } S = RC/E_c. \quad \dots\dots\dots(19)$$

Where,  $E_c$  is the control voltage which also controls the frequency of the input sine wave to the modulator.

Thus slope can be varied by R, C and  $E_c$  for a multiplier integrator.  $E_c$  change the frequency of the input modulating signal. Similarly, R can be varied easily by using a voltage control resistor.

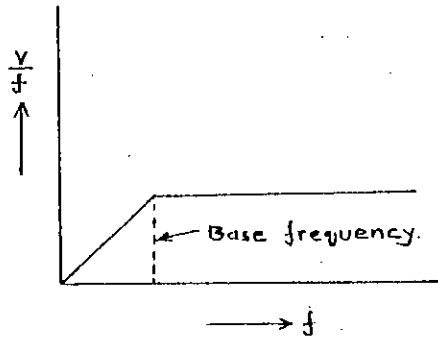


Fig.-36 : Graphical representation of  $V/f$  with respect to frequency. Frequency at  $V/f =$  constant is the base frequency.

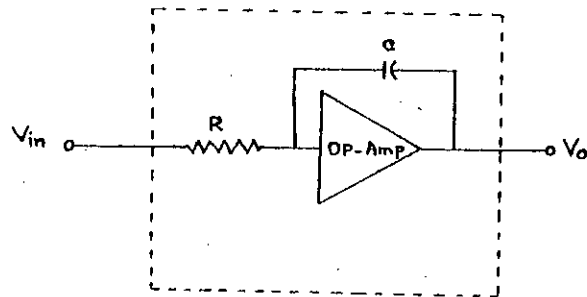


Fig.-37 : Normal integrator of a DM.

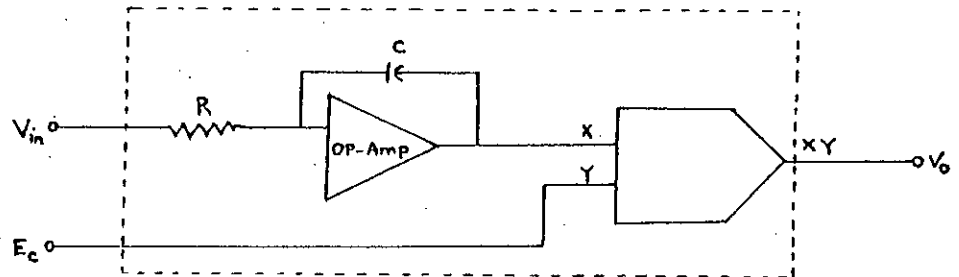


Fig.-38 : Multiplier integrator of a DM.

Tuning of delta modulator allows on-line parameter variation and provides means to change modulator wave form according to need. This type of on-line parameter variation cannot be obtained in other sine pwm modulators so easily.

### 2.3 SWITCHING POINT DETERMINATION OF DM:

Switching points of the modulator are required to determine the Fourier series of the converter output voltages. The switching points of a rectangular wave hysteresis delta modulator can be determined as follows :

Case I : Modulator with hard limiter in the feed forward path

For the wave forms of Fig.-33(a), the switching points of the modulated wave can be found from the following expressions :

$$b(t) = \text{sign} [n(t) - \bar{n}(t-T)] \quad \dots\dots\dots(20)$$

$$\bar{n}(t) = \bar{n}(t-T) + \Delta b(t) \quad \dots\dots\dots(21)$$

$$e(t) = n(t) - \bar{n}(t) \quad \dots\dots\dots(22)$$

$$m(t) = V \text{ sign} [e(t)] \quad \dots\dots\dots(23)$$

at every switching instant  $e(t) = 0$ .



Where,  $n(t)$  = input sin wave signal

$\bar{n}(t)$  = estimated signal, reconstructed by  
the filter from the modulated wave  
at the encoder

$\Delta$  = step size in the vertical direction

$T$  = step size in the horizontal  
direction

$b(t)$  = +ve or -ve sign of the difference of  
actual input to the estimated input  
of the previous step and

$m(t)$  = the equation of the modulated wave.

Solving the equations 20 to 23, the switching points  $t_i$ 's can  
be determined for the modulator of case I.

Case II : Rectangular Pulse modulator - hard limiter with  
hysteresis band

For rising slope, (Fig.-33(b))

$$S = [\Delta V/2 + V_m \sin \omega t_i - (-\Delta V/2 + V_m \sin \omega t_{i-1})]/[\omega(t_i - t_{i-1})]$$
$$\Rightarrow S\omega(t_i - t_{i-1}) = \Delta V + V_m (\sin \omega t_i - V_m \sin \omega t_{i-1})$$
$$\Rightarrow (t_i - t_{i-1}) = [\Delta V + V_m (\sin \omega t_i - V_m \sin \omega t_{i-1})]/S\omega$$
$$\Rightarrow t_i = t_{i-1} + [\Delta V + V_m (\sin \omega t_i - V_m \sin \omega t_{i-1})]/S\omega$$

For falling slope,

$$\begin{aligned}
 S &= [\Delta V/2 + V_m \sin \omega t_{i-1} - (-\Delta V/2 + V_m \sin \omega t_i)] / [\omega(t_i - t_{i-1})] \\
 \Rightarrow S\omega(t_i - t_{i-1}) &= \Delta V - V_m (\sin \omega t_i - V_m \sin \omega t_{i-1}) \\
 \Rightarrow (t_i - t_{i-1}) &= [\Delta V - V_m (\sin \omega t_i - V_m \sin \omega t_{i-1})] / S\omega \\
 \Rightarrow t_i &= t_{i-1} + [\Delta V - V_m (\sin \omega t_i - V_m \sin \omega t_{i-1})] / S\omega
 \end{aligned}$$

In general,

$$t_i = t_{i-1} + [\Delta V + (-1)^{i+1} V_m (\sin \omega t_i - V_m \sin \omega t_{i-1})] / S\omega \quad \dots\dots\dots(24)$$

Solving equation 24, switching points  $t_i$ s can be determined for a sine wave input.

Once the switching points  $t_i$ s of the modulated wave are known, the switching waveforms before filtering can be expressed in general as,

$$\begin{aligned}
 m(t) &= ga(t, t_1, t_2) - ga(t, t_2, t_3) + ga(t, t_3, t_4) - \\
 &\quad ga(t, t_4, t_5) + \dots\dots\dots \\
 &= \Sigma (-1)^{i+1} ga(t, t_i, t_{i+1}) \quad \dots\dots\dots(25)
 \end{aligned}$$

Thus, for the SMPS,

$$V_o = \frac{V_{dc}}{T} \Sigma (-1)^{i+1} ga(t, t_i, t_{i+1}) + \frac{V_{dc}}{T} \Sigma ga(t, t_i + T/2, t_{i+1} + T/2) \quad \dots\dots\dots(26)$$

The Fourier components of the waveforms of the above equations are obtained by the FAST FOURIER transform of  $V_c$ , using commercially available software MATLAB (Appendix)

$$\text{fft}(V_0) = \text{Fourier Series.}$$

The parametric variation causes modulated wave to exhibit various features which are studied by FFT on simulated modulated SMPS output voltages. Following sections elaborate the results of these parametric variation studies.

## 2.4 CHANGE OF MODULATOR PARAMETERS:

### 2.4.1 CHANGE OF MODULATOR PARAMETER TO FIND EFFECT ON MODULATED SMPS WAVE :

To find effective method of voltage regulation by DM technique, the following parameters of DM were varied,

1. Frequency of the input sine wave,  $f$
2. Window width of the hysteresis band,  $\Delta V$
3. Slope of the carrier wave,  $S$  and . .
4. Amplitude of the input sine wave,  $V_m$ .

These parameters vary the harmonics of the output voltage. Salient observations made from these studies are,

#### Case I. Frequency variation :

Fig.-39, 40, 41 and 42 describes the harmonic characteristics for varying  $f$  from 1000 Hz. to 4000 Hz. (keeping  $\Delta V$ ,  $S$  and  $V_m$  constant.) Output voltage [refer to Fig.-39(d), 40(d), 41(d), 42(d)] increases with the increasing frequency [refer to Fig.-39(a), 40(a), 41(a), 42(a)] upto  $f = 4000$  Hz. Beyond this frequency, output voltage remain constant. This result is as expected and described previously.

Case II. width variation :

Fig.-43, 44, 45, 46, 47 and 48 describes harmonic characteristics for varying  $\Delta V$  from 1.5V to 6V, with all other parameters constant. It is seen that, output voltage increases with increasing  $\Delta V$  and at  $\Delta V = 6V$ , output voltage is constant.

Case III. Slope variation :

Fig.-49, 50, 51, 52 and 53 describes the effect of varying slope of the carrier wave of the DM. Slope varies from 150,000 V/Sec. to 500,000 V/Sec. and it is observed that the output voltage decreases with increasing slope with all other parameters constant.

Case IV. Amplitude variation :

The effect of variation of the amplitude of the sine wave is described in Fig.-54, 55, 56, 57 and 58. It is seen that the average output voltage increases with increasing the amplitude with all other parameters constant. Amplitude is varied here from 5V to 8.5V and it is seen that at 8.5V, output voltage is constant.

#### 2.4.2 DISCUSSION :

From the above results it can be inferred that the output voltage variation is possible by varying any of the parameters. In an SMPS, the input sine wave of the DM is generated from a Voltage Control Oscillator (VCO). The input voltage of the VCO is the difference between the feedback voltage from the load and a reference voltage. When the feedback voltage from the load increases, the frequency of the output of the VCO (i.e, input sine wave of the DM) decreases which again decreases the output voltage of the DM (case.I) and hence the average load voltage. Similarly, as the load voltage of the SMPS decreases, the feedback voltage decreases, frequency of the input sine wave of the DM increases and hence output voltage of DM increases (case.I) which again increases the load voltage. Thus it is possible to maintain a constant load voltage.

96828

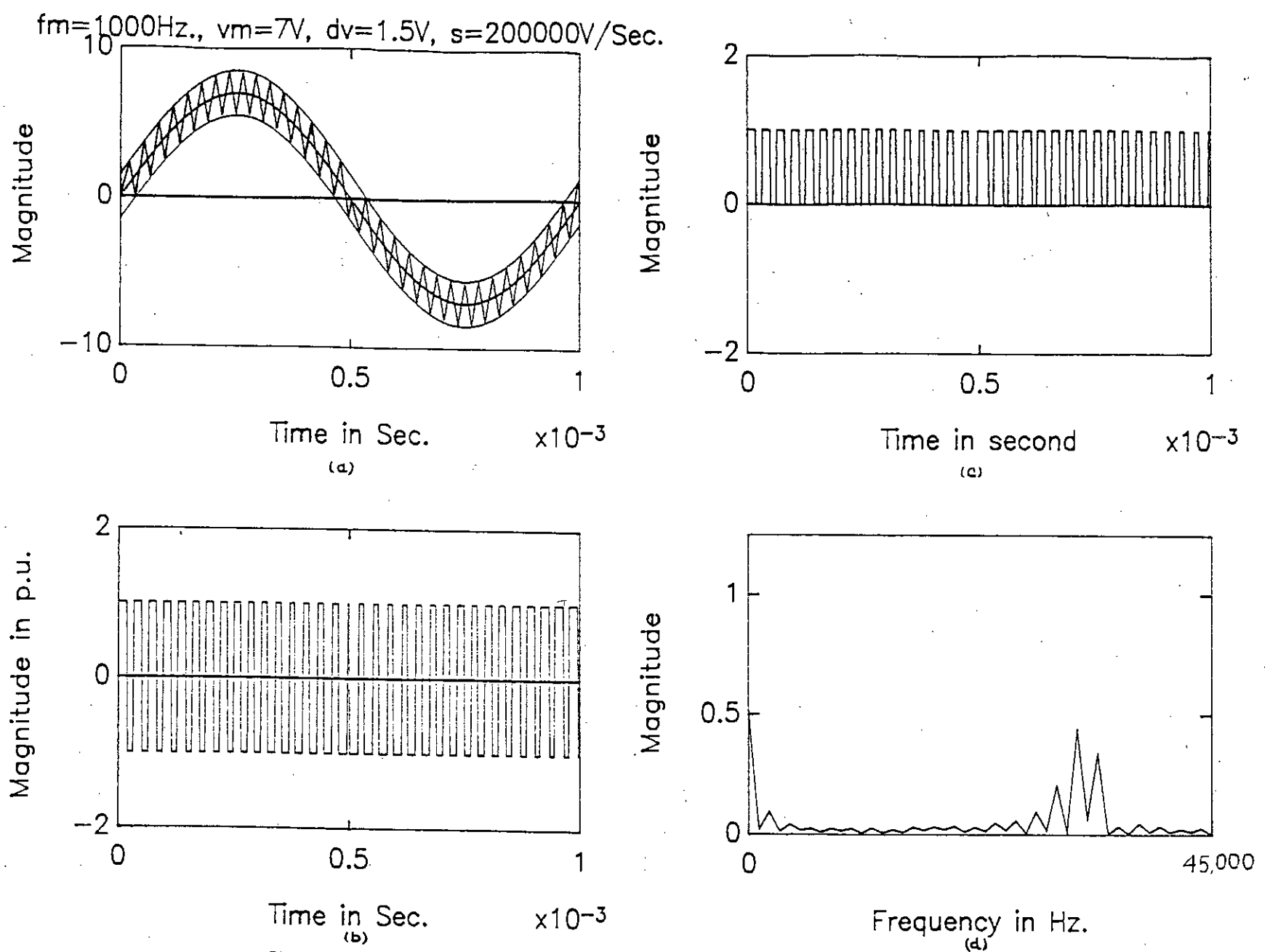


Fig.-39 : Simulated waveform of delta modulator and SMPS voltage waveform (a) modulator waveforms (b) modulated output of modulator (c) SMPS output (d) spectrum of SMPS output.  $f_m = 1,000 \text{ Hz.}, V_m = 7 \text{ V}, \Delta V = 1.5 \text{ V}, S = 200,000 \text{ V/Sec.}$

$f_m=2000\text{Hz.}, v_m=7\text{V}, dv=1.5\text{V}, s=200000\text{V/Sec.}$

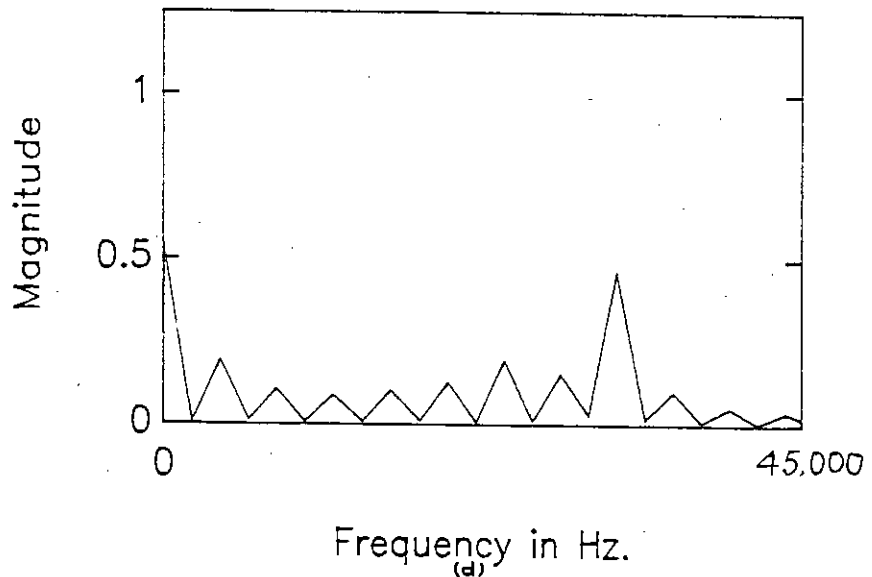
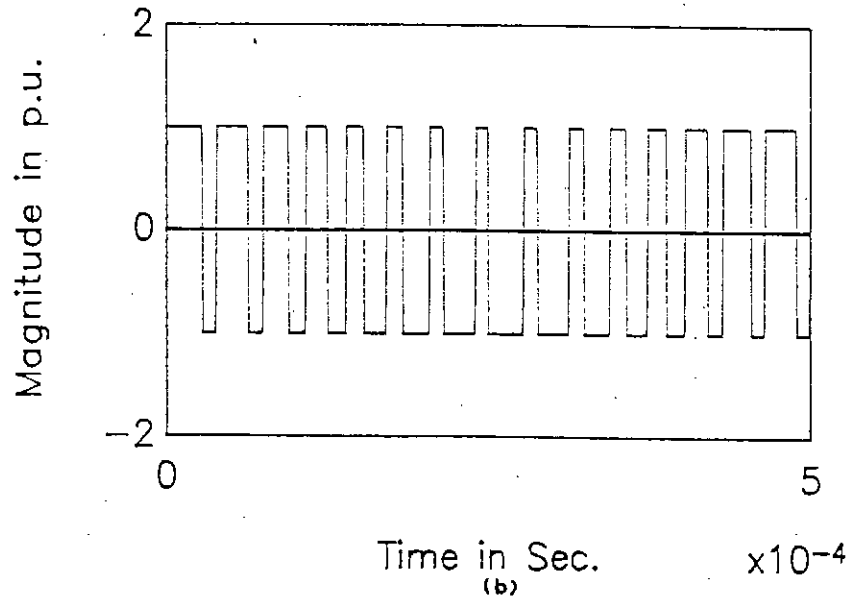
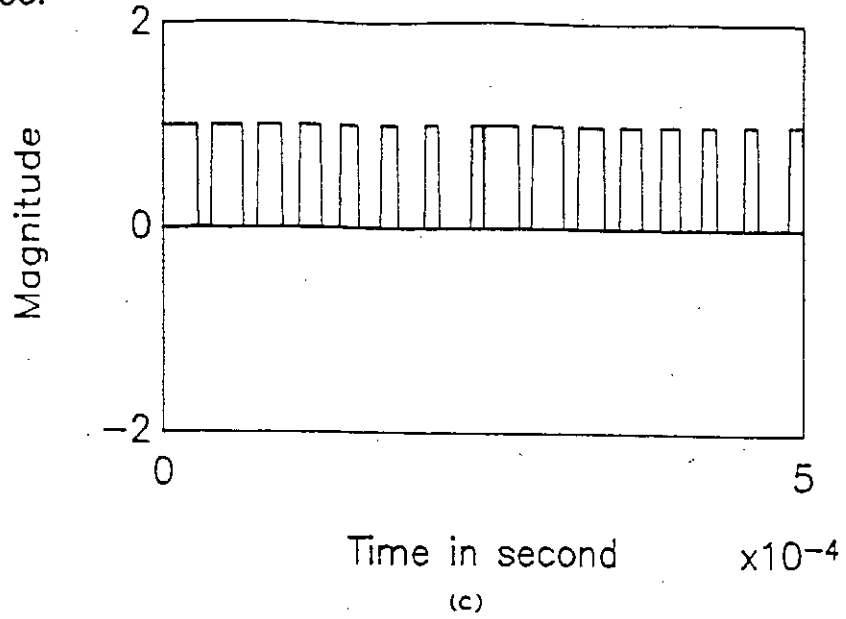
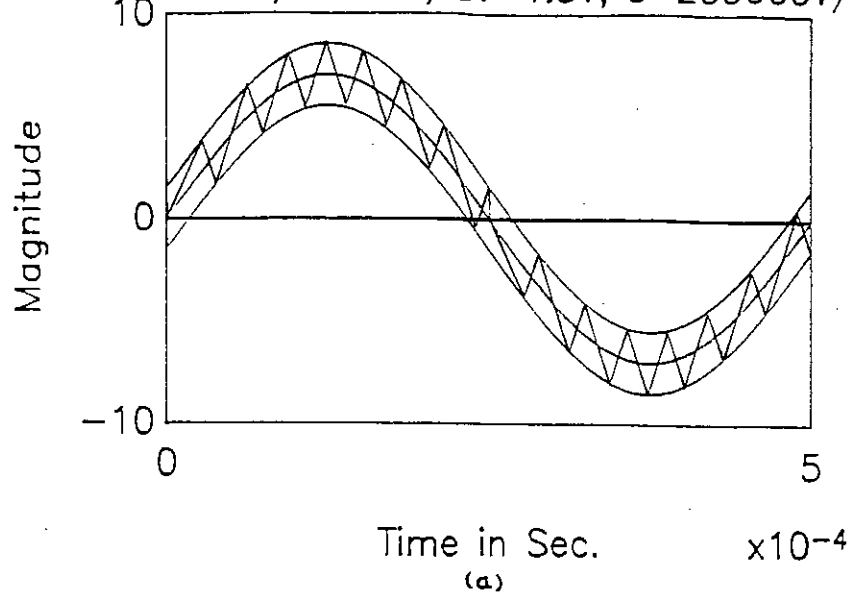


Fig.-40 : Simulated waveform of delta modulator and SMPS voltage waveform (a) modulator waveforms (b) modulated output of modulator (c) SMPS output (d) spectrum of SMPS output.  $f_m=2,000\text{ Hz.}, V_m=7\text{V}, AV=1.5\text{V}, S=200,000\text{V/Sec.}$



$f_m=3000\text{Hz.}, v_m=7\text{V}, dv=1.5\text{V}, s=200000\text{V/Sec.}$

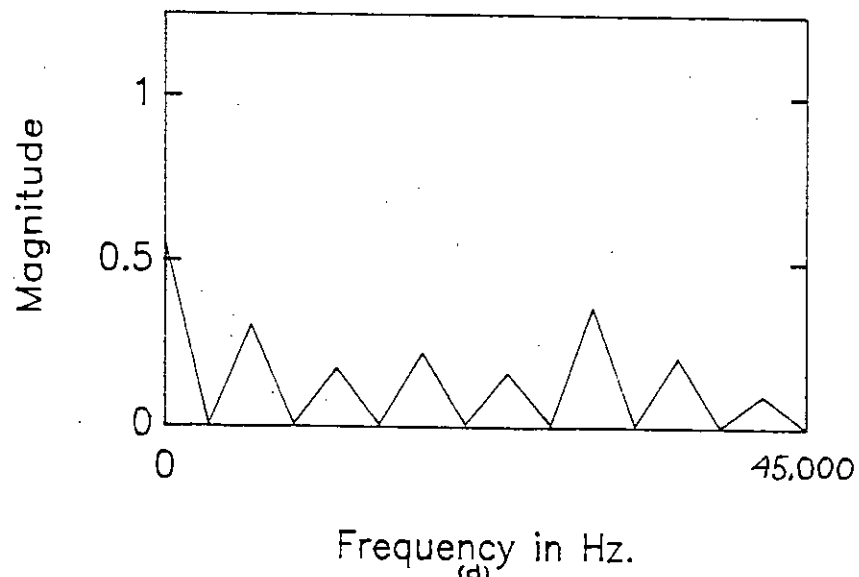
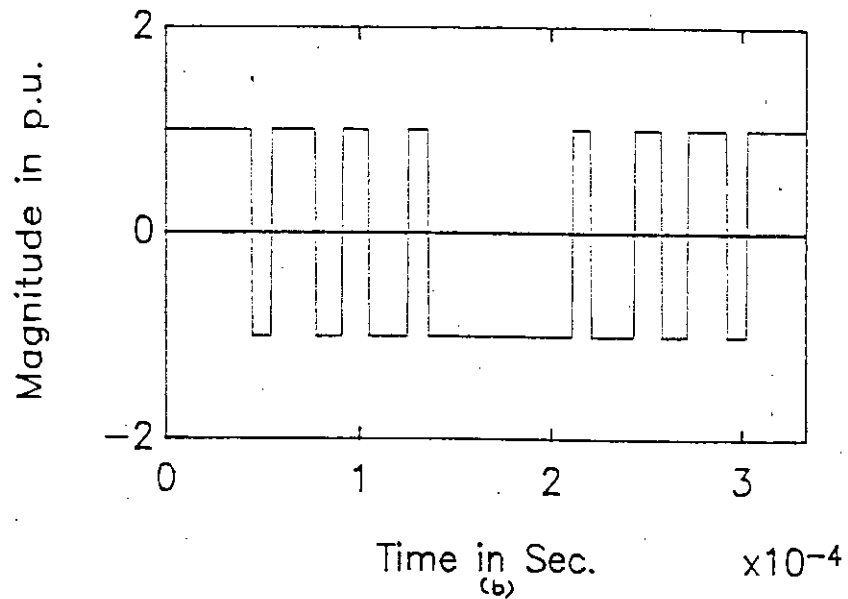
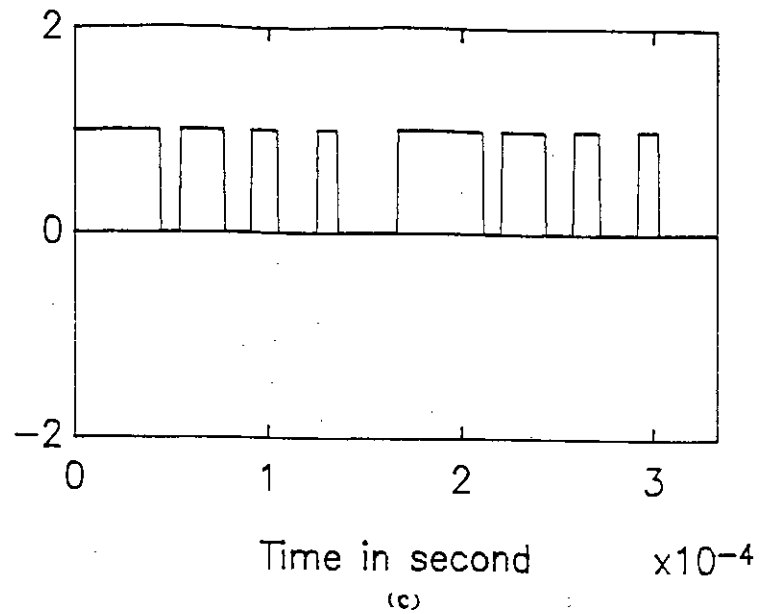
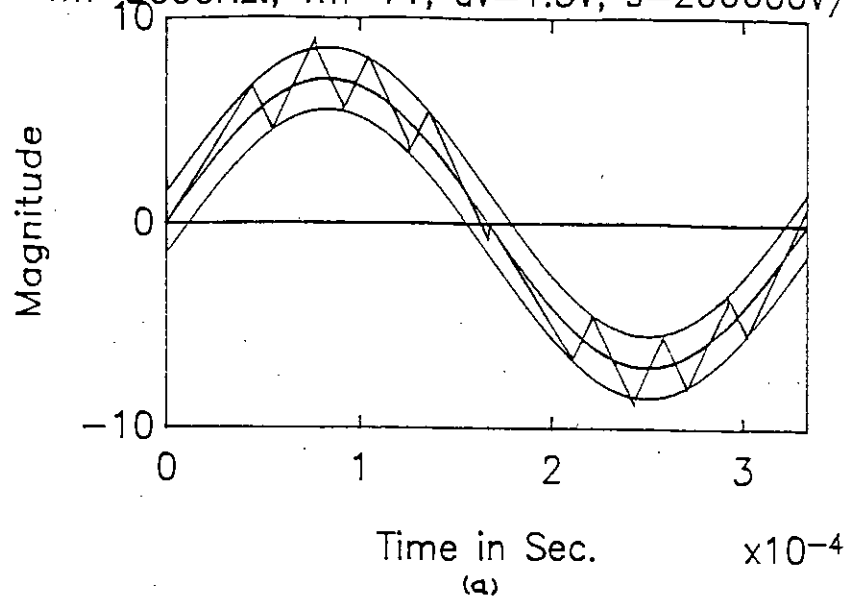


Fig.-41 : Simulated waveform of delta modulator and SMPS voltage waveforms (a) modulator waveforms (b) modulated output of modulator (c) SMPS output (d) spectrum of SMPS output.  $f_m=3,000\text{ Hz.}, V_m=7\text{V}, \Delta V=1.5\text{V}, S=200,000\text{V/Sec.}$

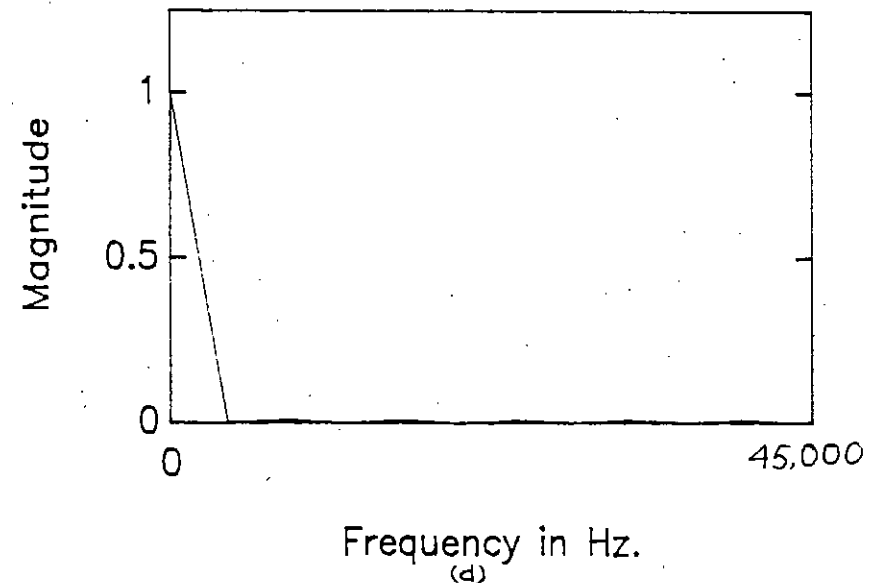
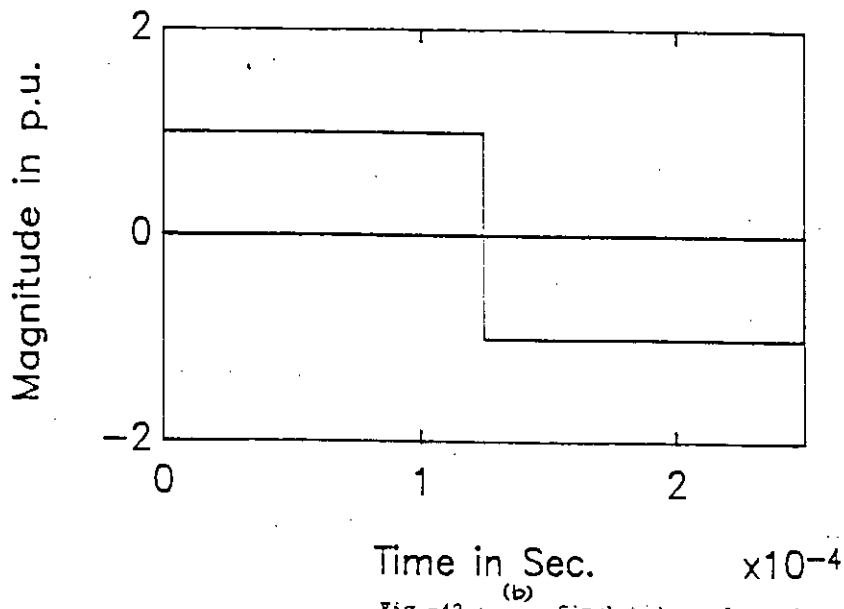
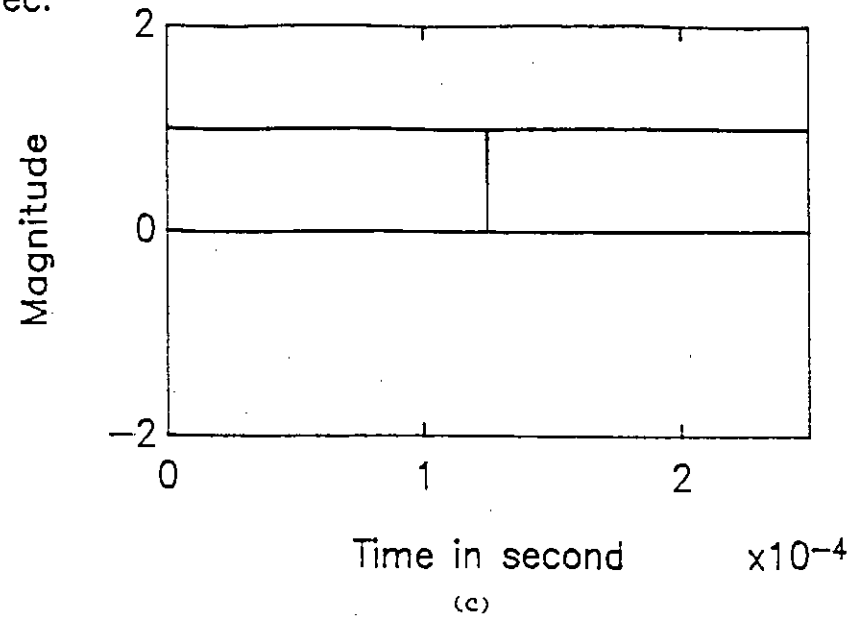
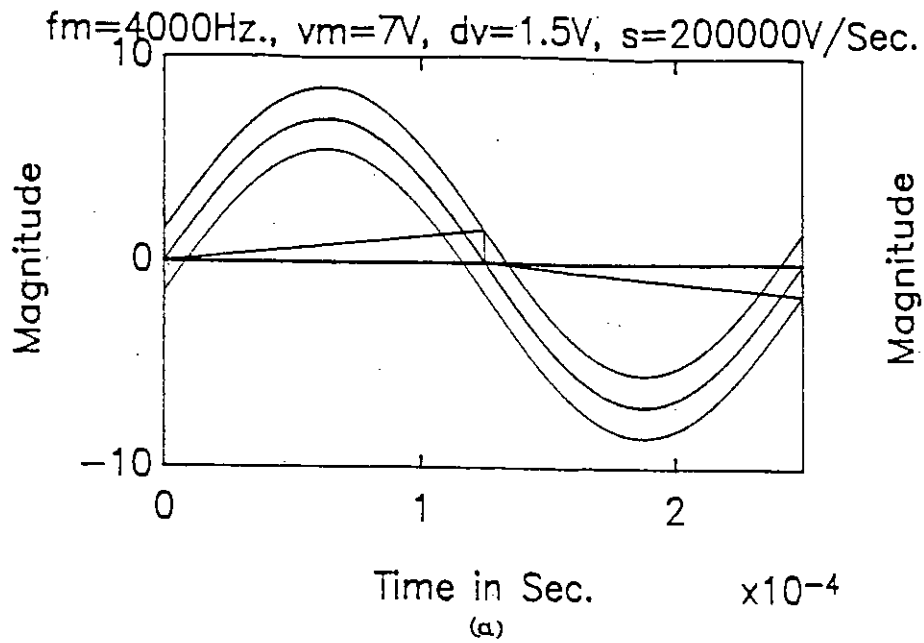


Fig.-42 : (a) Simulated waveform of delta modulator and SMPS voltage waveform (a) modulator waveforms (b) modulated output of modulator (c) SMPS output (d) spectrum of SMPS output.  $f_m=4,000\text{ Hz.}, V_m=7\text{V}, \Delta V=1.5\text{V}, S=200,000\text{V/Sec.}$

$f_m=3000\text{Hz.}, v_m=7\text{V}, dv=1.5\text{V}, s=200000\text{V/Sec.}$

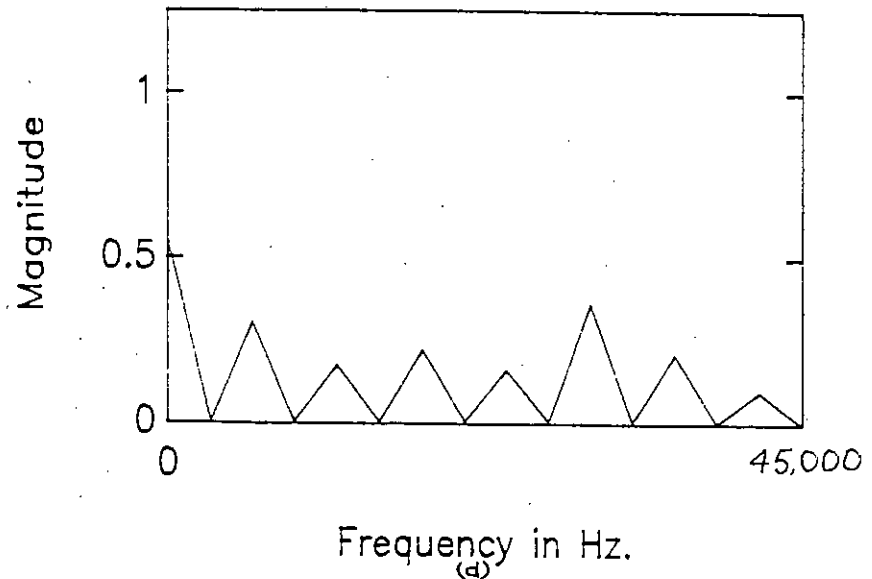
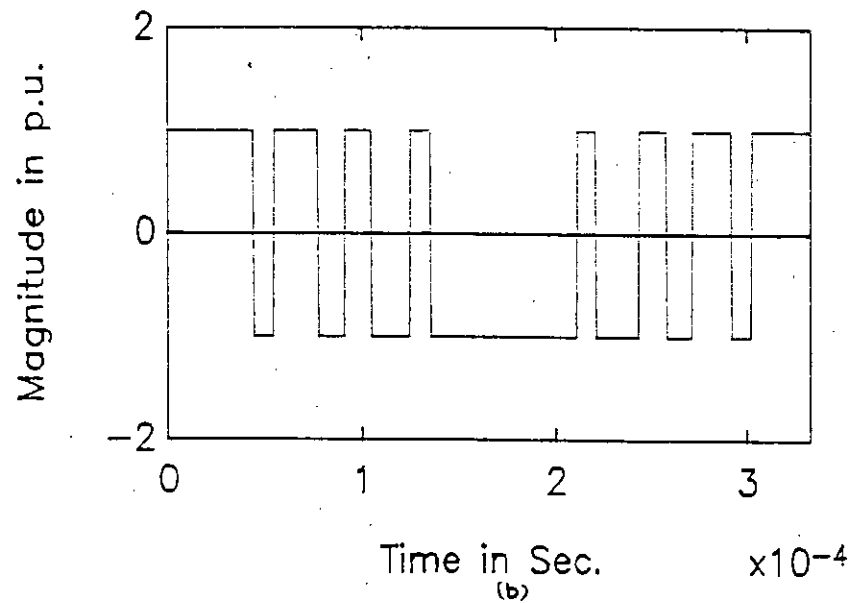
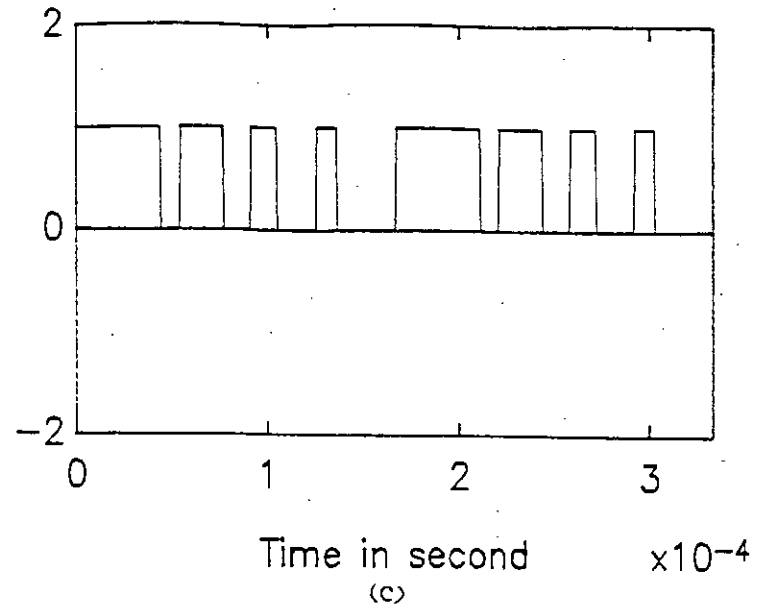
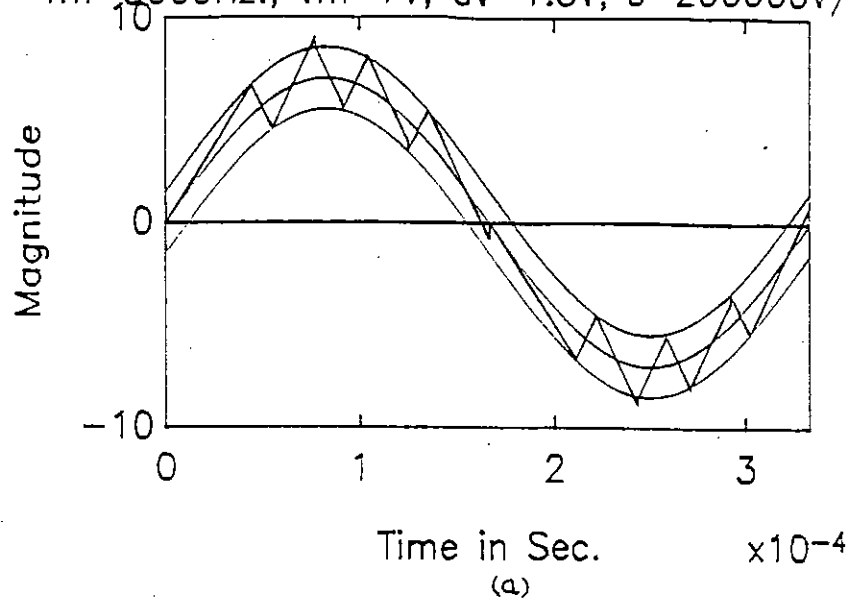


Fig.-43 : (a) Simulated waveform of delta modulator and SHPS voltage waveform (a) modulator waveforms (b) modulated output of modulator (c) SHPS output (d) spectrum of SHPS output.  $f_m=3,000\text{ Hz.}, V_m=7\text{V}, AV=1.5\text{V}, S=200,000\text{V/Sec.}$

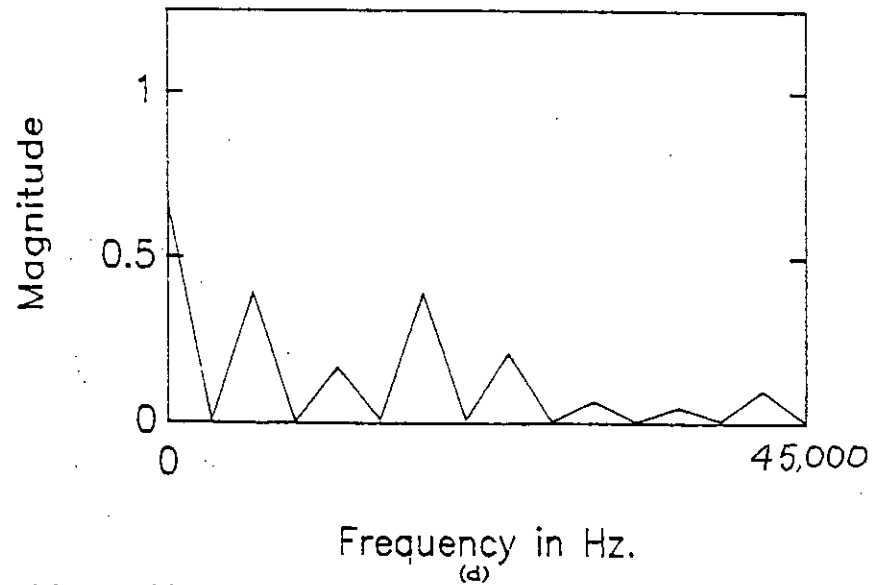
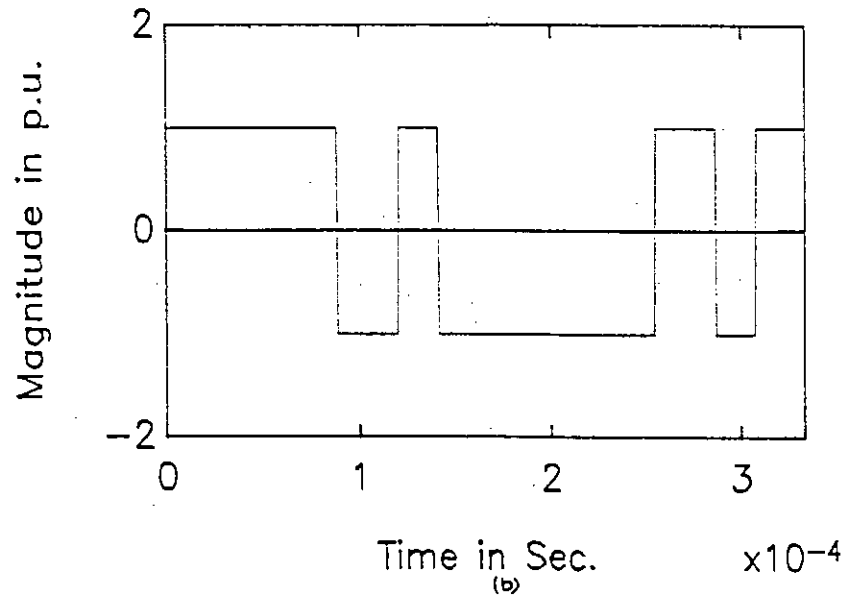
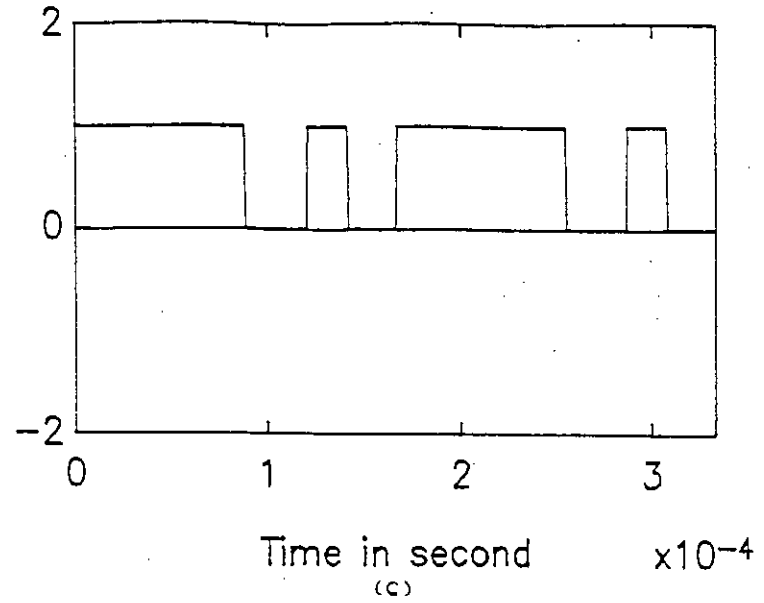
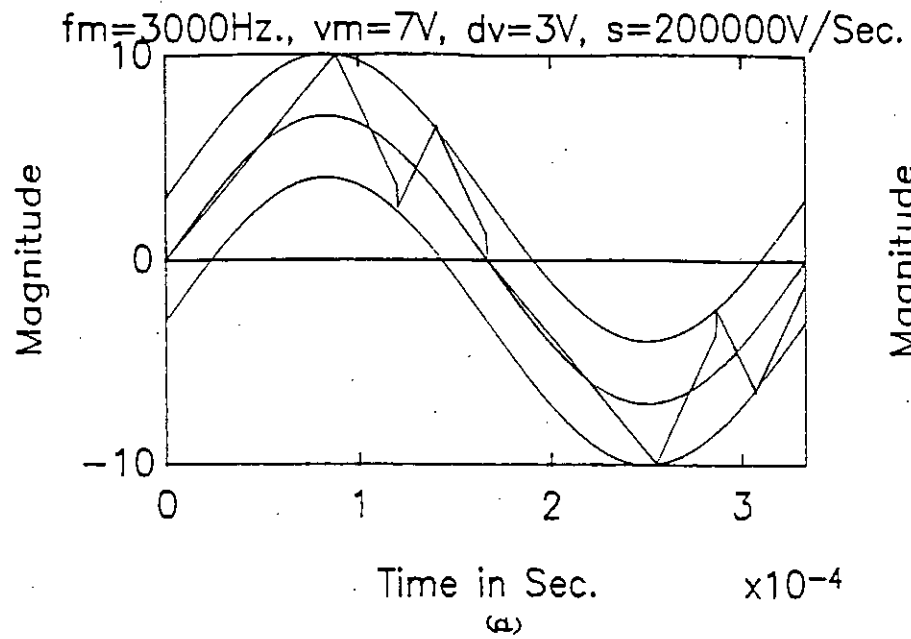


Fig.-44 : Simulated waveform of delta modulator and SMPS voltage waveform (a) modulator waveforms (b) modulated output of modulator (c) SMPS output (d) spectrum of SMPS output.  $f_m=3,000\text{ Hz.}, V_m=7\text{V}, \Delta V=3\text{V}, S=200,000\text{V/Sec.}$

$f_m=3000\text{Hz.}, v_m=7\text{V}, dv=4\text{V}, s=200000\text{V/Sec.}$

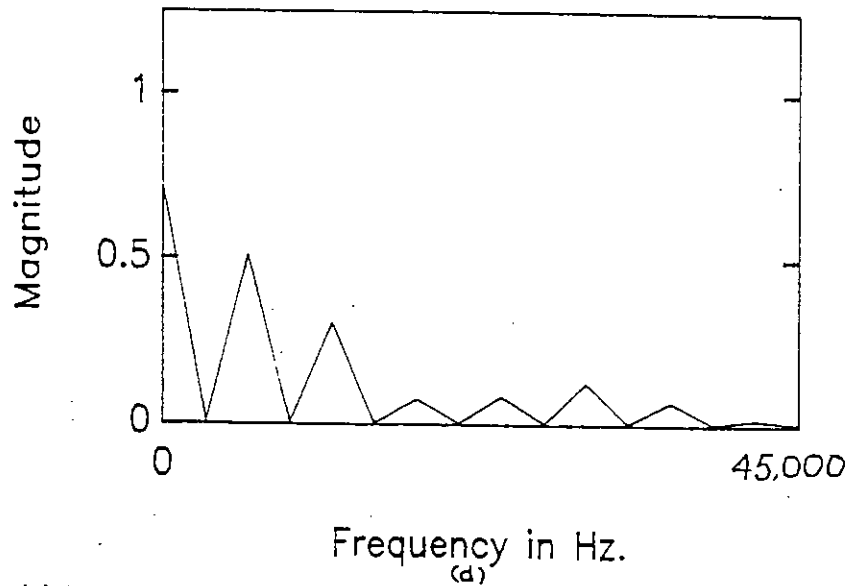
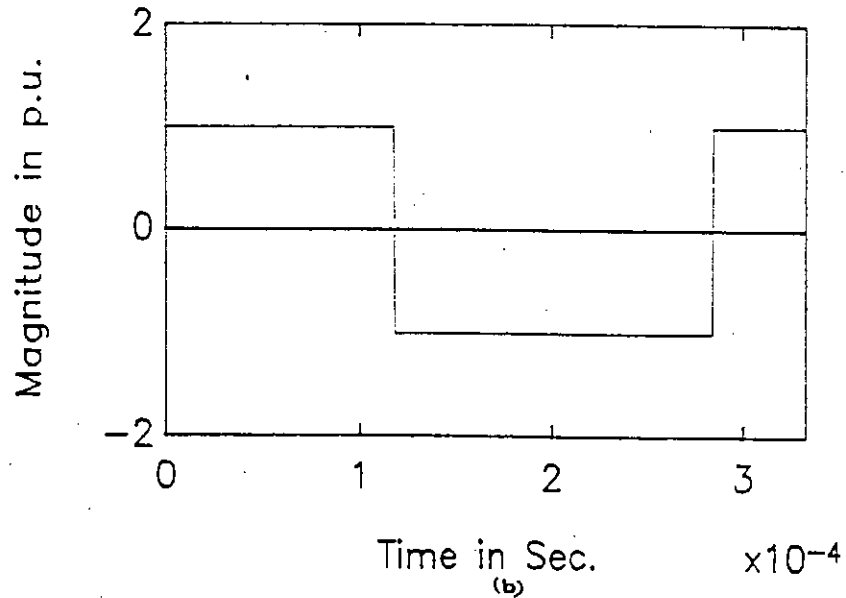
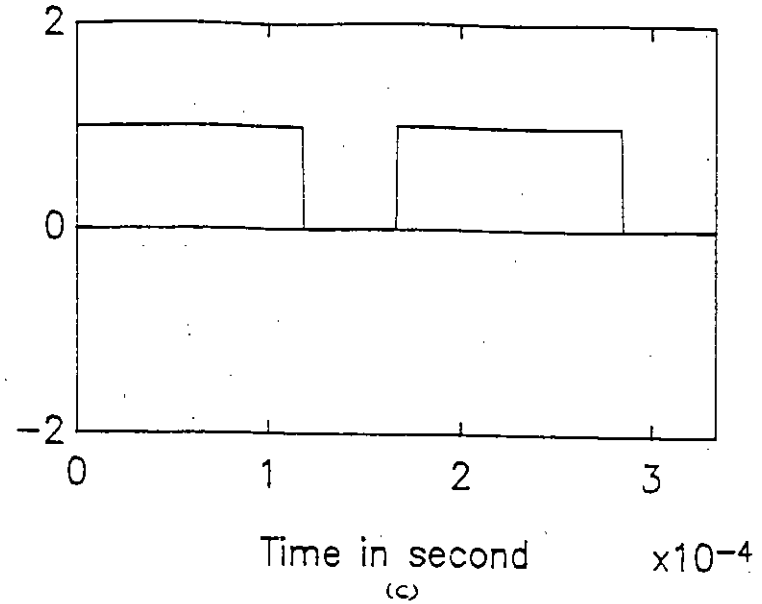
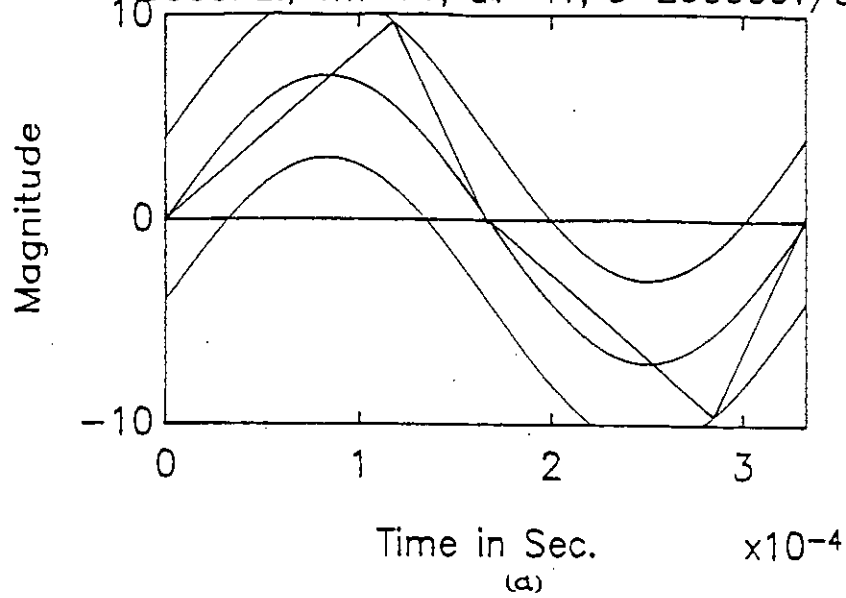


Fig.-45 : Simulated waveform of delta modulator, and SMPS voltage waveform (a) modulator waveforms (b) modulated output of modulator (c) SMPS output (d) spectrum of SMPS output.  $f_m=3,000\text{ Hz.}, V_m=7\text{V}, \Delta V=4\text{V}, S=200,000\text{V/Sec.}$

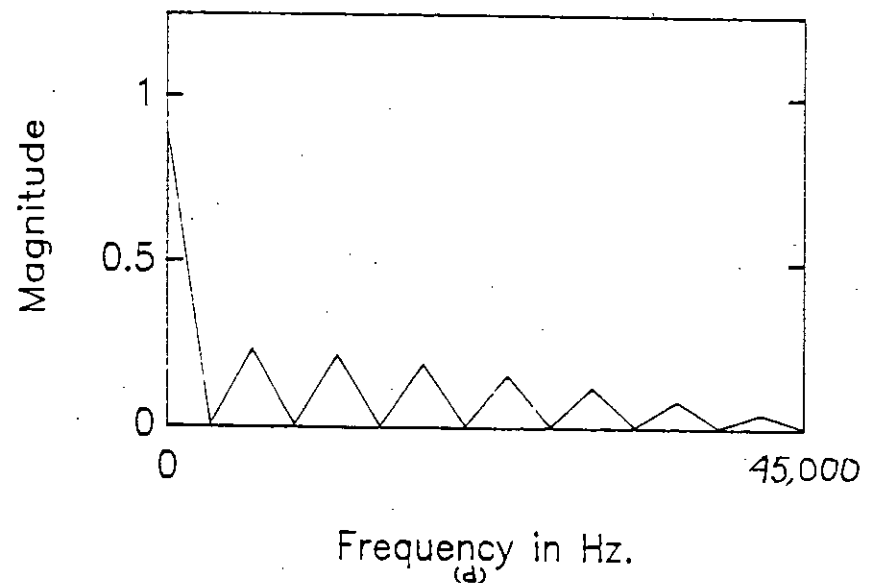
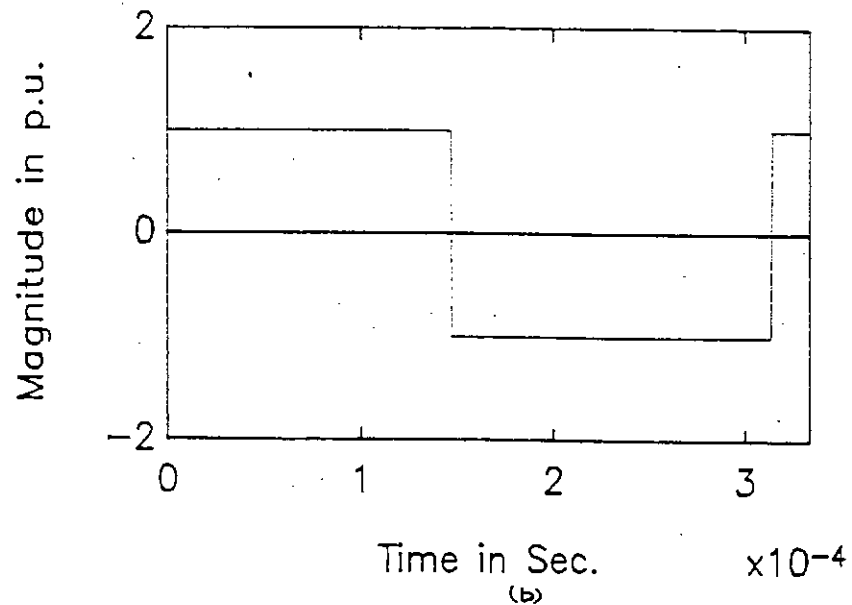
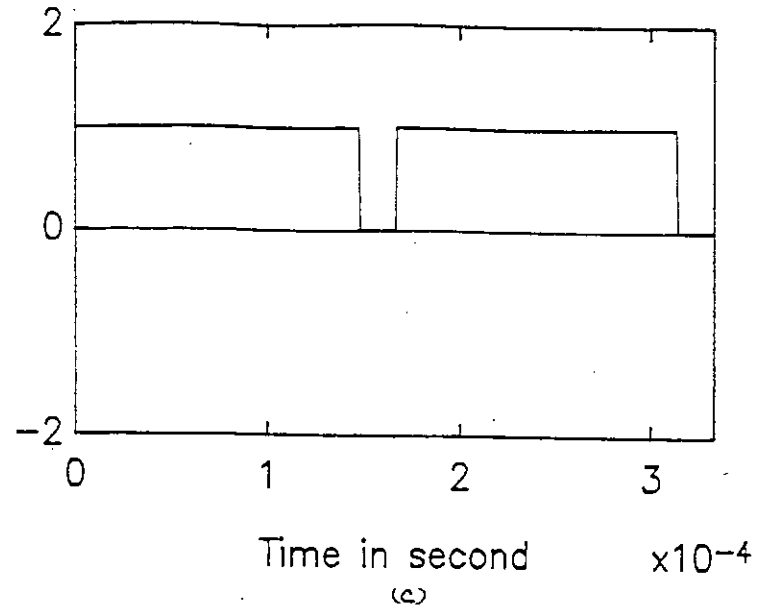
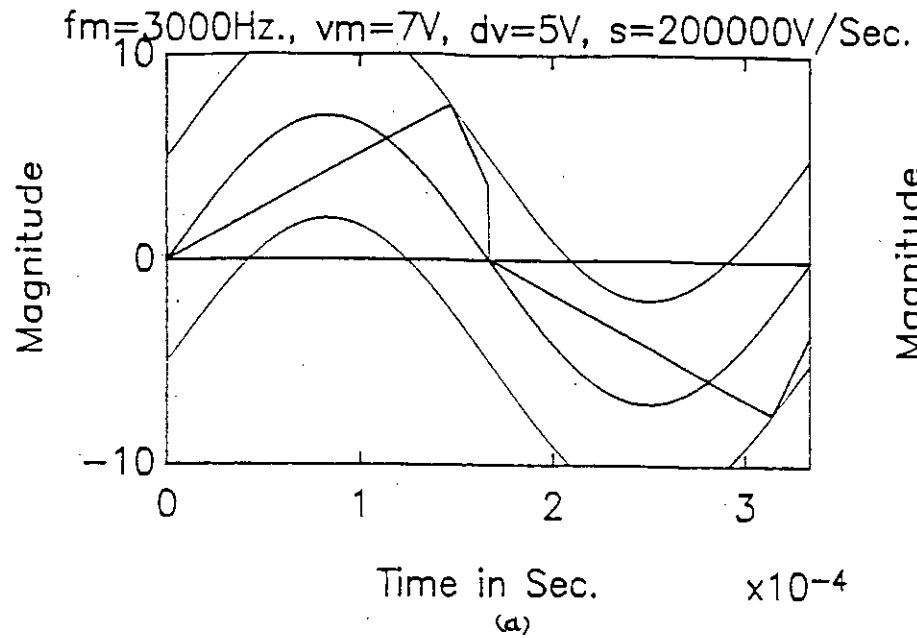
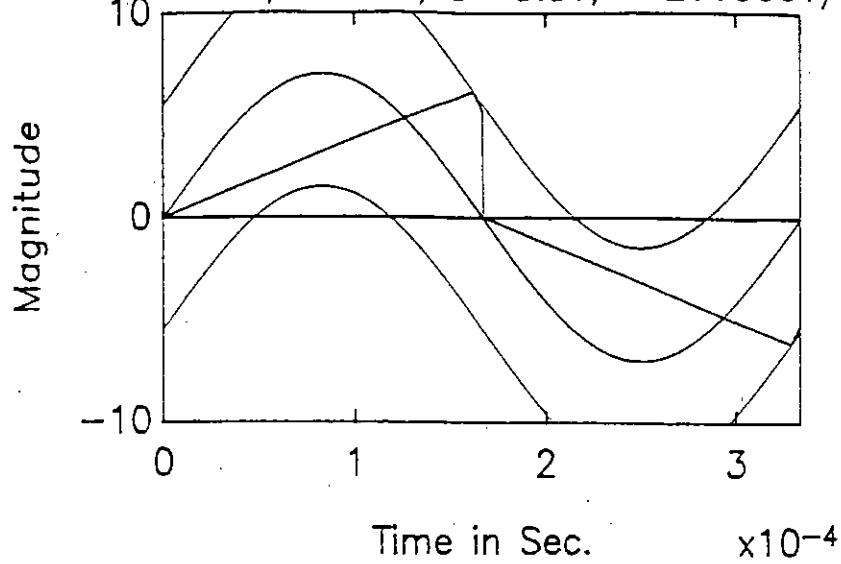
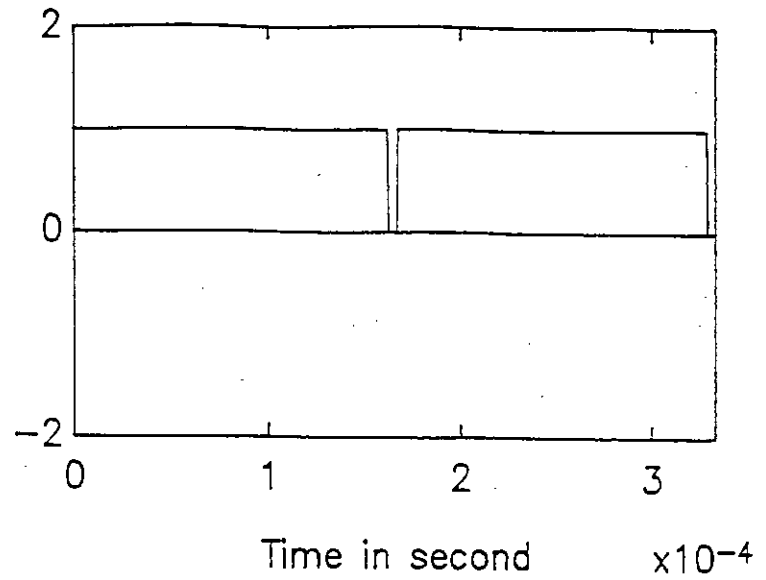


Fig.-46 : Simulated waveform of delta modulator and SMPS voltage waveform (a) modulator waveforms (b) modulated output of modulator (c) SMPS output (d) spectrum of SMPS output.  $f_m=3,000\text{ Hz.}, V_m=7\text{V}, \Delta V=5\text{V}, S=200,000\text{V/Sec.}$

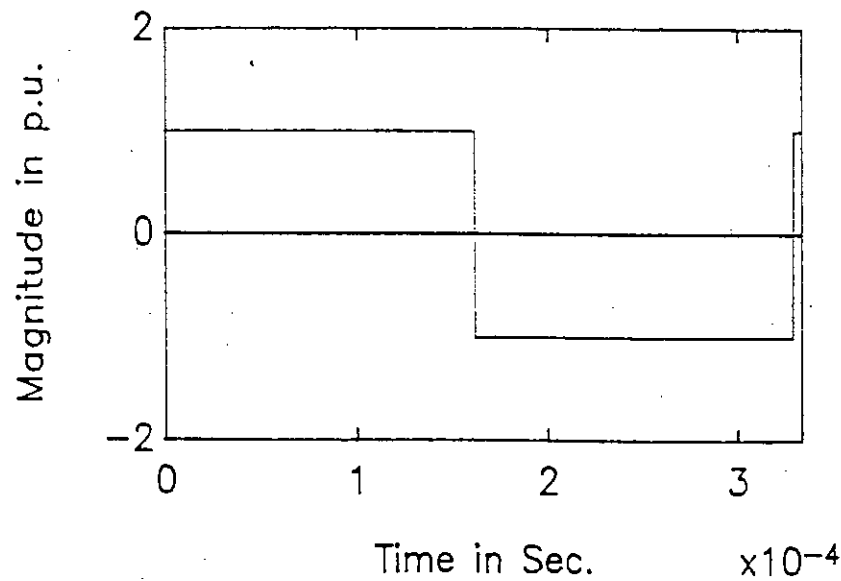
$f_m=3000\text{Hz.}, v_m=7\text{V}, dv=5.5\text{V}, s=200000\text{V/Sec.}$



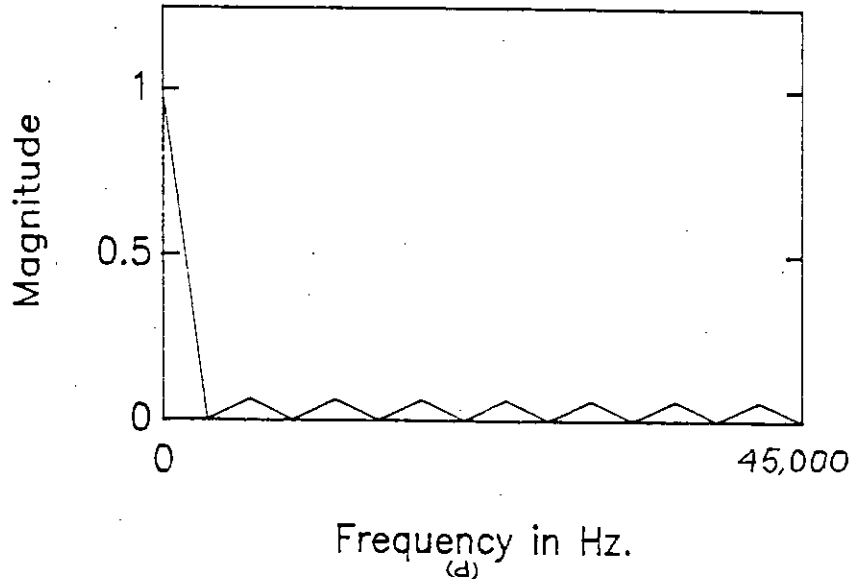
(a)



(c)



(b)



(d)

Fig.-47 : Simulated waveform of delta modulator and SMPS voltage waveform (a) modulator waveforms (b) modulated output of modulator (c) SMPS output (d) spectrum of SMPS output.  $f_m=3,000\text{ Hz.}, V_m=7\text{V}, \Delta V=5.5\text{V}, S=200,000\text{V/Sec.}$

$f_m=3000\text{Hz.}, v_m=7\text{V}, \Delta v=6\text{V}, s=200000\text{V/Sec.}$

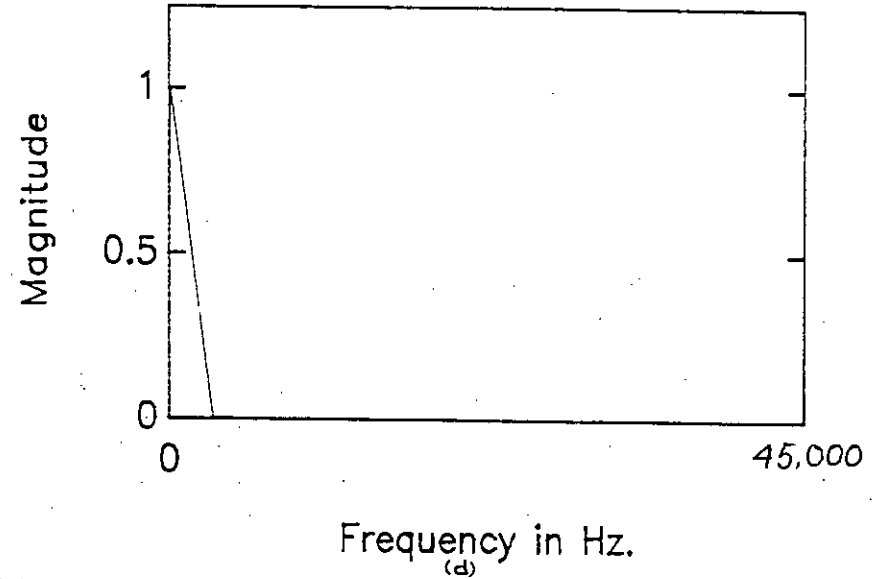
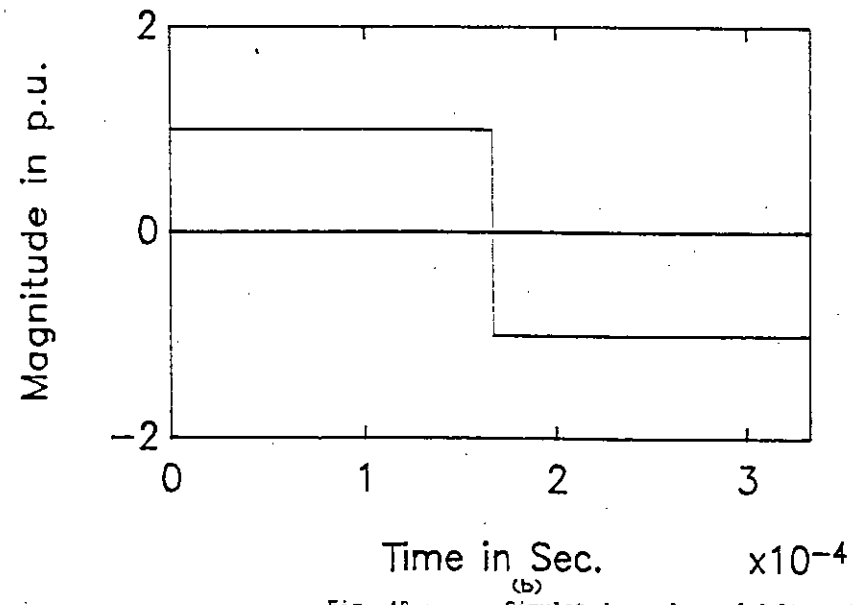
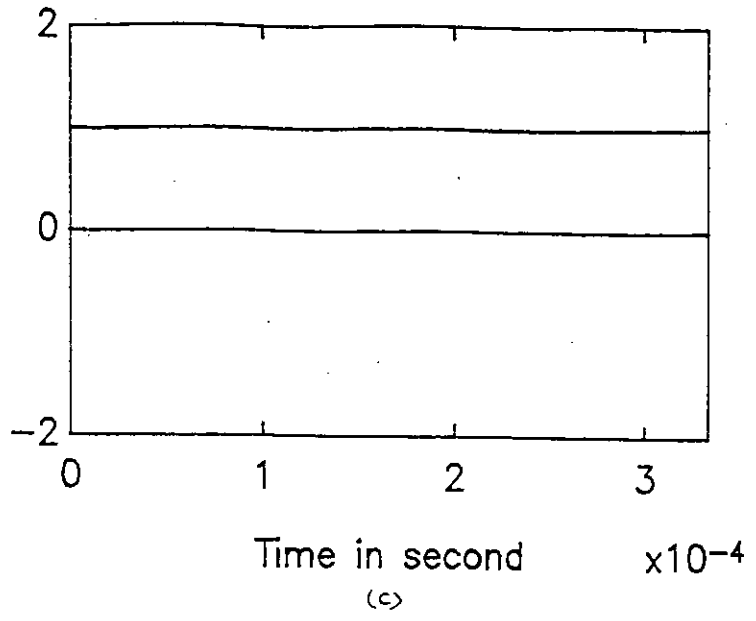
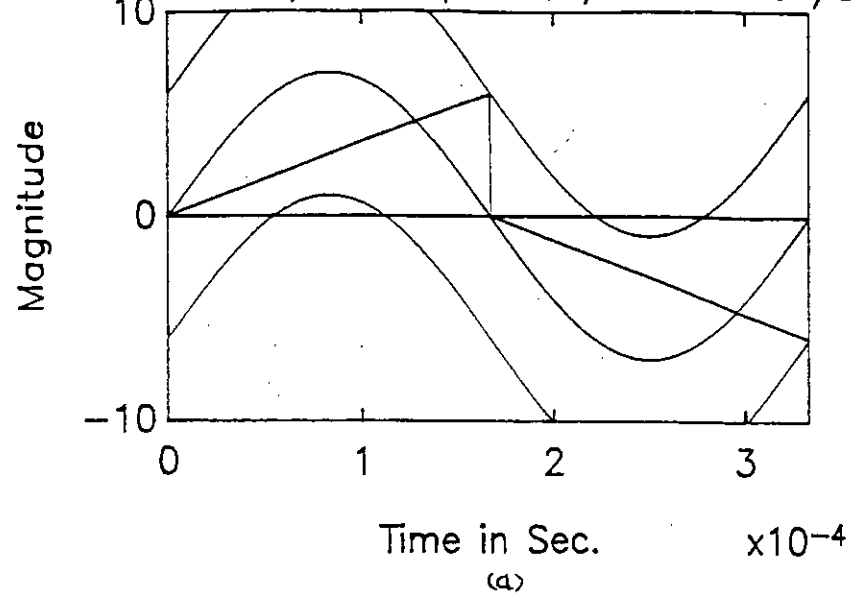
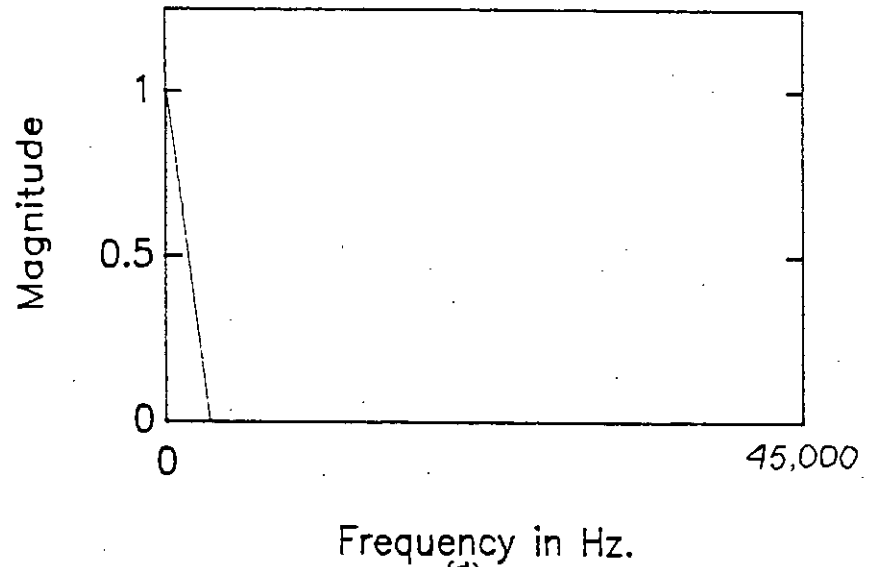
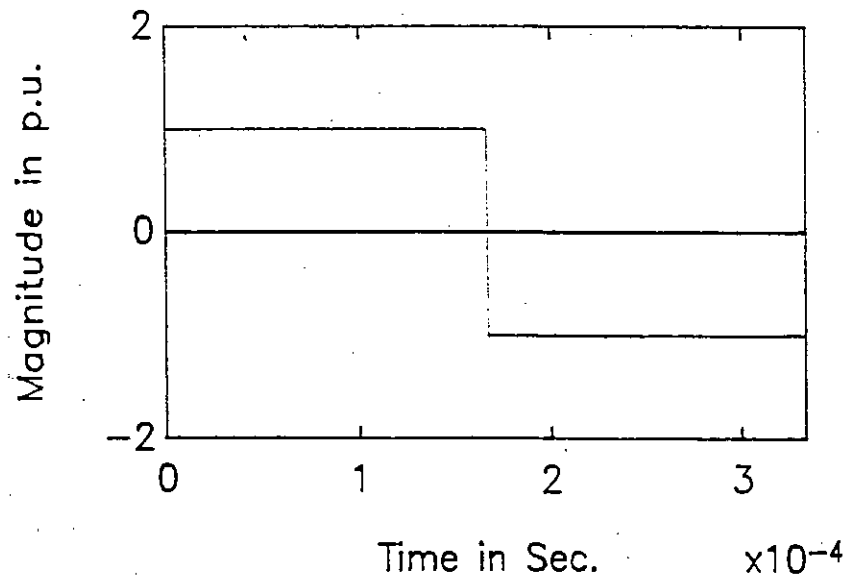
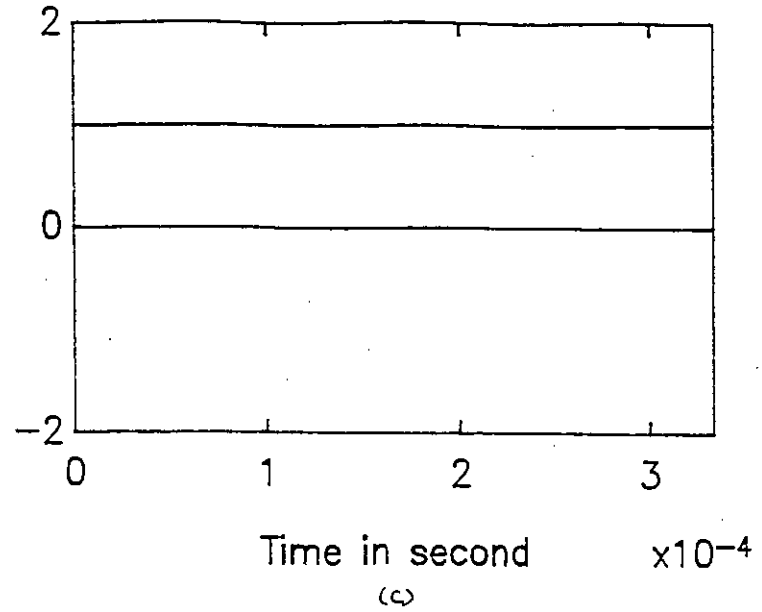
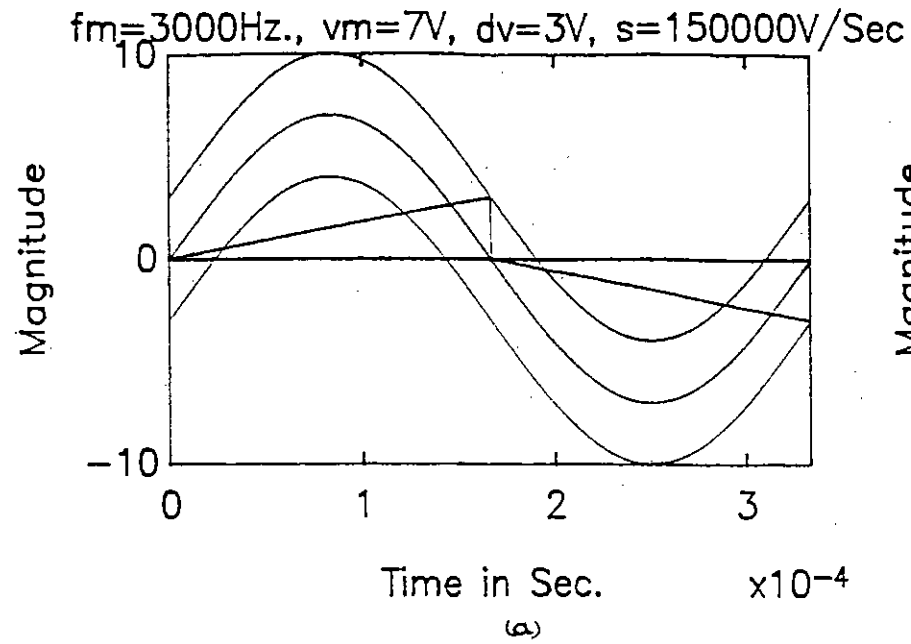


Fig.-48 : Simulated waveform of delta modulator and SHPS voltage waveform (a) modulator waveforms (b) modulated output of modulator (c) SHPS output (d) spectrum of SHPS output.  $f_m=3,000\text{ Hz.}, V_m=7\text{V}, \Delta V=6\text{V}, S=200,000\text{V/Sec.}$





Time in Sec.  $\times 10^{-4}$

Frequency in Hz.

Fig.-49 : (b) Simulated waveform of delta modulator and SMPS voltage waveform (a) modulator waveforms (b) modulated output of modulator (c) SMPS output (d) spectrum of SMPS output.  $f_m=3,000\text{ Hz.}, V_m=7\text{V}, \Delta V=3\text{V}, S=150,000\text{V/Sec.}$

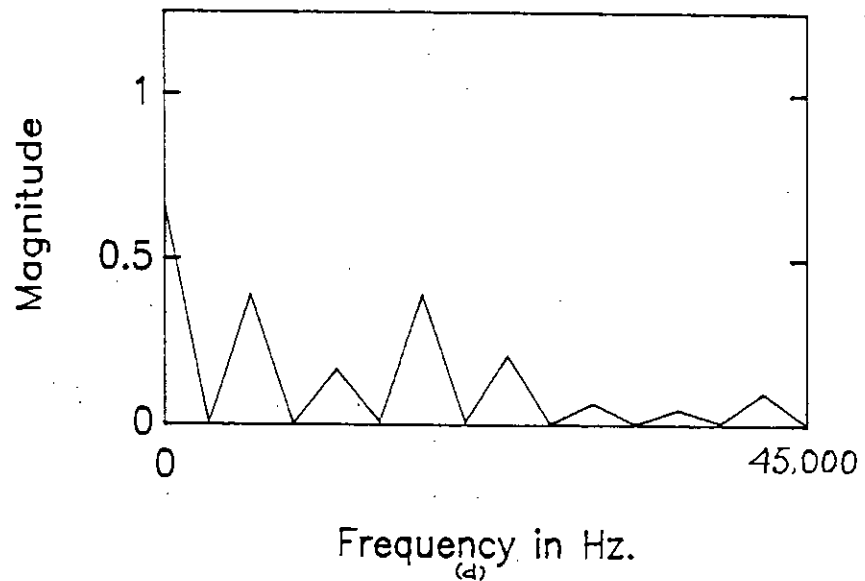
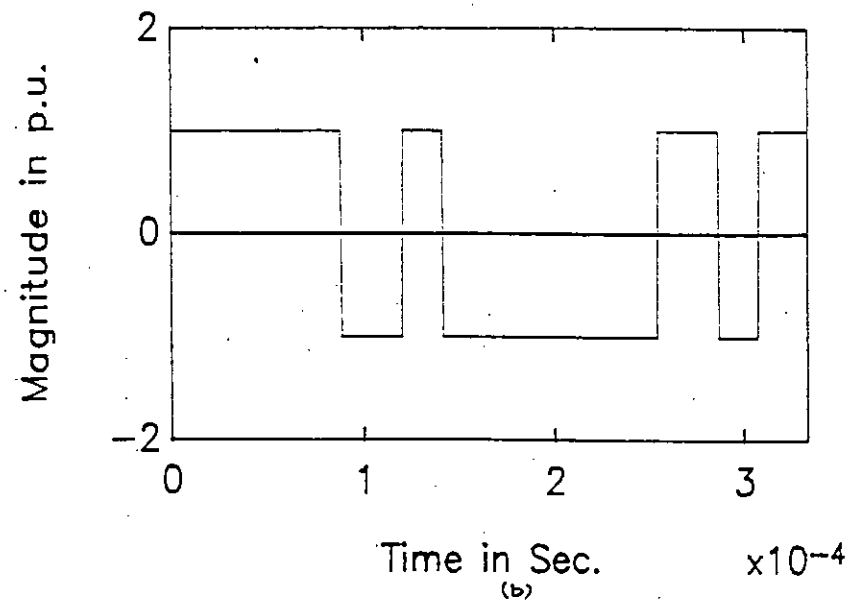
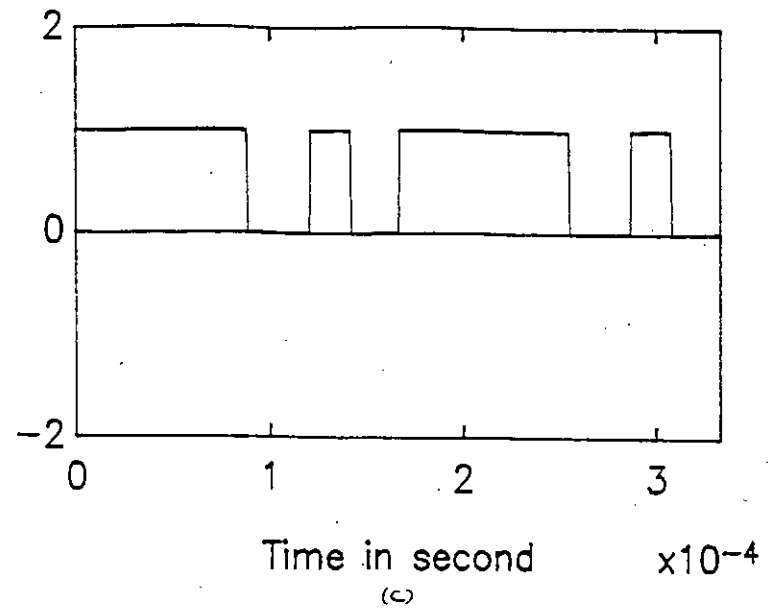
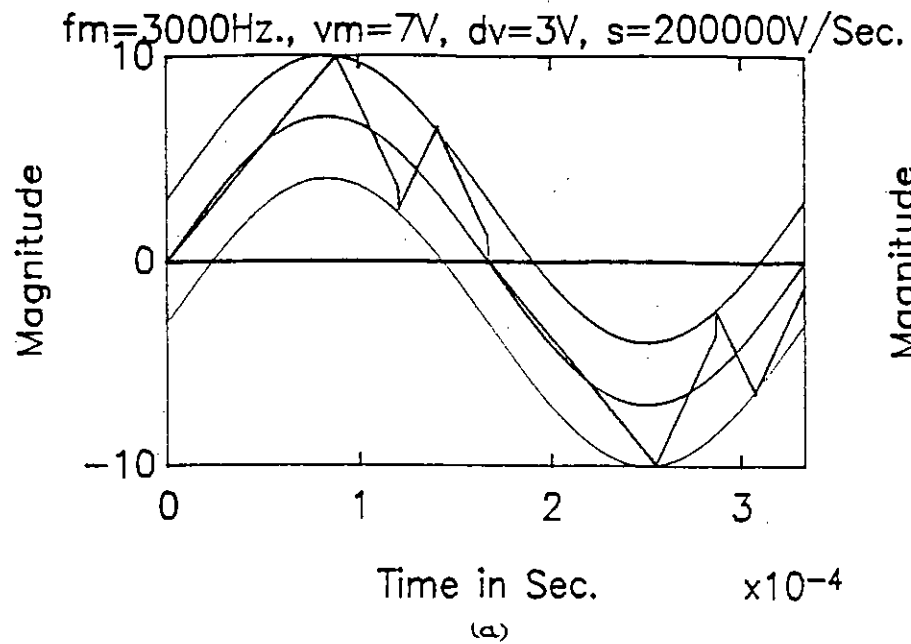


Fig.-50 : Simulated waveform of delta modulator and SMPS voltage waveform (a) modulator waveforms (b) modulated output of modulator (c) SMPS output (d) spectrum of SMPS output.  $f_m=3,000\text{ Hz.}, V_m=7\text{V}, \Delta V=3\text{V}, S=200,000\text{V/Sec.}$

$f_m=3000\text{Hz.}, v_m=7\text{V}, dv=3\text{V}, s=300000\text{V/Sec.}$

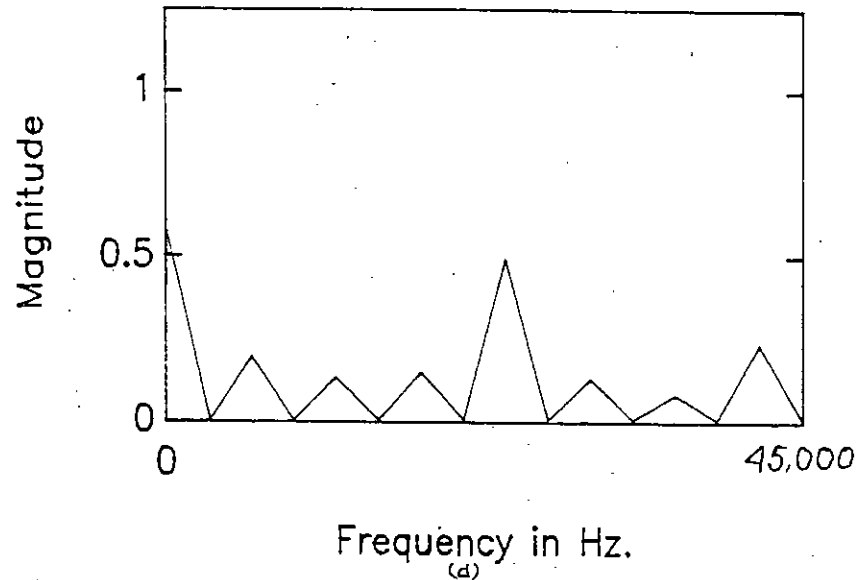
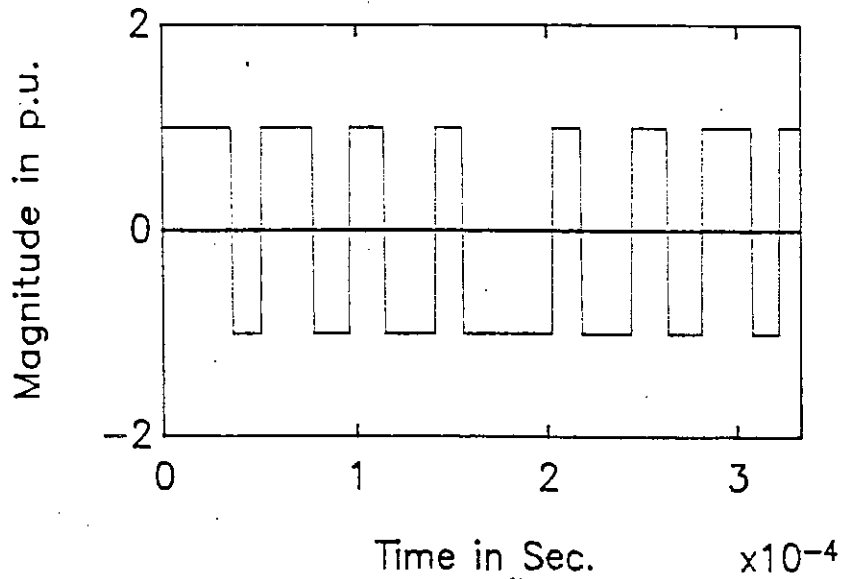
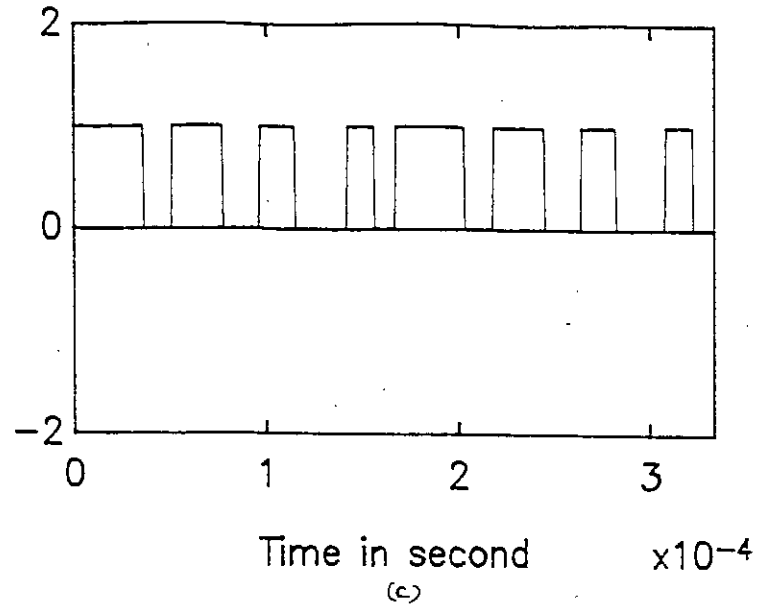
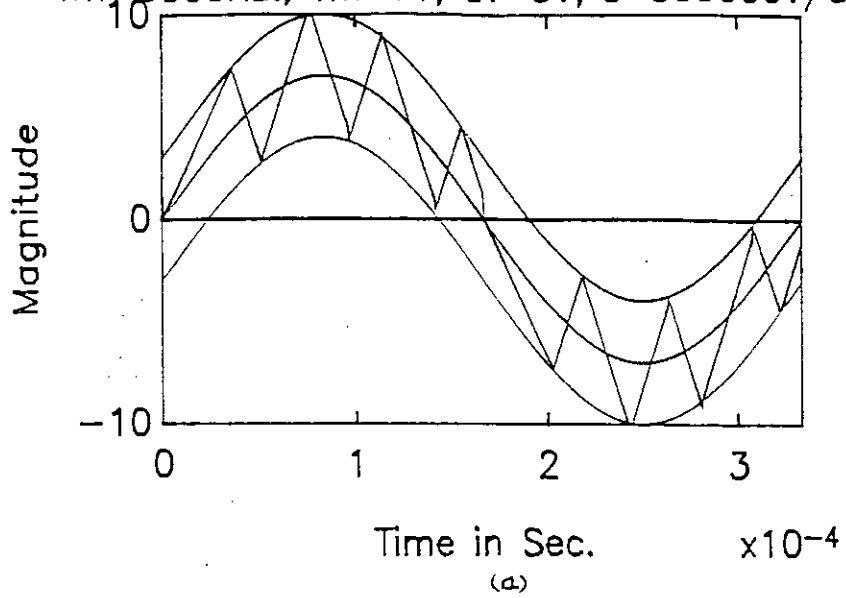


Fig.-51 : (b) Simulated waveform of delta modulator and SHPS voltage waveform (a) modulator waveforms (b) modulated output of modulator (c) SHPS output (d) spectrum of SHPS output.  $f_m=3,000\text{ Hz.}, V_m=7\text{V}, \Delta V=3\text{V}, S=300,000\text{V/Sec.}$

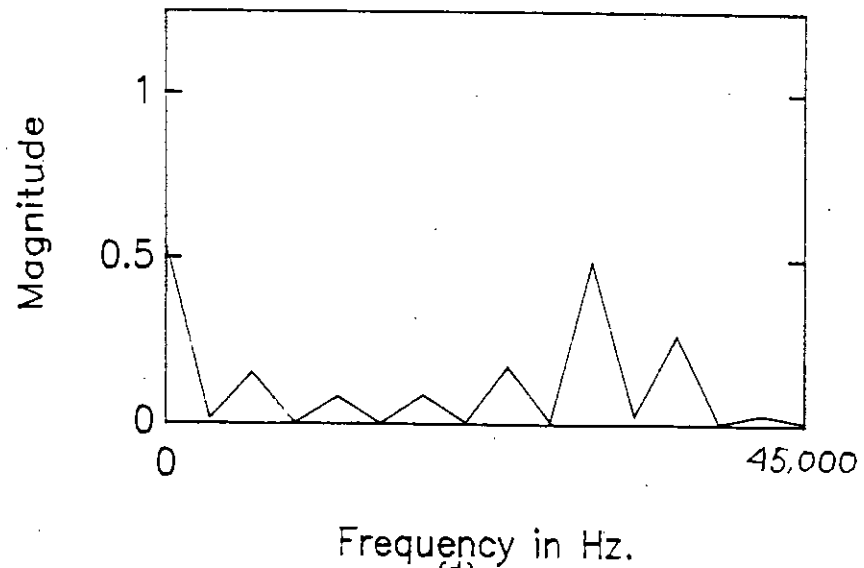
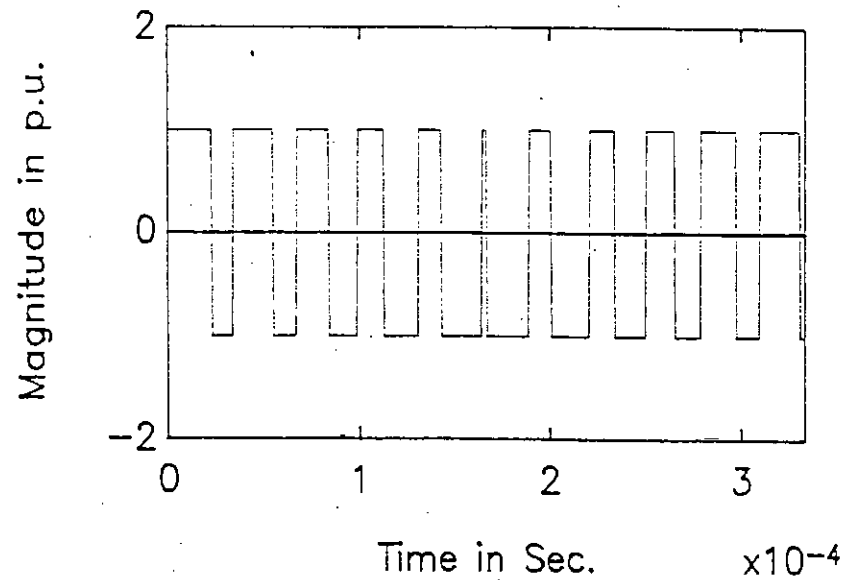
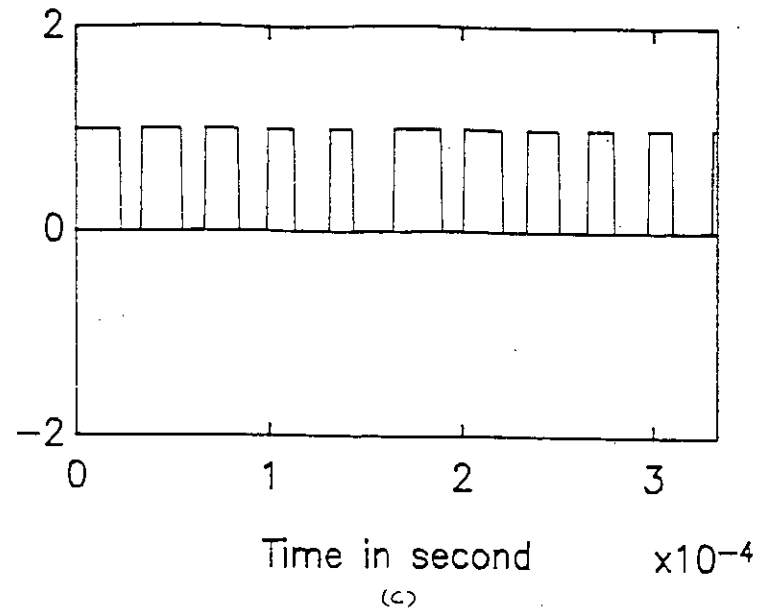
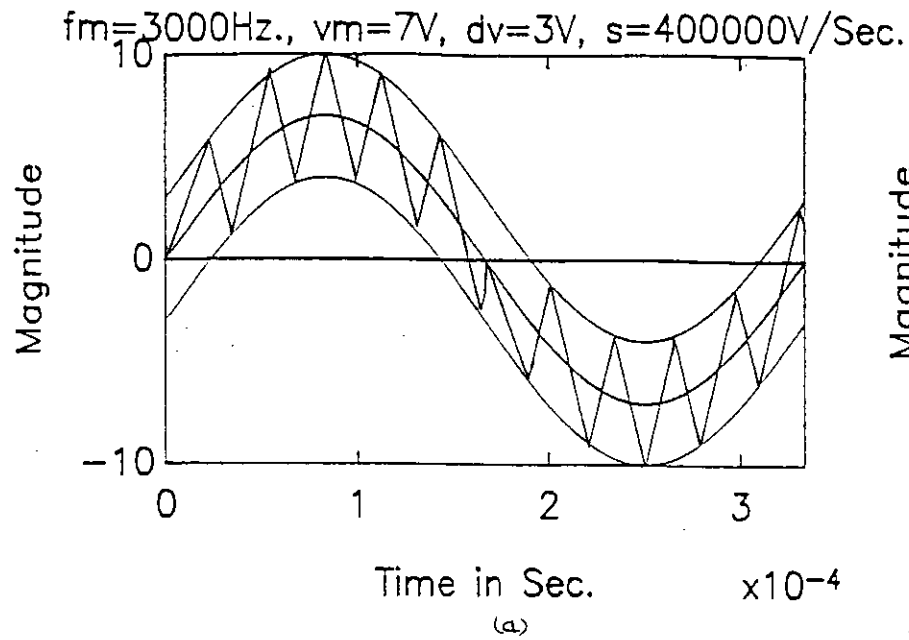
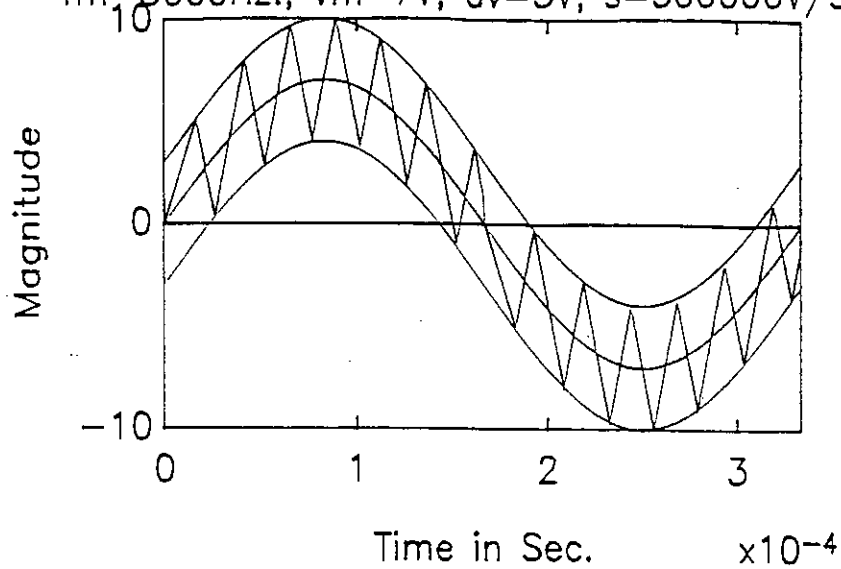
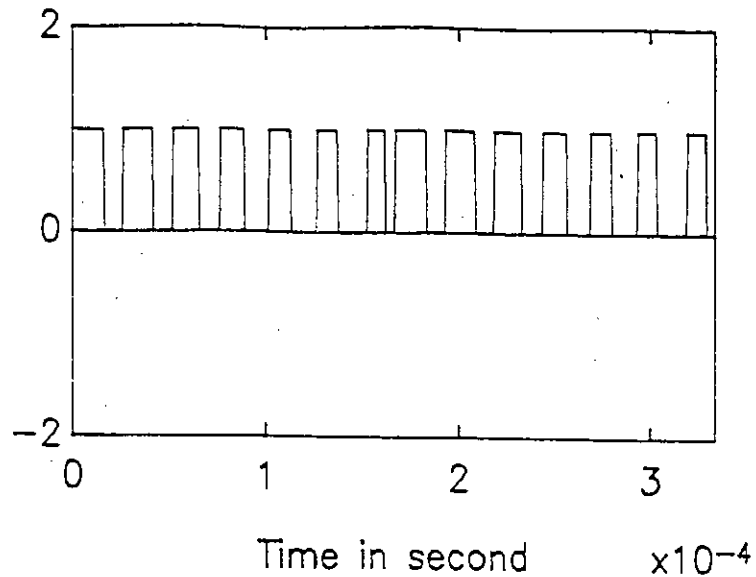


Fig.-52 : (b) Simulated waveform of delta modulator and SHPS voltage waveform (a) modulator waveforms (b) modulated output of modulator (c) SMPS output (d) spectrum of SHPS output.  $f_m=3,000\text{ Hz.}, V_m=7\text{V}, \Delta V=3\text{V}, S=400,000\text{V/Sec.}$

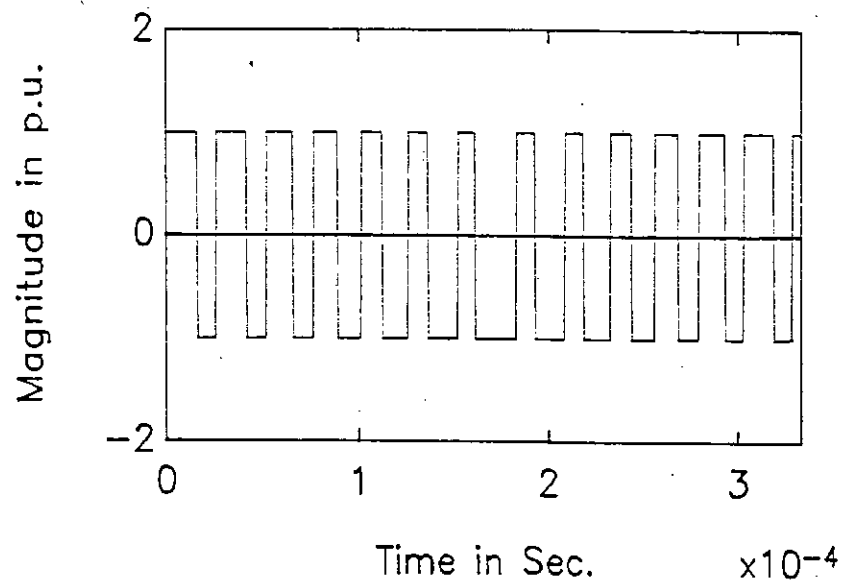
$f_m=3000\text{Hz.}, v_m=7\text{V}, dv=3\text{V}, s=500000\text{V/Sec.}$



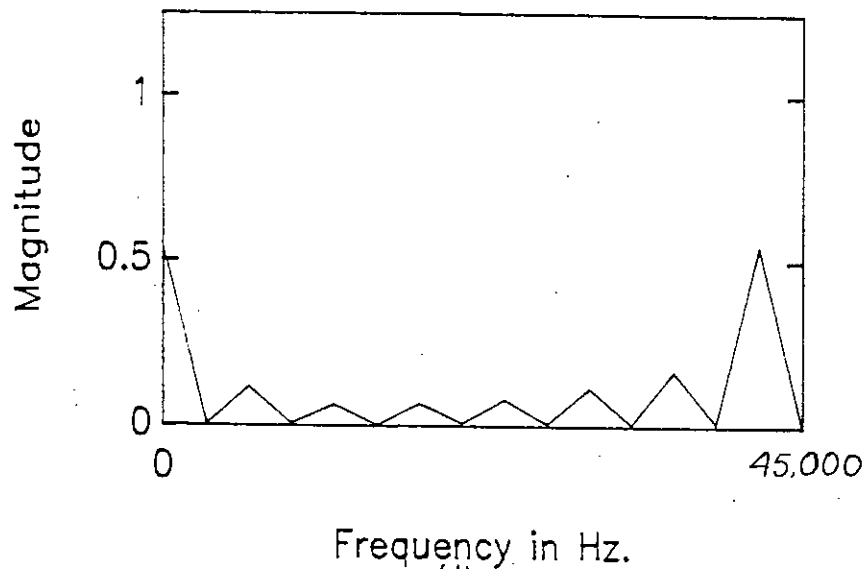
(a)



(c)



(b)



(d)

Fig.-53 : Simulated waveform of delta modulator and SMPS voltage waveform (a) modulator waveforms (b) modulated output of modulator (c) SMPS output (d) spectrum of SMPS output.  $f_m=3,000\text{ Hz.}, V_m=7\text{V}, \Delta V=3\text{V}, S=500,000\text{V/Sec.}$

$f_m=3000\text{Hz.}, v_m=5\text{V}, dv=4\text{V}, s=200000\text{V/Sec.}$

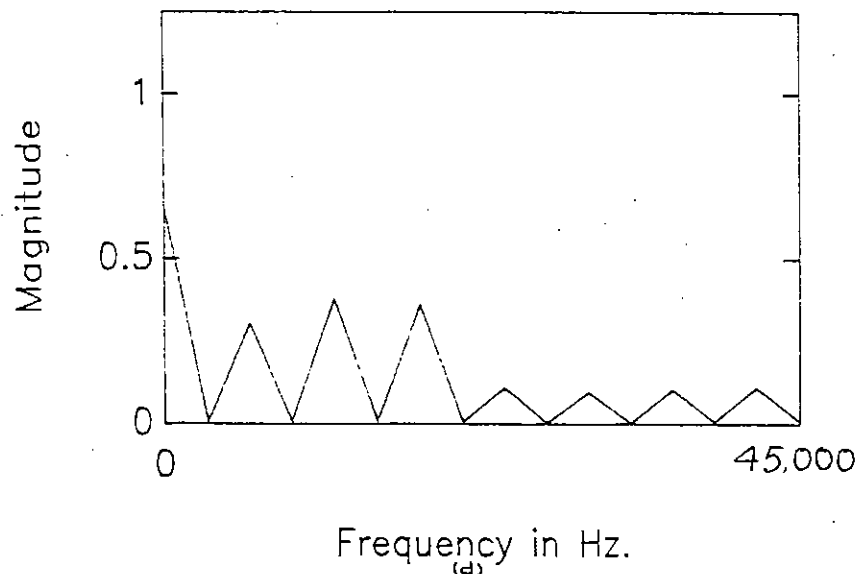
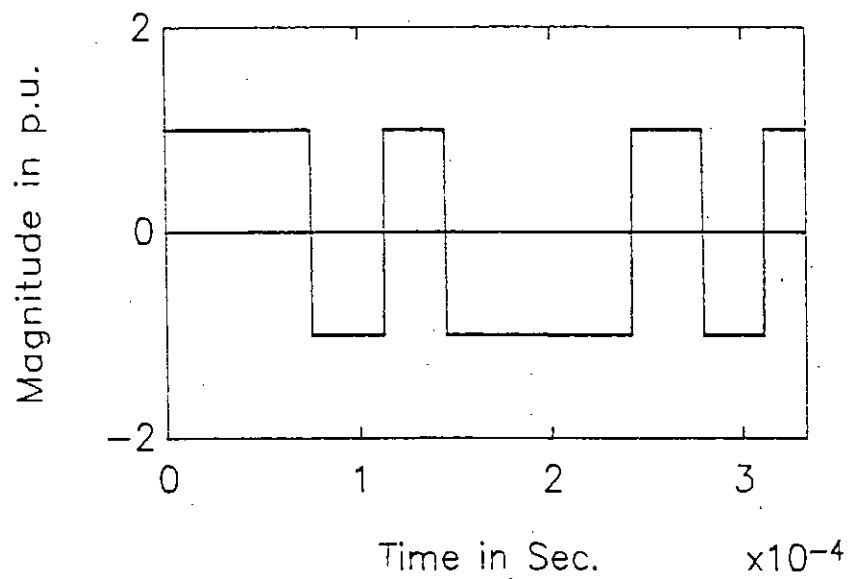
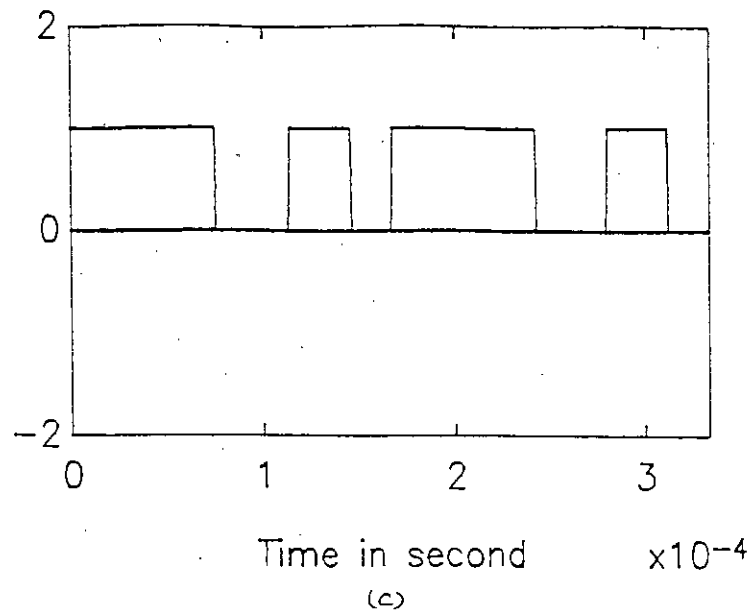
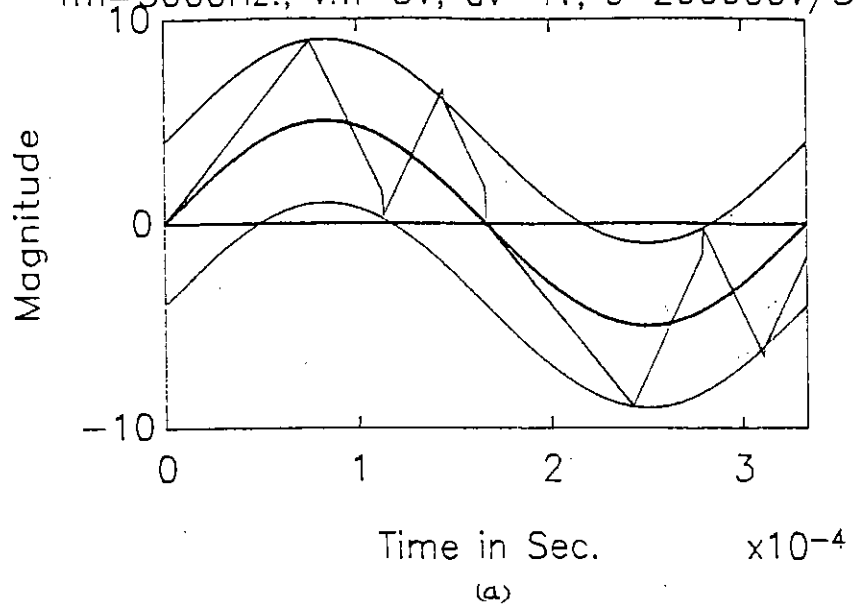


Fig.-54 : (b) Simulated waveform of delta modulator and SHPS voltage waveform (a) modulator waveforms (b) modulated output of modulator (c) SHPS output (d) spectrum of SHPS output.  $f_m=3,000\text{ Hz.}, V_m=5\text{V}, \Delta V=3\text{V}, S=200,000\text{V/Sec.}$

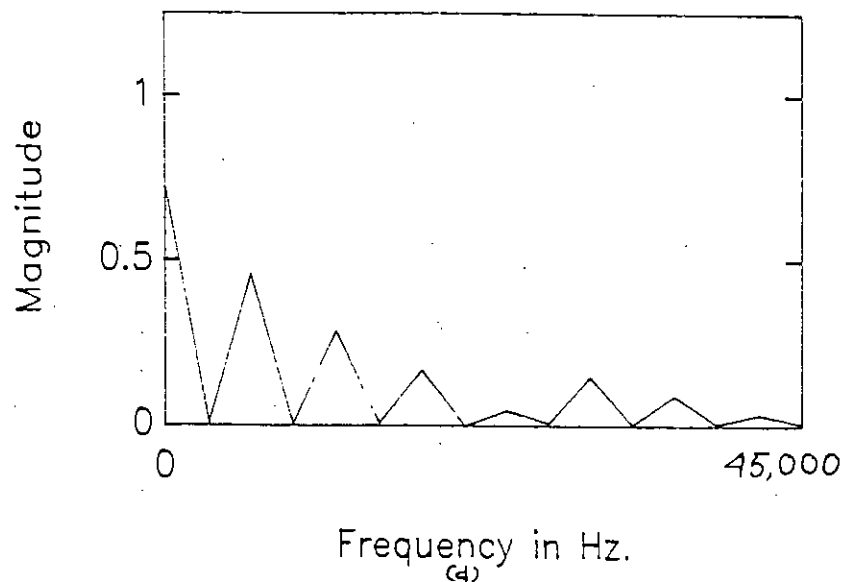
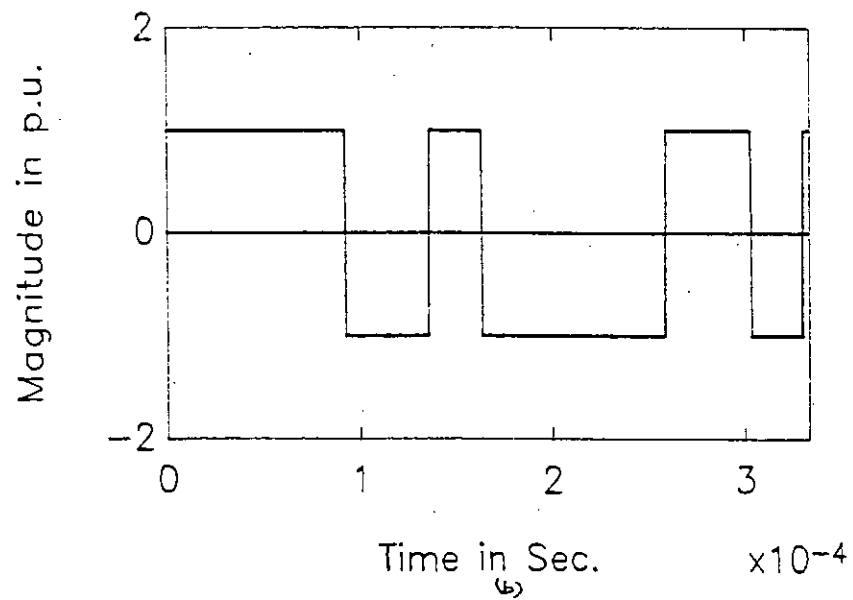
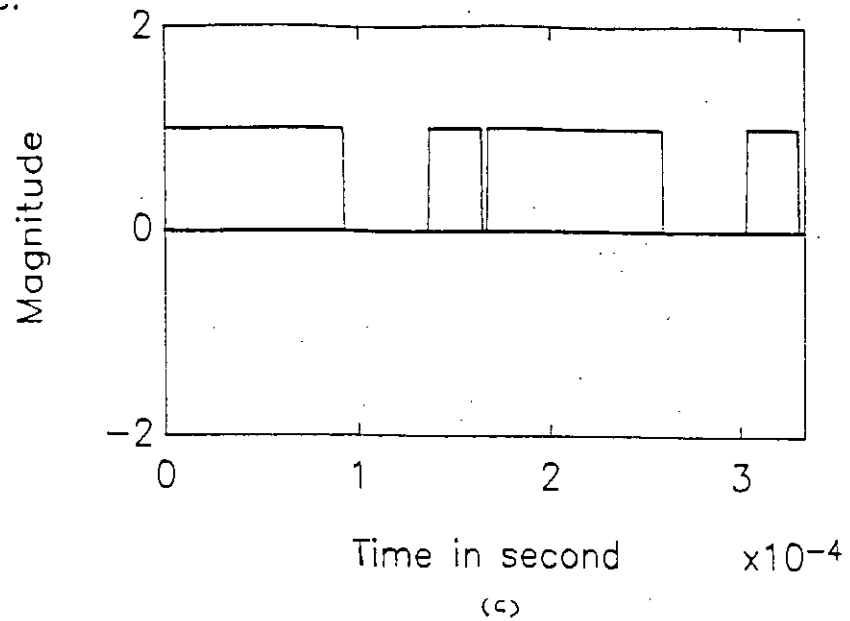
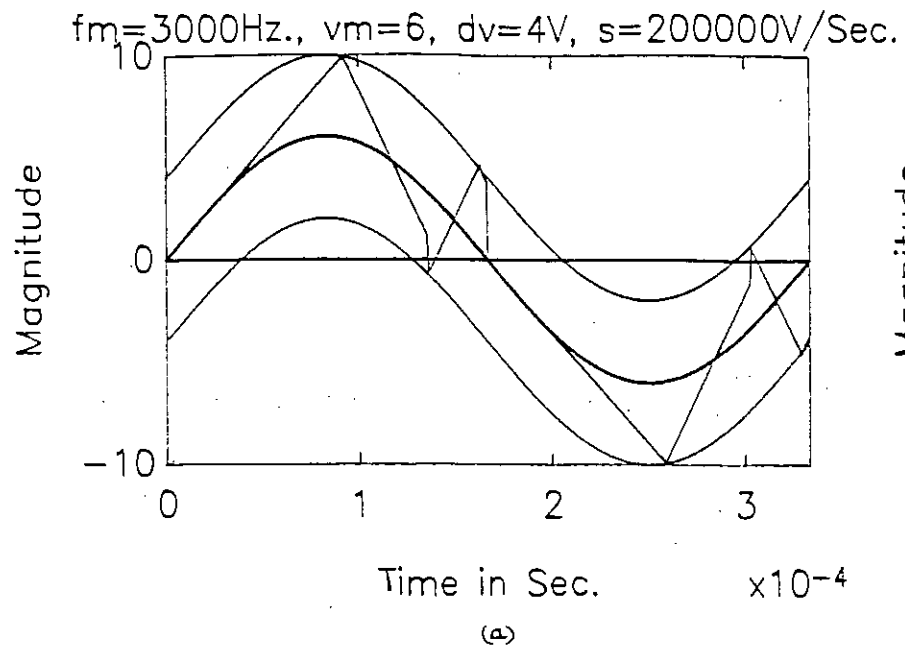


Fig.-55 : Simulated waveform of delta modulator and SMPS voltage waveform (a) modulator waveforms (b) modulated output of modulator (c) SMPS output (d) spectrum of SMPS output.  $f_m=3,000\text{ Hz.}, V_m=6V, AV=4V, S=200,000V/\text{Sec.}$

$f_m=3000\text{Hz.}, v_m=7\text{V}, dv=4\text{V}, s=200000\text{V/Sec.}$

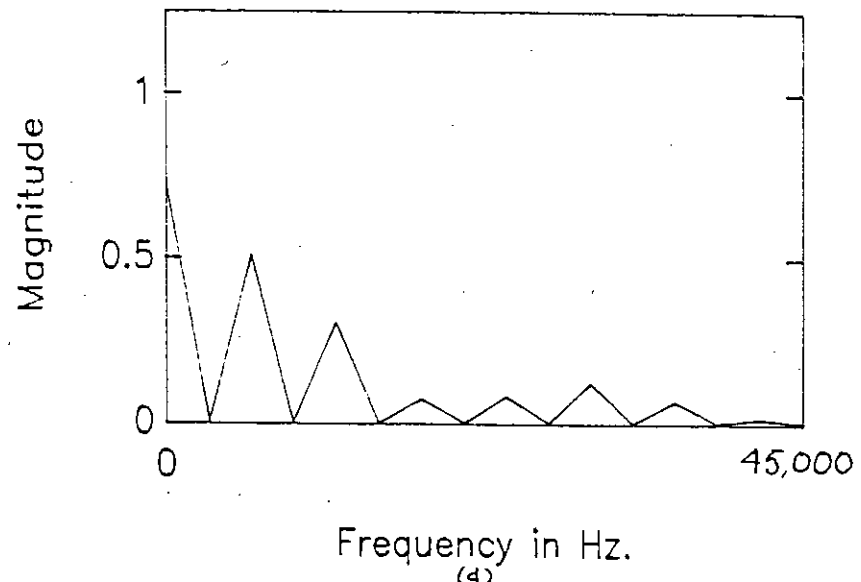
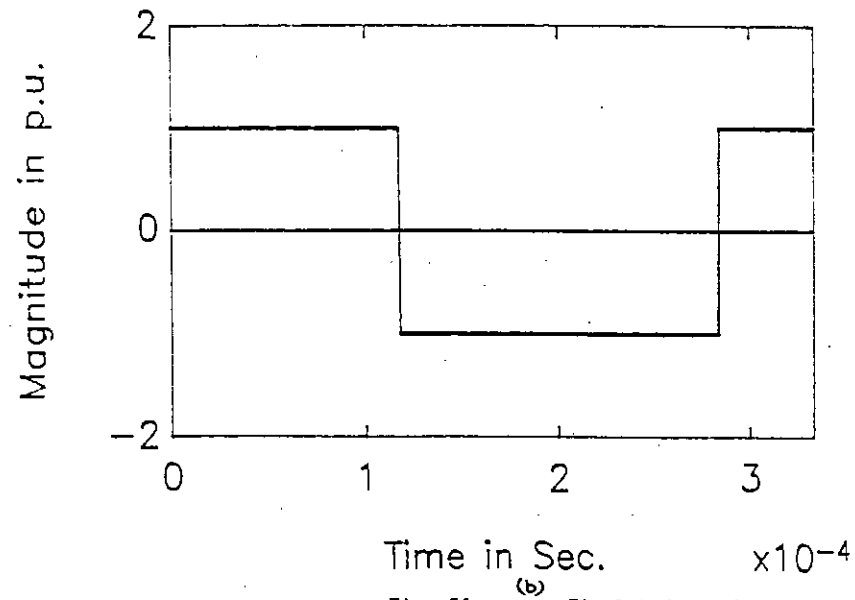
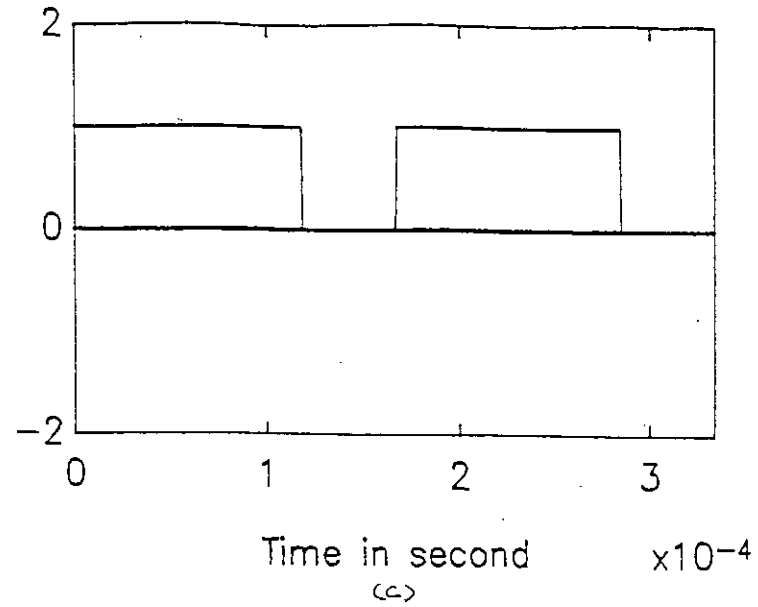
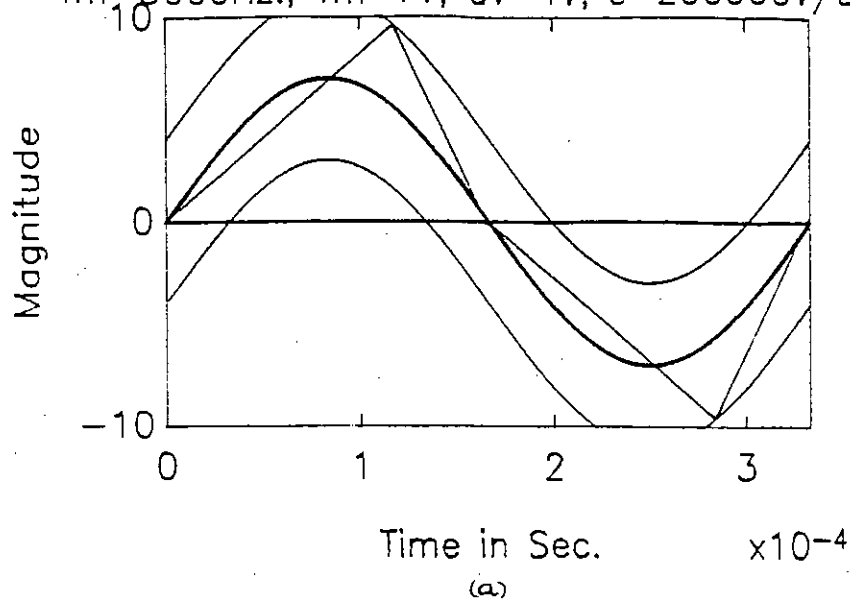


Fig.-56 : (a) modulator waveforms (b) modulated output of modulator (c) SMPS output (d) spectrum of SMPS output.  $f_m=3,000\text{ Hz.}, V_m=7\text{V}, \Delta V=4\text{V}, S=200,000\text{V/Sec.}$



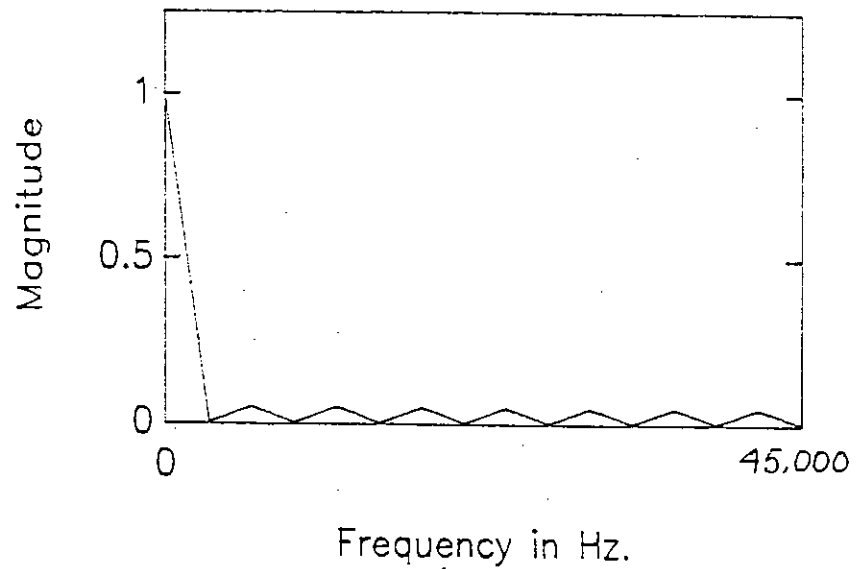
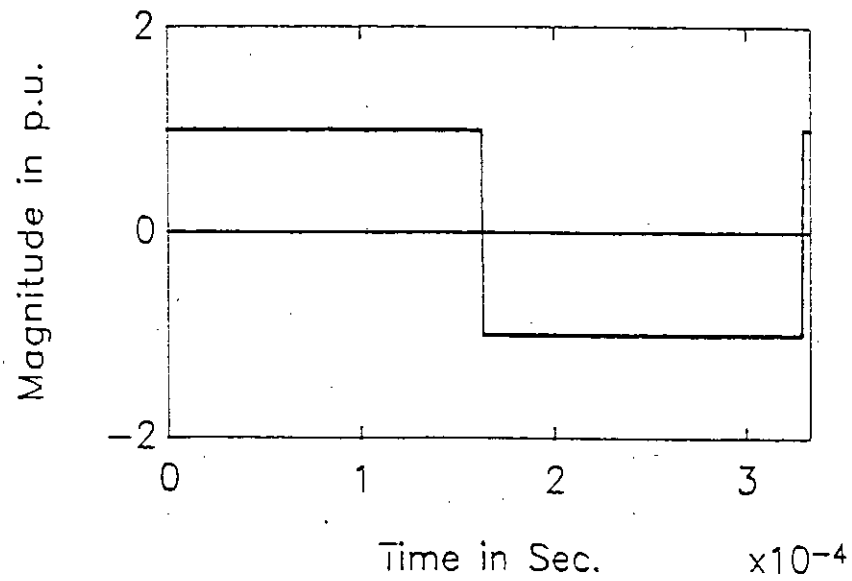
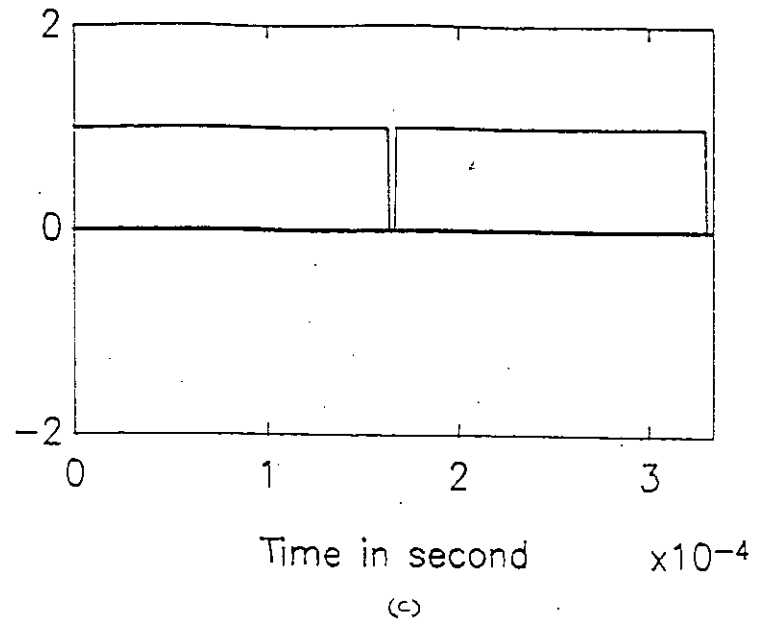
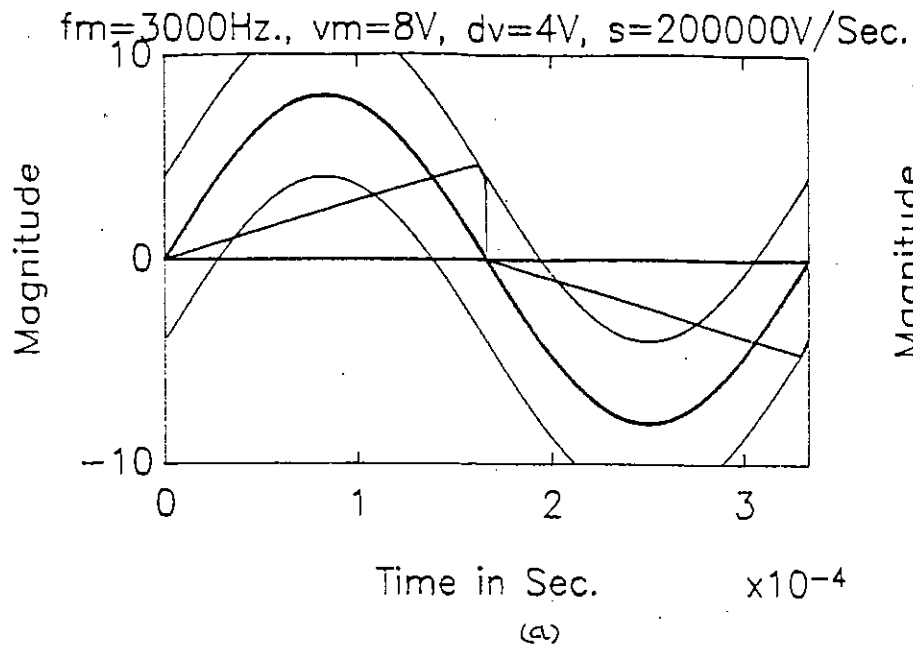


Fig.-57 : (b) Simulated waveform of delta modulator and SMPS voltage waveform (a) modulator waveforms (b) modulated output of modulator (c) SMPS output (d) spectrum of SMPS output.  $f_m=3,000\text{ Hz.}, V_m=8\text{V}, \Delta V=4\text{V}, E=200,000\text{V/Sec.}$

$f_m=3000\text{Hz.}, v_m=8.5\text{V}, dv=4\text{V}, s=200000\text{V/Sec.}$

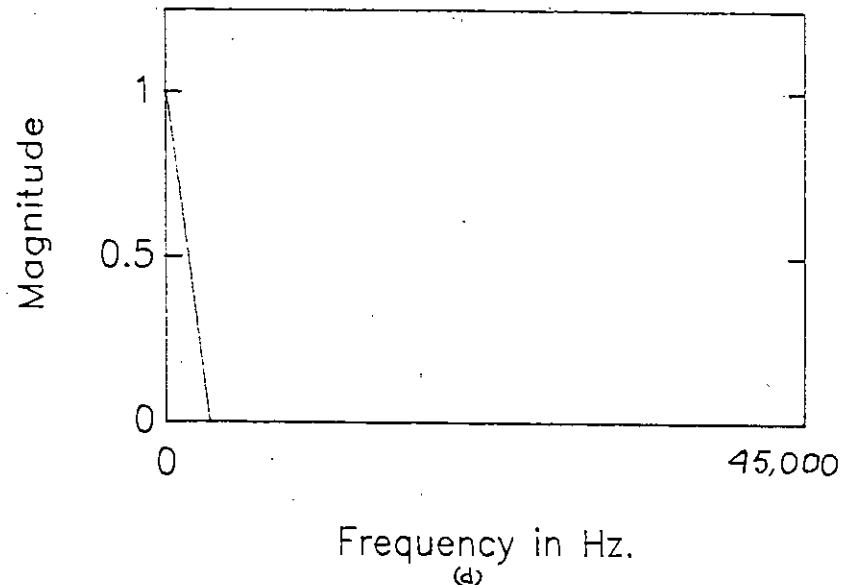
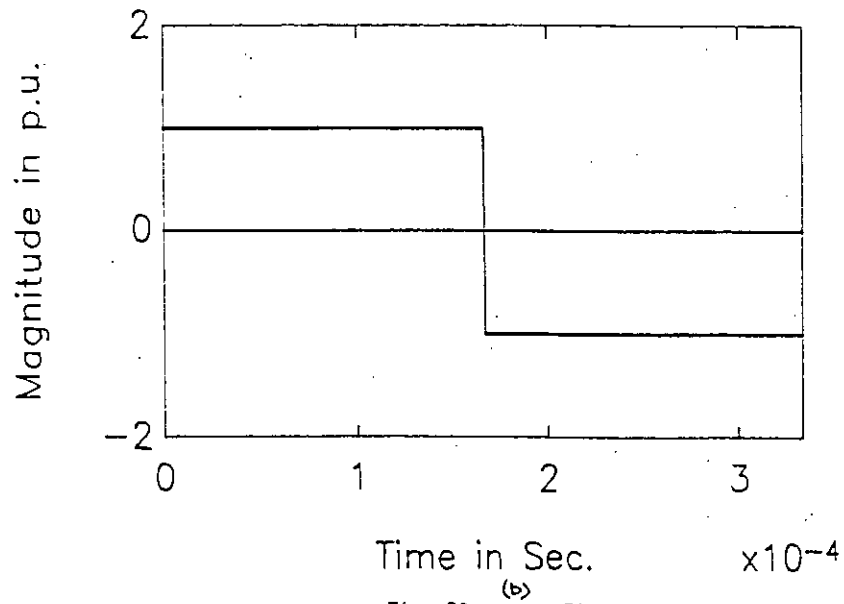
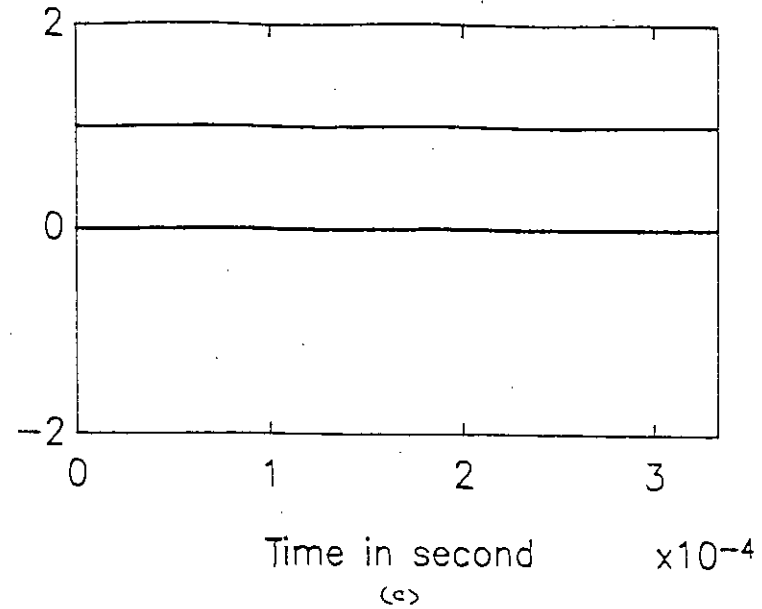
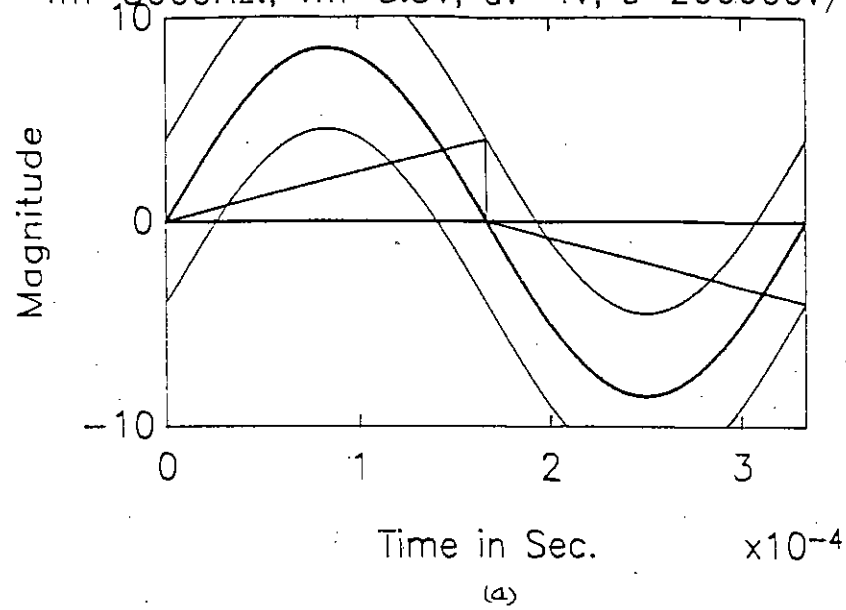


Fig.-58 : Simulated waveform of delta modulator and SMPS voltage waveform (a) modulator waveforms (b) modulated output of modulator (c) SMPS output (d) spectrum of SMPS output.  $f_m=3,000\text{ Hz.}, V_m=8.5\text{V}, \Delta V=4\text{V}, S=200,000\text{V/Sec.}$

## Chapter - 3

### Practical Implementation

#### 3.1 IMPLEMENTATION OF DELTA MODULATION CONTROL CIRCUIT

##### FOR PULSE WIDTH MODULATED SMPS :

The delta modulation technique requires simple circuitry to generate switching waveforms for switching the device (transistor, MOSFET etc.) of an SMPS. Fig.-59 is an analog circuit which is capable of producing the waveforms shown in Fig.-60.

The operation of the circuit can be described as follows :  
Sine reference or modulating wave  $V_R$  is supplied to the input of the comparator  $A_1$  and the carrier  $V_T$  is generated in the following manner; wherever the output voltage of  $A_2$  exceeds the upper or lower window boundary (preset by  $R_2/R_3$  ratio), the comparator  $A_1$  reverses the polarity of  $V_T$  at the input of  $A_2$ . It forces carrier wave  $V_T$  to oscillate around the reference waveform  $V_R$  at ripple frequency  $f_r$ . The switching waveform is obtained at the output  $A_1$ .

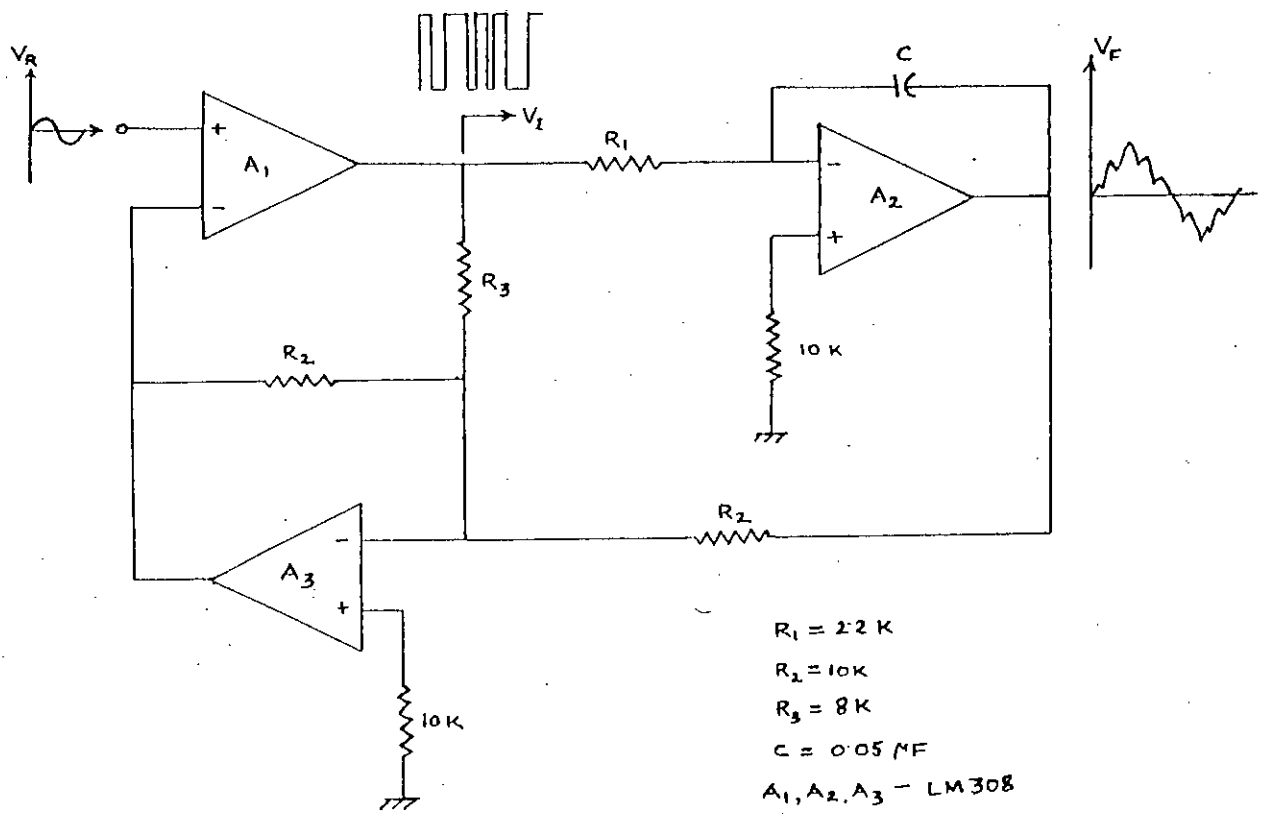


Fig.-59 : A practical circuit for producing switching waveform of delta modulated inverters.

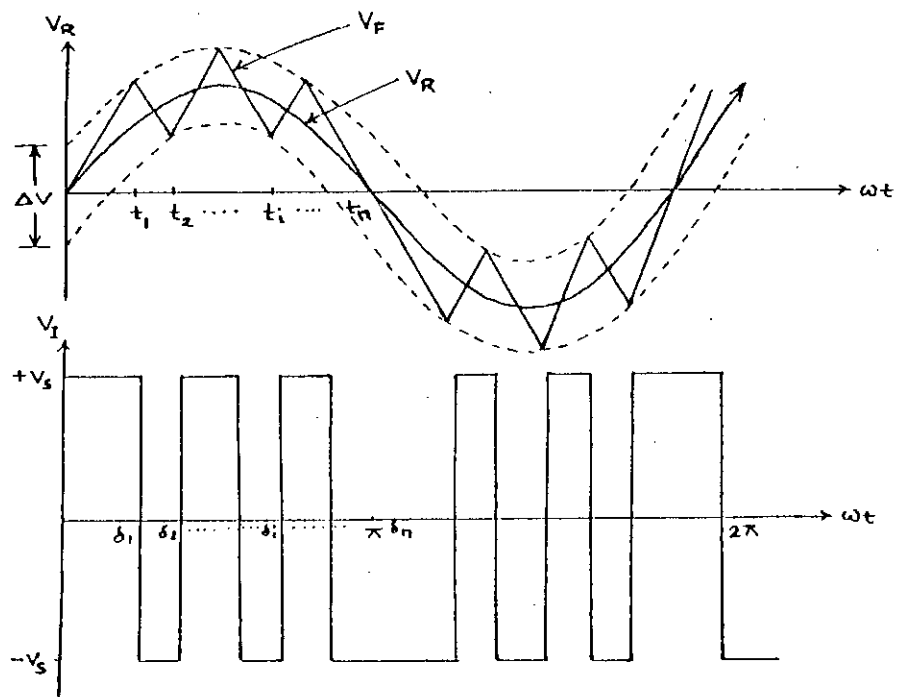


Fig.-60 : Graphical illustration of DM technique for the SMPS.

### 3.2 EXPERIMENTAL DELTA MODULATION FOR STATIC CONVERTERS :

This section deals with experimental verification of analytical results of delta modulation carried out so far. The implementation of the logic circuits and verification of the main features of delta modulation are described.

#### 3.2.1 Implementation of the logic circuits:

The basic circuit used for the delta modulation is shown in Fig.-59. The output waveform of this circuit are shown in Fig.-61 through Fig.-69. Different outputs of the modulator are obtained by changing

1. Frequency,  $f$  of the input Signal to the DM.
2. Window width,  $\Delta V$  of the hysteresis band of the DM  
and
3. Slope  $S$ , of the carrier wave of the DM.

Fig.-61 shows the carrier wave and the output of the DM with a sine input. Frequency of the input sine wave is 40 Hz.

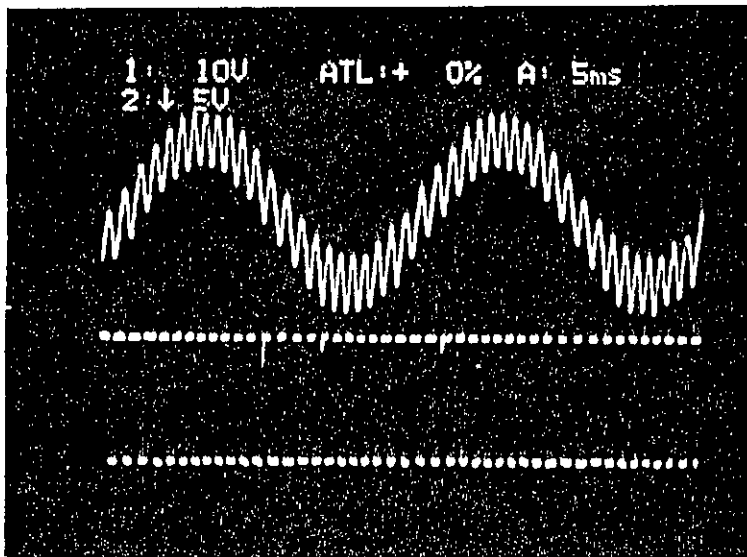


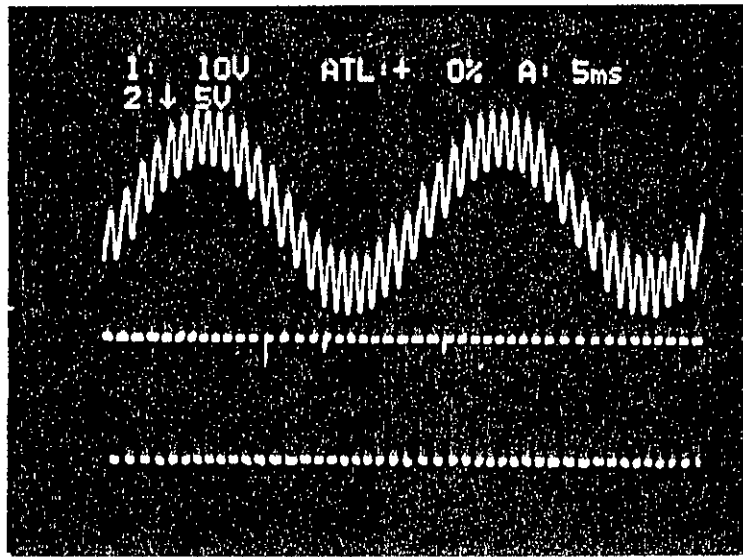
Fig.-61 : Illustration of practical waveforms of delta modulation circuit,  $f = 40$  Hz.

### 3.2.2 Effect of change of frequency of the input sine wave to the DM :

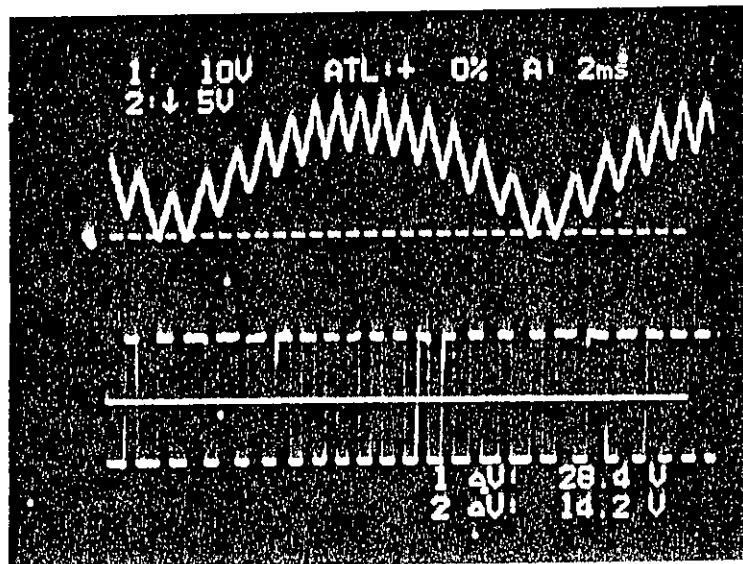
For comparative study Fig.-62(a) again describes Fig.-61 and Fig.-62(b) describes the rectified carrier wave and output wave of the DM for  $f=40$  Hz. and  $\Delta V=4$  Volt.

Frequency of the input sine wave is then increased to 60 Hz. keeping  $\Delta V=4$  Volt. This is shown in Fig.-63(b). By comparing Fig.-63(a) and 63(b), it is seen that the pulse width of the output of DM increases. The same thing happens when frequency increases from 80 to 100 Hz (Fig.-64 and Fig.-65 ). This indicates that as the frequency of reference sine wave is increased, the modulated wave changes having wider pulses. As a result dc voltage of the modulated wave increases. Also, as frequency is increased number of pulses/half cycle (number of switching) decreases .



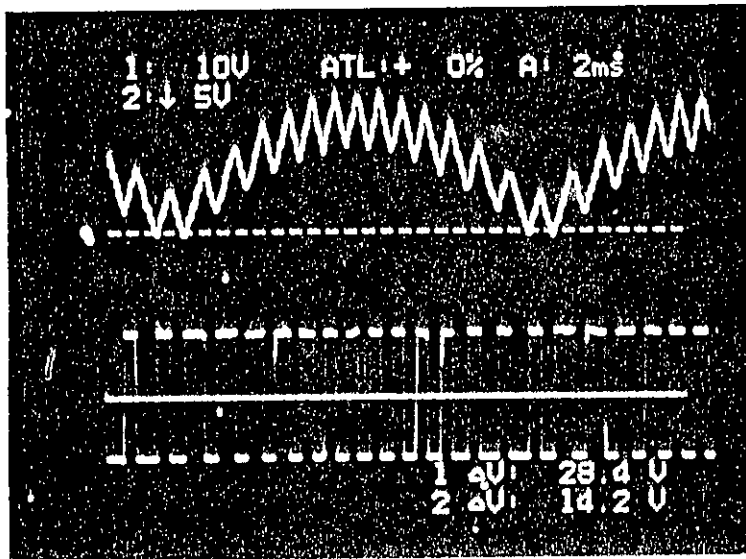


(a)

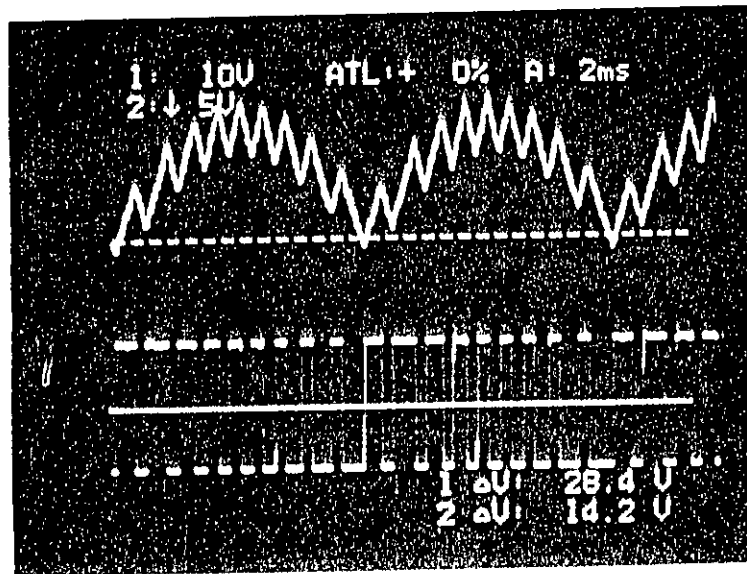


(b)

Fig.-62 : Carrier and modulated output of a DM circuit for  $f=40$  Hz.,  $\Delta V=4$  Volt,  $S=5,405$  V/Sec.

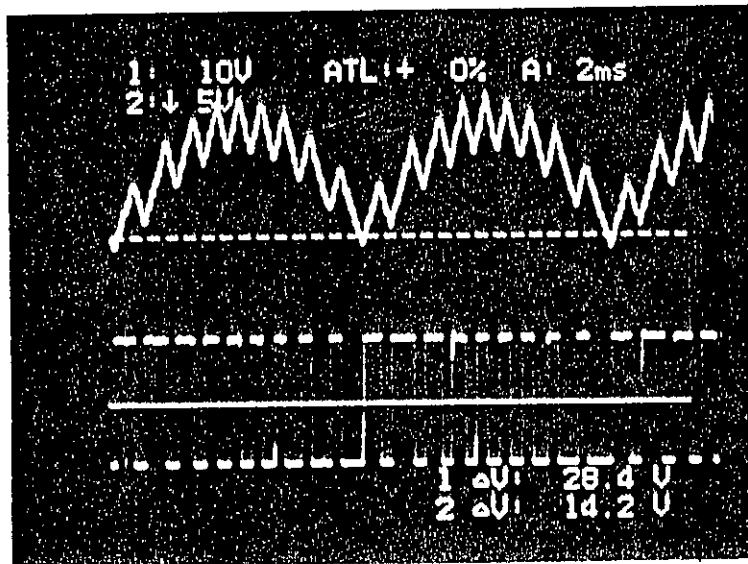


(a)

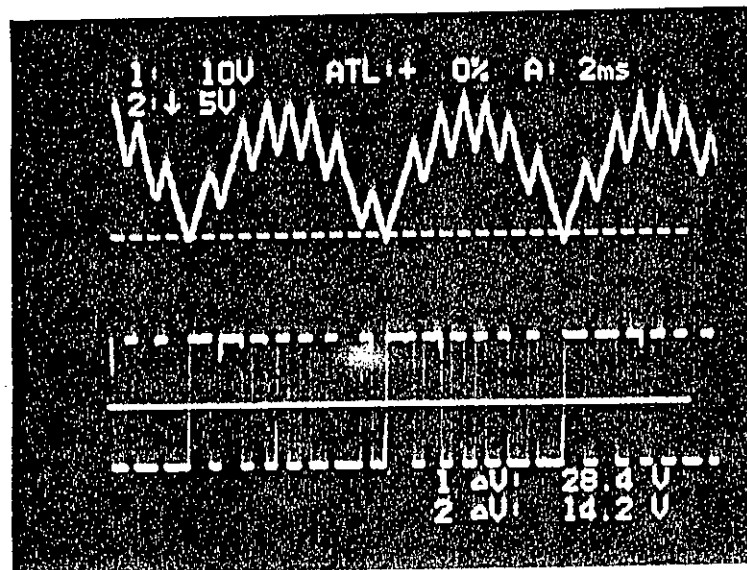


(b)

Fig.-63 : Carrier and modulated output of a DM circuit for  $f=40$  Hz. and  $60$  Hz.,  $\Delta V=4$  Volt,  $S=5,405$  V/Sec.

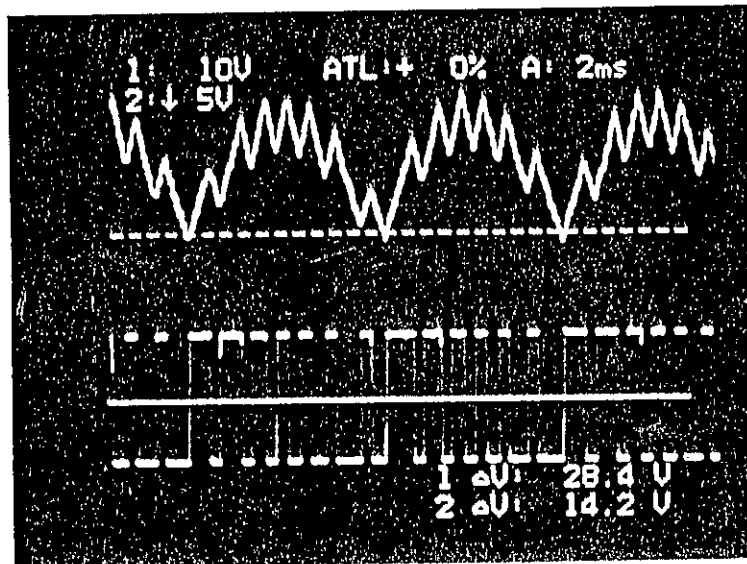


(a)

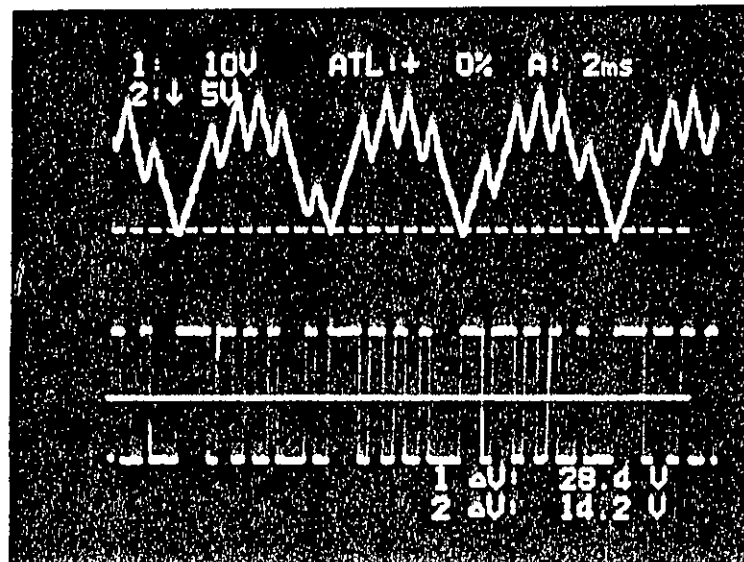


(b)

Fig.-64 : Carrier and modulated output of a DM circuit for  $f=60$  Hz. and  $80$  Hz.,  $\Delta V=4$  Volt,  $S=5,405$  V/Sec.



(a)

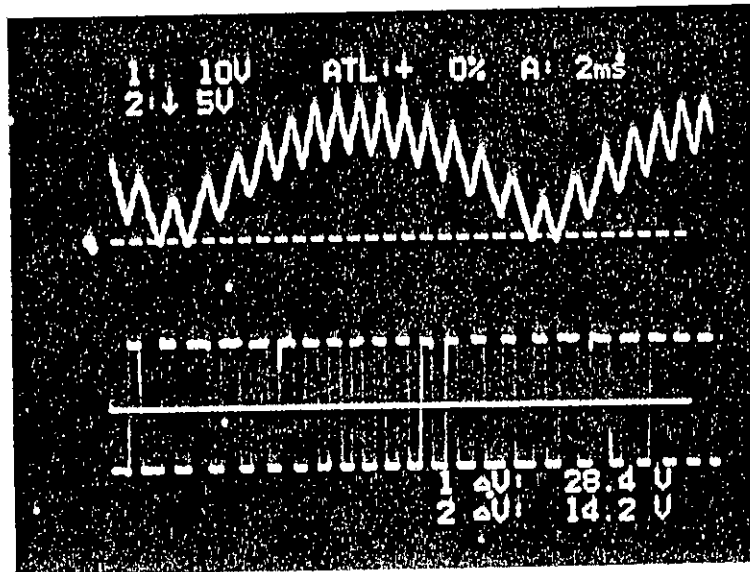


(b)

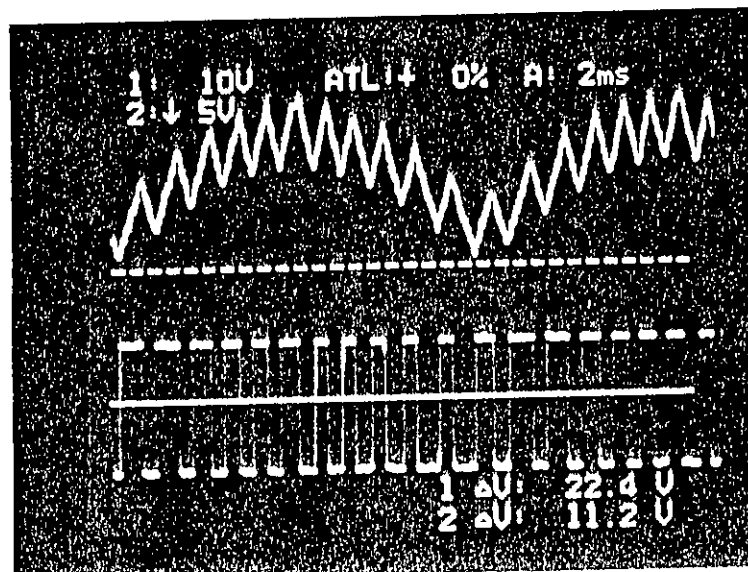
Fig.-65 : Carrier and modulated output of a DM circuit for  $f=80$  Hz. and  $100$  Hz.,  $\Delta V=4$  Volt,  $S=5,405$  V/Sec.

### 3.2.3 Effect of change of window width of the Hysteresis band of the DM :

Fig.-66(a) shows the waveforms when  $f=40$  Hz and  $\Delta V=4$  Volt. By keeping the frequency constant ( $f=40$ Hz),  $\Delta V$  is changed to 7V and the output is shown in Fig.-66(b). Comparing these two illustrations it is clear that the pulse width of the output of DM the increases with increasing  $\Delta V$ . The effect of change of output due to change of  $\Delta V$  for another constant frequency ( $f=100$  Hz) is illustrated in Fig.-67, where it is again clear that the output pulse width increases with increasing  $\Delta V$ . The result of increasing window width  $\Delta$  has same effect as increasing the frequency of the modulated wave. Both the parameters can therefore be used to control the output voltage of the modulator and also to control harmonic content of the modulated output.

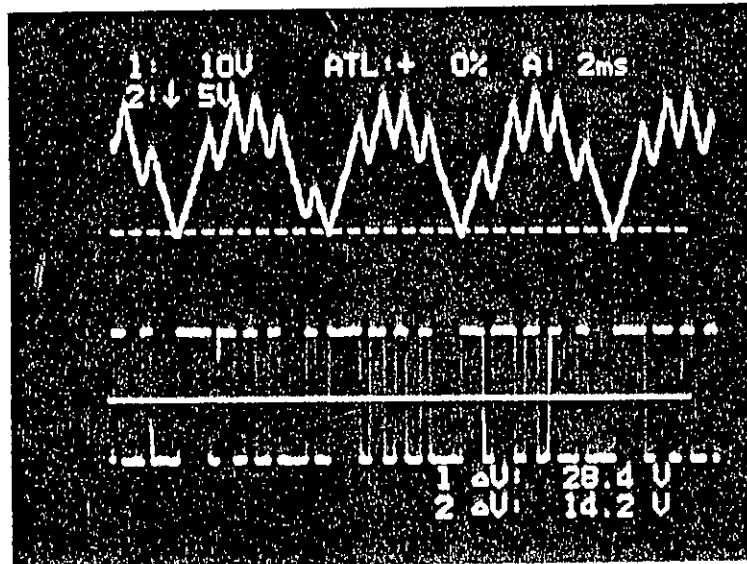


(a)

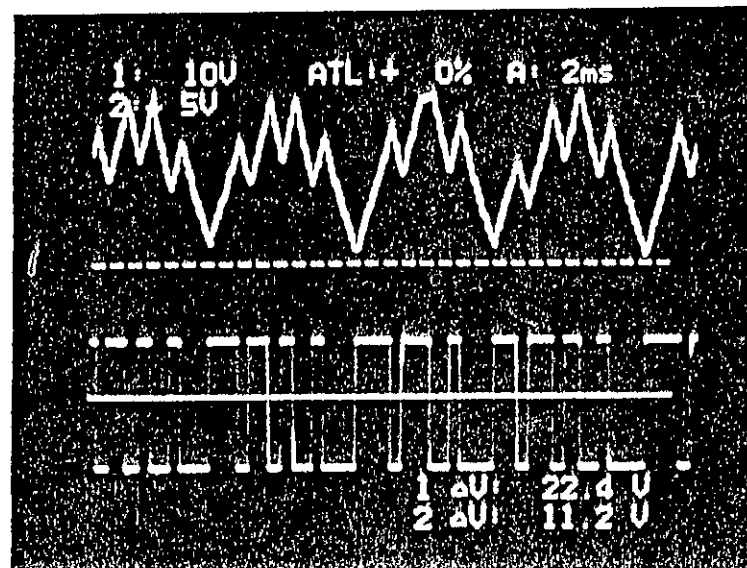


(b)

Fig.-66 : Carrier and modulated output of a DM circuit for  $f=40$  Hz.,  $\Delta V=4$  Volt and 7 Volt,  $S=5,405$  and  $9,459$  V/Sec.



(a)



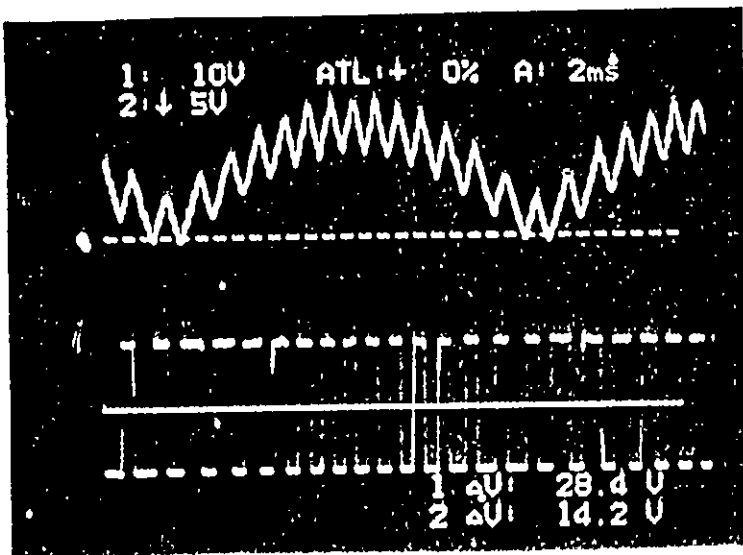
(b)

Fig.-67 : Carrier and modulated output of a DM circuit for  $f=100$  Hz.,  $\Delta V=4$  Volt and 7 Volt,  $S=5,405$  and  $9,459$  V/Sec.

3.2.4 Effect of change of slope (Volt/Sec) of the carrier wave:

The slope of the carrier wave also effects the output of the DM like window width. As slope increases the pulse width of the output of the DM decreases. This is clearly described in Fig.-68 (for  $f=40$  Hz.) and Fig.-69 (for  $f=100$  Hz.).

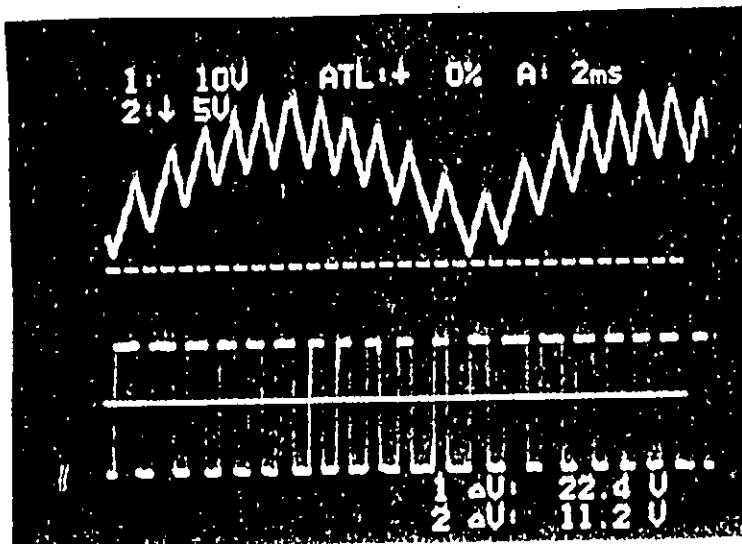




(a)

$$f = 40 \text{ Hz.}$$

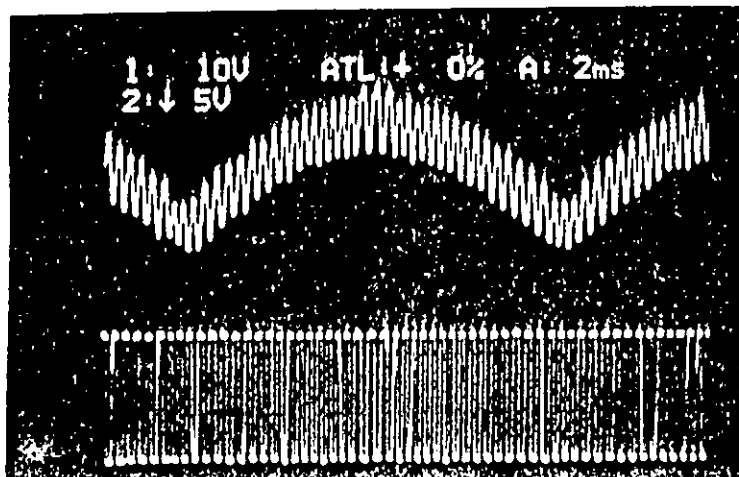
$$S = \frac{4 \text{ V}}{740 \times 10^{-6} \text{ sec.}} = 5,405 \text{ V/sec.}$$



(b)

$$f = 40 \text{ Hz.}$$

$$S = \frac{7 \text{ V}}{740 \times 10^{-6} \text{ sec.}} = 9,459 \text{ V/sec.}$$

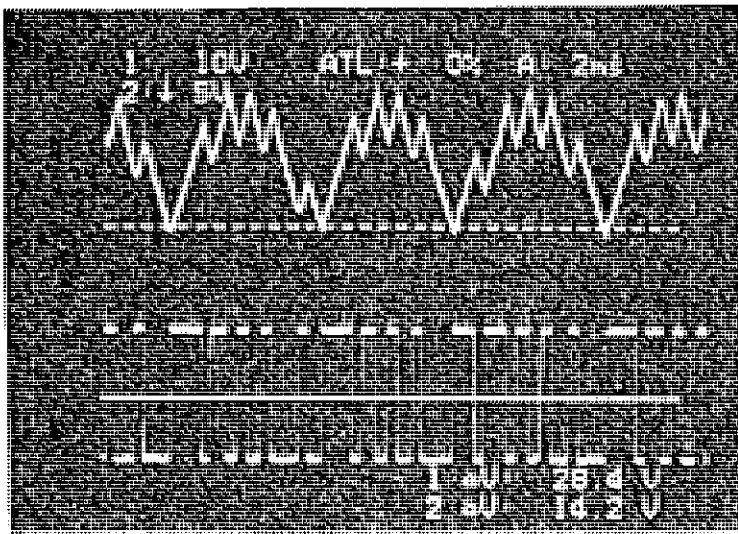


(c)

$$f = 40 \text{ Hz.}$$

$$S = \frac{5.8 \text{ V}}{160 \times 10^{-6} \text{ sec.}} = 3,6250 \text{ V/sec.}$$

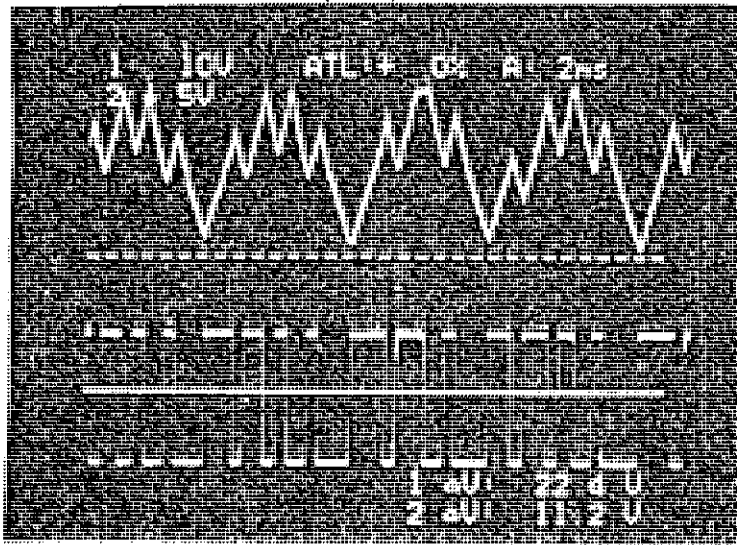
Fig.-68 : Effect of change of slope of the carrier wave with constant frequency ( $f=40 \text{ Hz.}$ ).



(a)

$$f = 100 \text{ Hz.}$$

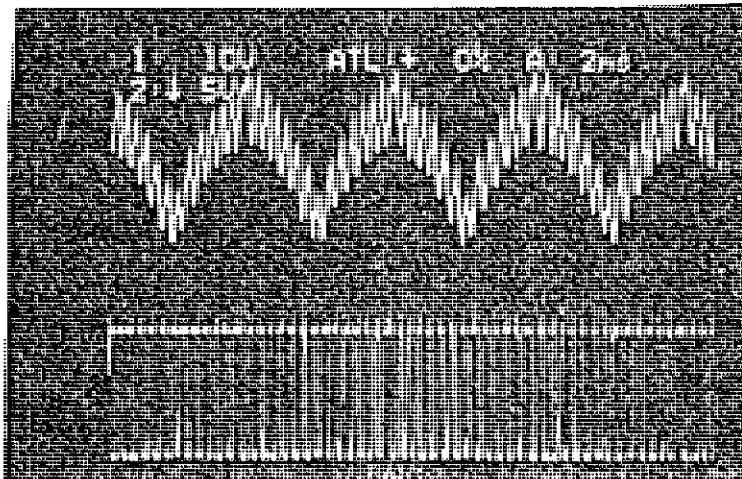
$$S = \frac{4V}{740 \times 10^{-6} \text{ Sec.}} = 5,405 \text{ v/sec.}$$



(b)

$$f = 100 \text{ Hz.}$$

$$S = \frac{7V}{740 \times 10^{-6} \text{ Sec.}} = 9,459 \text{ v/sec.}$$



(c)

$$f = 100 \text{ Hz.}$$

$$S = \frac{5.8V}{160 \times 10^{-6} \text{ Sec.}} = 36,250 \text{ v/sec.}$$

Fig.-69 : Effect of change of slope of the carrier wave with constant frequency ( $f=100 \text{ Hz.}$ ).

### 3.2.5 Discussion:

It is clear that by changing any of the parameter ( $f$ ,  $\Delta V$ ,  $S$ ) of the DM, the output pulse width can be increased or decreased. These pulses are given to the gate of the MOSFET (or base of the transistor) which acts as the switch of the SMPS. As the pulse width can increase or decrease, the OFF/ON time of the switch can be increased or decreased controlling the switching time of the SMPS. Any of the parameters like frequency, window width or slope can be chosen as the control parameter of the modulator to control output voltage of an SMPS. However, in our work we have investigated the method of changing the frequency of the modulating wave. The change of other two parameters can be incorporated in the SMPS control with further advantages such as harmonic elimination/reduction and better filter size etc. Such work can be a part of future work.

### 3.3. Practical SMPS requirements : [1]

This section describes the operation of the total SMPS system. The complete SMPS system is shown in Fig.-72. Before describing this circuit. Let us examine the key ideas behind a switching regulator. Fig.-70 illustrates such a switching regulator. A string of pulses drives the base of the transistor. When the base voltage is high, the transistor is saturated. When the base voltage is low, the transistor is cutoff. The main idea is that the transistor acts like a

switch. Ideally, a switch dissipates no power when it is closed or open. In reality, the transistor switch is not perfect, and so it does dissipate some power, but this power is less than that dissipated by a series regulator.

A diode is connected from the emitter to ground. This is necessary because of 'inductive kick back'. An inductor will try to keep the current constant through it. When the transistor cuts off, the diode continues to provide a path for current through the inductor. Without the diode, the inductive kickback would produce enough reverse voltage to destroy the transistor.

By controlling the duty cycle out of the pulse generator, we control the duty cycle of the input voltage to the LC filter. Ideally this input voltage varies from 0 to  $V_{in}$  as shown. Although obsolete in ordinary power supplies the LC filter is very popular in switching regulators because the switching frequency is above 5 Kz. As a result a small inductor and capacitor can be used. The output of the LC filter is dc voltage with only a small ripple. This dc voltage depends on the duty cycle, and is given by,

$$V_{out} = DV_{in} \dots\dots\dots 27.$$

The output voltage is fed back to the pulse generator. In most switching regulators, the duty cycle is inversely proportional to the output voltage. If the output voltage increases the duty cycle will decrease. This means that narrower pulses will drive the LC filter and its output will decrease. In effect, we have negative feed back. Since the output voltage is being sampled and fed back, output voltage is the quantity being stabilized.

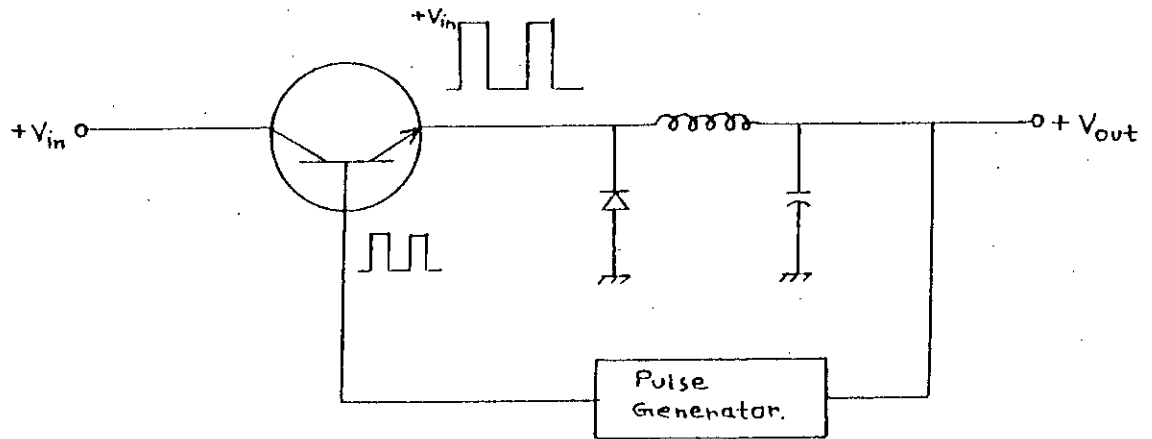


Fig.-70 : Transistor acting as a switch in an SMPS.

For a concrete idea of how a conventional switching regulator works, Fig.-71 shows a low power design. The relaxation oscillator produces a square wave whose frequency is set by  $R_3$  and  $C_3$ . The square wave is integrated to get a triangular wave, which drives the non inverting input of a triangular-to-pulse converter. The pulse train out of this circuit drives the transistor. The output of the LC filter is sensed by a voltage divider, sending a feedback voltage to the comparator. This feed back voltage is compared with a reference voltage. The output of the comparator then drives the inverting input of the triangular to pulse generator.

If the regulated output voltage tries to increase the comparator produces a higher output raising the reference voltage of the triangular-to-pulse converter. This means that the narrower pulses drive the base of the pass transistor. Since the duty cycle is low the filtered output is less canceling the original increase in output voltage.

Conversely, if the regulated output voltage tries to decrease the output of comparator decreases the reference voltage of triangular to pulse converter. Since wider pulses drive the transistor higher voltage results at the output of the LC filter. The net effect is to cancel the original decrease in output voltage.

There is enough open-loop gain in the system to ensure a well-regulated output voltage. The boot strap effect in the comparator implies that,

$$V_{\text{ref}} = [R_2 / (R_1 + R_2)] V_{\text{out}} \dots\dots\dots 28.$$

$$\text{or, } V_{\text{out}} = [(R_1 / R_2) + 1] V_{\text{ref}} \dots\dots\dots 29.$$



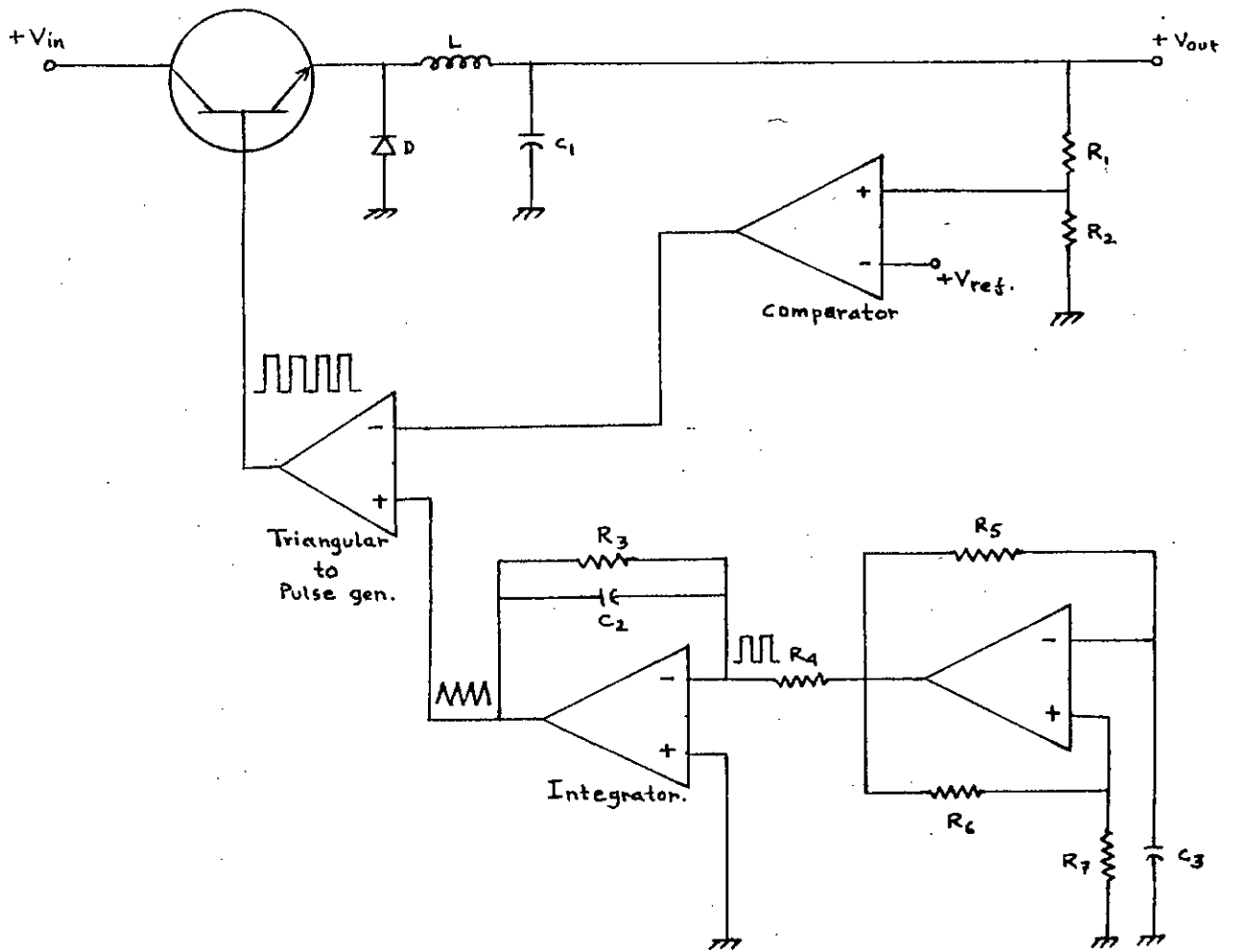


Fig.-71 : Conventional switching regulator [25].

This thesis give emphasis on the control circuit of the SMPS which is different from that used in the conventional circuit. The input 50 volt AC (Can be 220 V AC with changing the rating of all other components of the circuit) at 50 Hz is rectified by a bridge rectifier and then filtered by a capacitor filter. The dc is switched by a switch (MOSFET) and the output of the switch is again filtered by a LC filter and finally fed to the load. Main attention is given to the control circuit of the switch which is discussed in the following section.

### 3.3.1 Incorporation of DM in SMPS controller :

Attempt is taken to make a 50 volt, 50 Hz AC to 5V dc SMPS. A feed back voltage is achieved by using a divider circuit and the available feed back voltage is,

$$[5/(1 \times 10^6 + 470 \times 10^3)] \times 470 \times 10^3 = 1.59 \approx 1.6 \text{ Volt.}$$

A reference voltage is provided by using a capacitor divider circuit and a 10V Zener diode. Though ideally the Zener is 10V practically its output is 9.6V. This voltage is inverted to -9.6V by using an inverting amplifier and -9.6 V is used as reference voltage of the circuit. The feed back voltage and the reference voltage is then compared by a comparator. The output of the comparator is,

$$\begin{aligned} V_{\text{feed back}} - V_{\text{ref.}} \\ = 1.6 - (-9.6) \\ = 11.2 \text{ Volt.} \end{aligned}$$

The output of the comparator is fed to the Pin 8 of a sine oscillator IC 8038. The basic construction of this chip is described below :

### 3.3.1 Voltage controlled oscillator, ICL 8038 :

The ICL 8038 waveform generator is a monolithic integrated circuit capable of producing high accuracy sine, square, triangular, sawtooth and pulse waveforms with very few external components. The frequency can be selected extremely from 0.001 Hz to more than 300 KHz using either resistors or capacitors or by frequency modulation achieved by sweeping with an external voltage.

The frequency of the waveform generated is a direct function of the dc voltage at terminal 8. By altering this voltage, frequency modulation is achieved. For correct operation, the sweep voltage should be within the range,

$$[(2/3)V_{\text{supply}} + 2V] < V_{\text{sweep}} < V_{\text{supply}}$$

As the sweep voltage increases the frequency of the output sine wave at pin 2 decreases and vice versa. This a desired case for the control circuit of an SMPS. The capacitor (0.1  $\mu$ F) and the resistor (1.5 K) used at the output of pin 2 is for dc offset.

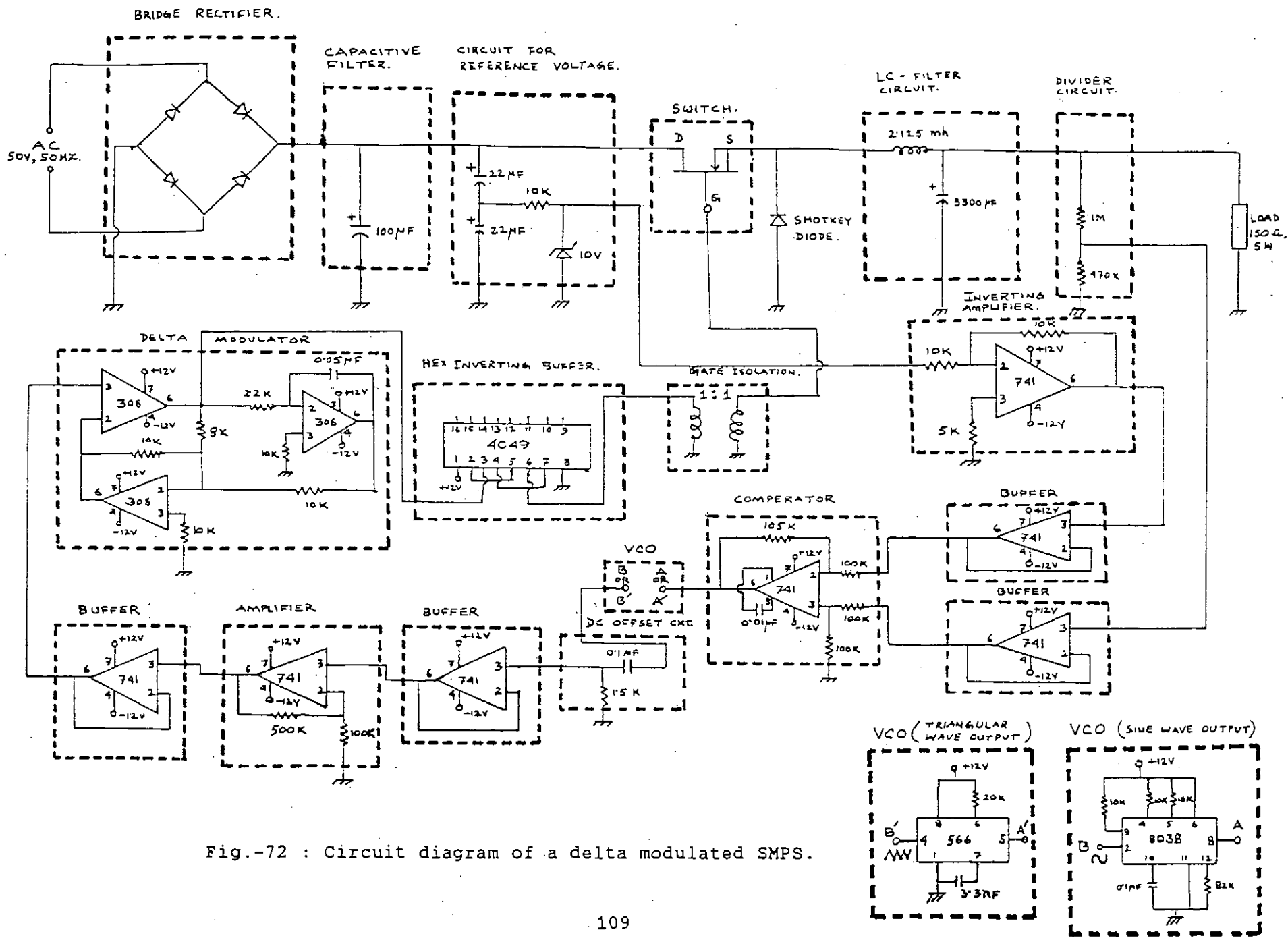


Fig.-72 : Circuit diagram of a delta modulated SMPS.

### 3.3.2 Amplification of the sine wave generated by VCO :

The amplitude of the sine wave generated by VCO is very low. This low amplitude sine wave can not perform delta modulation effectively. The amplifier shown in the circuit of Fig.-72 amplify this sine wave.

### 3.3.3 Rectification of sine wave :

This sine wave generated by the VCO is a full sine wave. DM smps required modulation of a rectified sine wave. An isolation transformer of 1:1 is used to isolate this sine wave form ground and then a bridge rectifier produces the required rectified sine wave. The output of this rectifier is fed to the input of the DM. The operation of the Delta modulator is described in section 3.1.

### 3.3.4 Necessity of Hex inverting buffer :

The ON/OFF time of the switch of the SMPS depends on the ON/OFF pulse width of the output of the DM. The design is made for a 5 V dc output at the load. Practically it is seen that the ON pulse width of the DM is wider than the OFF time which results more than 5 V at the load. Thus an Hex inverting buffer is used to invert the pulse of the DM output. Finally these pulses are fed to the gate of the MOSFET which acts as the switch of the SMPS.

3.4 Filter design : voltage ripple. [26]

The output of the switch is a train of pulses which is filtered by inductor and capacitor. The small switching ripple  $\Delta V$  of the converter (less than 1%) directly translates into idealized rectangular voltage waveform and triangular current waveform on the inductor.

Let us assume that the average inductor current  $I$  flows into the load resistance  $R$  to generate the dc voltage  $V = IR$ , while the inductor current ripple  $\Delta i_L$  flows into the output capacitor to generate the output voltage ripple  $\Delta V$  (Fig.-73). This is a good approximation for small switching ripple. The capacitor ripple current is triangular in shape. The stored charge  $\Delta Q$  corresponds to the area under inductor current ripple.

Hence from Fig.-73(e),

$$\begin{aligned} \Delta Q &= [1/2 \times (DT_s/2) \times (\Delta i_L/2)] + [1/2 \times (D'T_s/2) \times (\Delta i_L/2)] \\ &= 1/2 \times [(DT_s \times \Delta i_L)/4] + (D'T_s \times \Delta i_L)/4 \\ &= 1/8 \times T_s \Delta i_L (D+D') \\ &= 1/8 \times \Delta i_L T_s \quad [\because D+D' = 1] \dots\dots\dots 30. \end{aligned}$$

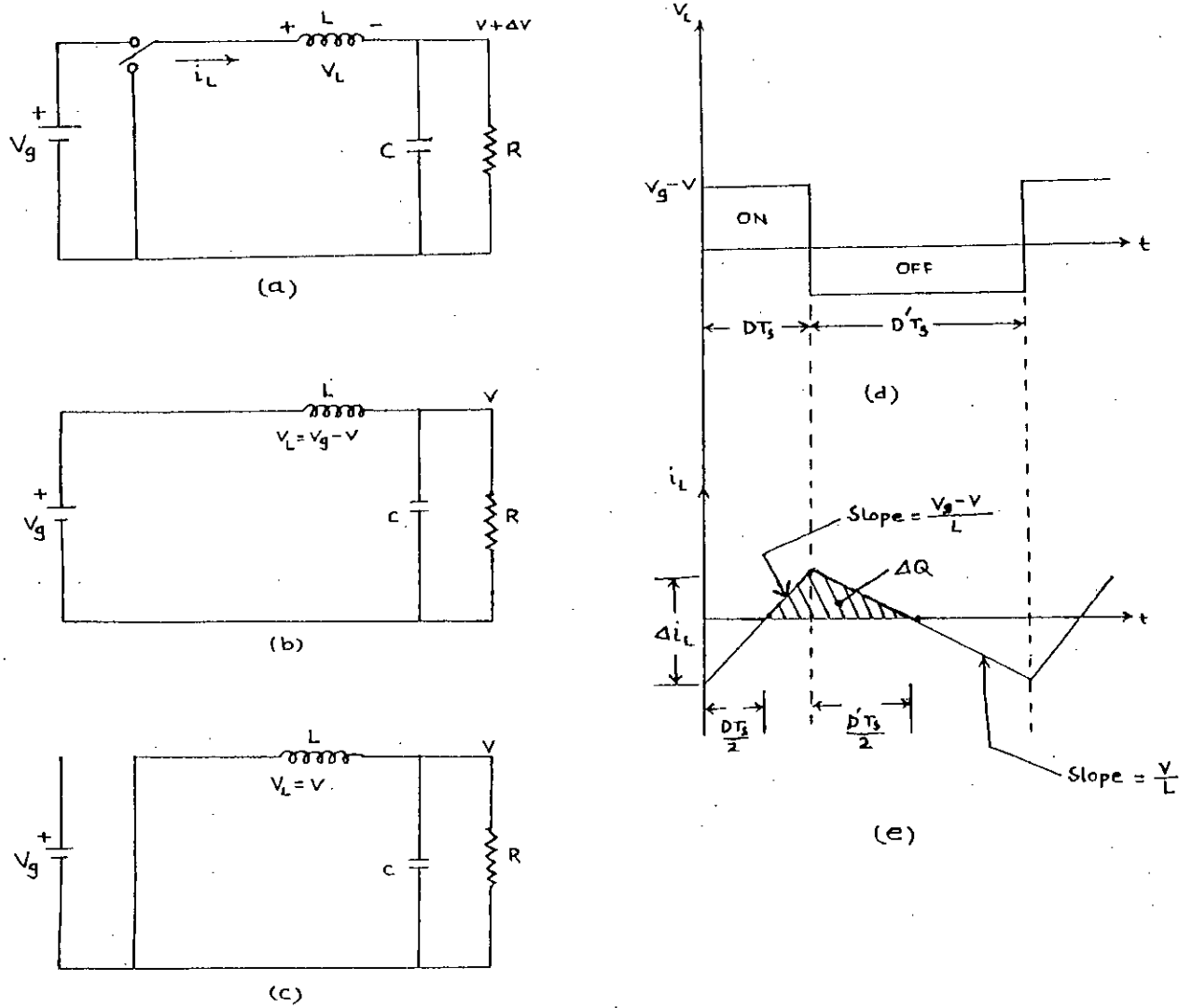


Fig.-73 : (a) Original circuit (b) when switch is ON  
(c) when switch is OFF (d) voltage waveform (e) inductor current waveform neglecting voltage ripple.

Again for the inductor,

$$\begin{aligned}V &= L(di/dt) \\ \Rightarrow di/dt &= V/L \\ \therefore \text{Slope} &= V/L \dots\dots\dots 31.\end{aligned}$$

Thus from the falling slope of inductor current,

$$\begin{aligned}\text{Slope} &= V/L \\ &= (\Delta i_L/2)/(D' T_s/2) \\ \Rightarrow V/L &= \Delta i_L/D' T_s \\ \Rightarrow \Delta i_L &= (V/L)D' T_s \dots\dots\dots 32.\end{aligned}$$

Now,

$$\begin{aligned}C &= Q/V \\ \Rightarrow V &= Q/C \\ \therefore \Delta V &= \Delta Q/C \\ &= 1/8 \times \Delta i_L \times T_s \times 1/C \\ &= 1/8 \times V/L \times D' T_s \times T_s \times 1/C \\ &= 1/8 \times D' T_s^2 \times 1/LC \times V \\ &= 1/8 \times (D' T_s^2)/LC \times V \dots\dots\dots 33.\end{aligned}$$

which is the absolute output voltage ripple.

$$\therefore \Delta V/L = 1/8 \times (D' T_s^2)/LC \dots\dots\dots 34.$$

is the expression for relative voltage ripple.



Corner frequency can be obtained as,

$$\begin{aligned}f_c &= 1/2\pi\sqrt{LC} \\ \Rightarrow f_c^2 &= 1/4\pi^2 LC \\ \Rightarrow 1/LC &= 4\pi^2 f_c^2 \\ \therefore \Delta V/V &= 1/8 \times D'T_s^2 4\pi^2 f_c^2 \\ &= (\pi^2 D')/2 \times (f_c/f_s)^2 \dots\dots\dots 35.\end{aligned}$$

Which is the expression for ripple in terms of corner frequencies and where  $T_s = 1/f_s$ .

This result for Buck convertor can be generalized for others switching convertors as well.

*Small switching ripple =>> natural frequencies << switching frequency.*

On the basis of small switching ripple requirements the voltage waveforms of the inductor in many convertors have the typical rectangular shape.

### 3.5 Semiconductor implementation of the switching action :[1]

A semiconductor implementation of the single pole double throw switch is desired for the full electronic control of the convertor.

Consider Fig.-74, the diode with a transistor operating in its cut off and saturation region. When the switch is ON, the input dc voltage reverse biases the diode and turns it OFF for the interval  $DT_s$ . During transistor OFF condition the diode is forward biased by the inductor voltage. However, this semiconductor implementation simulates the original ideal switch only in a limited fashion. Namely, while the ideal switch conducts current in either direction and can block voltage of either polarity the shown semiconductor version limits the current flow in one direction only and blocks voltage of any polarity. This implementation by nature limits the whole convertor to single quadrant operation (i.e, only one voltage and one current polarity are available at the output).

As the switch of the SMPS works at a very high frequency, the semiconductor diode used is a schotky diode rather than a normal diode.

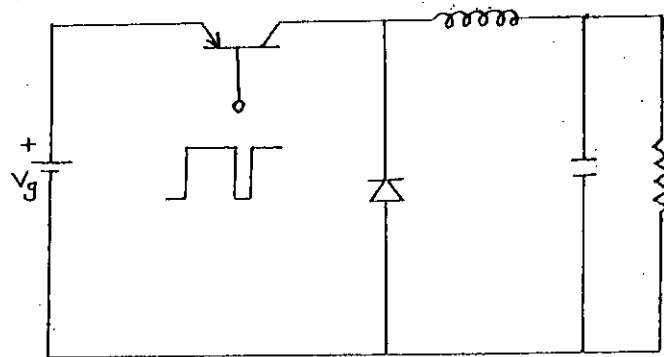
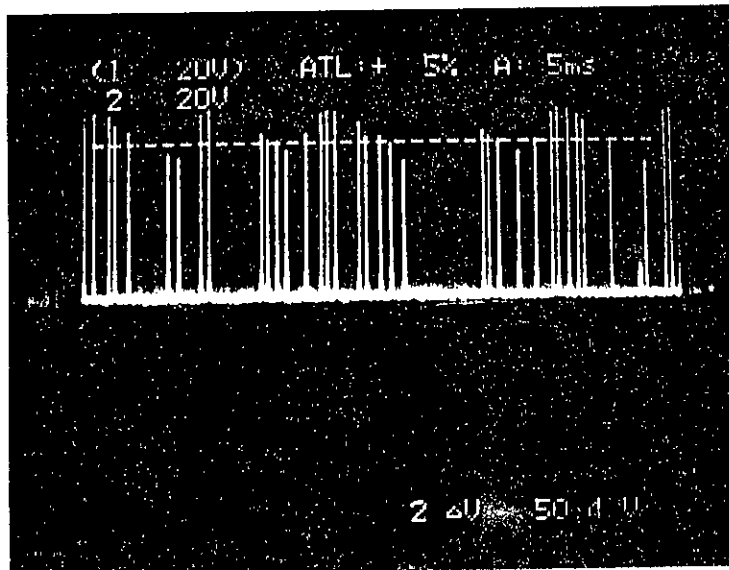


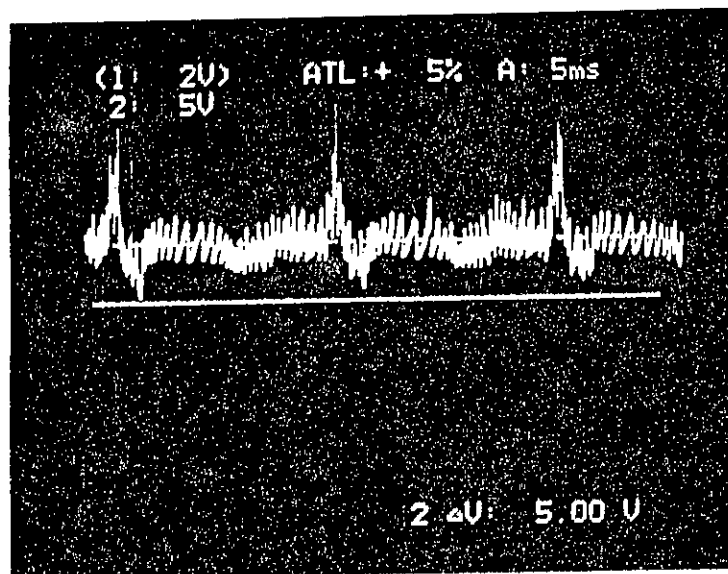
Fig.-74 : Semiconductor implementation of SMPS circuit.

### 3.6 Results:

Fig.-75 and Fig.-76 describe the output voltage waveform of the SMPS without feed back for various inductor and capacitor values. In the complete SMPS, the feed back voltage is compared with a reference voltage and the comparator output is used as a input voltage of the VCO. Considering the safety of the circuit, instead of the feed back voltage, another voltage from a different dc source is applied to the input of the VCO and by changing this voltage within the range  $(\frac{2}{3} V_{\text{supply}} + 2V) < V_{\text{sweep}} < V_{\text{supply}}$  it is observed that constant output 5V is obtained. Fig.-75(a) shows the output voltage without any filter. By using only inductive filter ( $L=0.125$  mh) the output is shown in Fig.-75(b). Fig.-76(a) describes when the filter have both inductor ( $L=0.125$  mh) and capacitor ( $C=22\mu\text{f}$ ). Keeping the same inductor value the output waveform improves (tends to be more dc) when the capacitor value is increased from 22  $\mu\text{F}$  to 3300  $\mu\text{F}$  which is shown is Fig.-76(b).

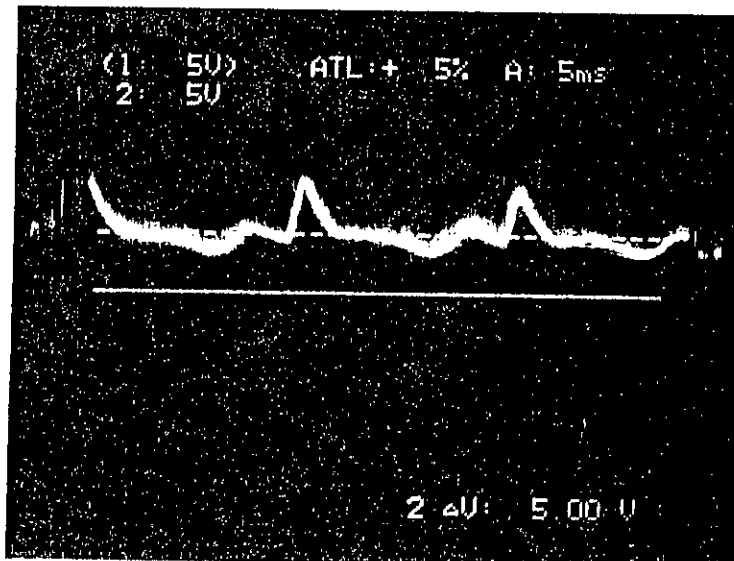


(a)

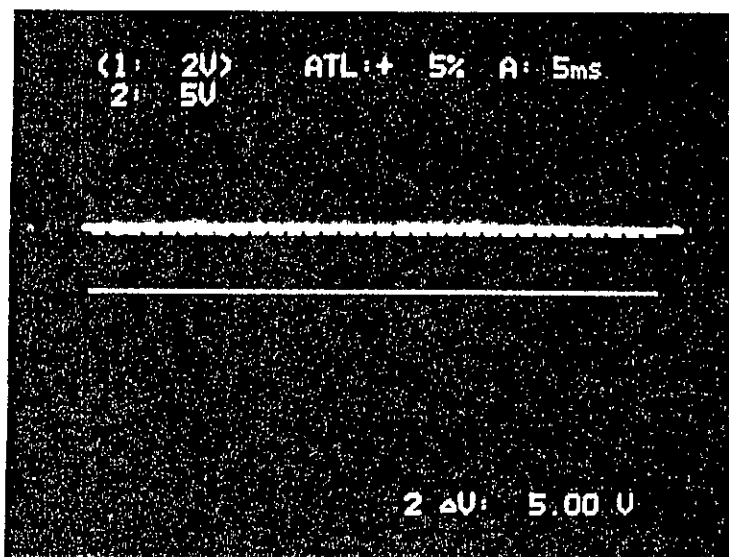


(b)

Fig.-75 : Output of the SMPS without feedback  
 (a) without any filter  
 (b) Inductive filter only.



(a)



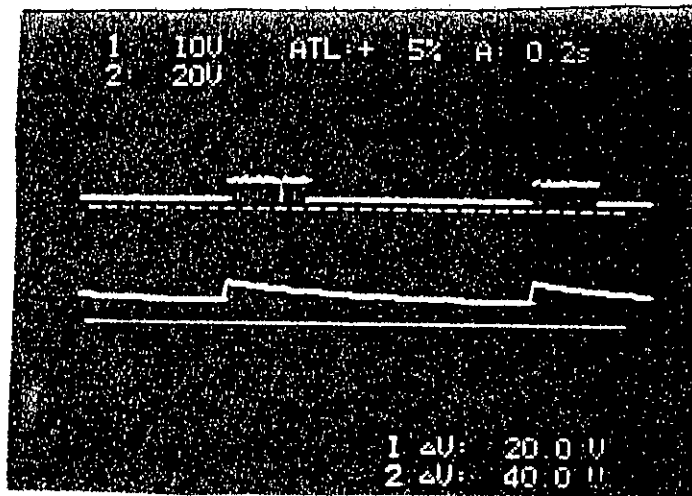
(b)

Fig.-76 : Output of the SMPS without feedback

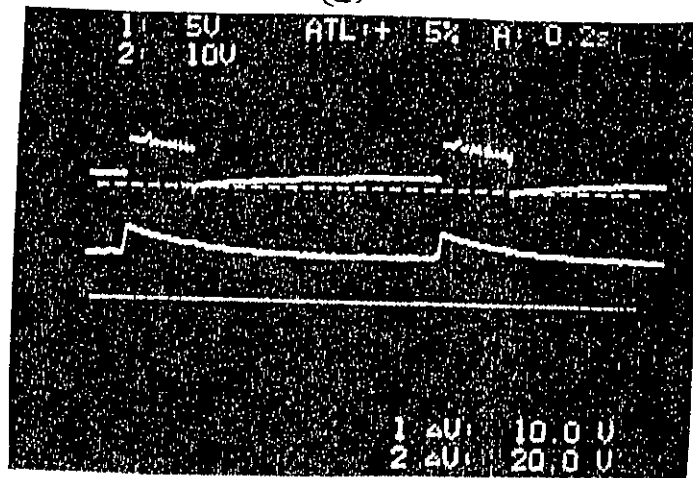
(a) Capacitor ( $22\mu\text{F}$ ) and inductor ( $0.125\text{mh}$ ) filter.

(b) Increased capacitor value ( $3300\mu\text{F}$ ) and same inductor value.

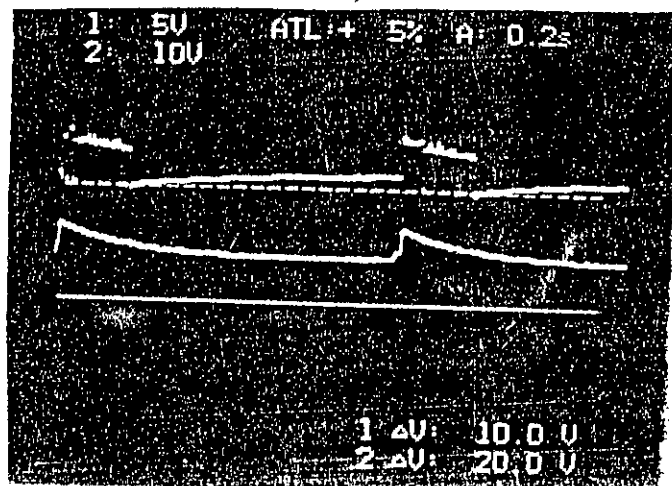
Output of the complete SMPS circuit with feed back is shown in Fig.-77 for varying input from 35V A.C. to 50V A.C. Upper waveform indicates switching wave and the lower indicates output wave.



(a)



(b)



(c)

Fig.-77 : Output of the SMPS with feedback :  
input (a) increased from 40 to 50 volt  
A.C. (b) decreased from 50 to 35 volt  
A.C. and (c) increased from 35 to 40 volt  
A.C.



## Chapter - 4

### Conclusions

DC to DC converters with isolation transformers can have multiple outputs of various magnitudes and polarities. The regulated power supply of this type has wide applications, particularly in computer systems, where a low voltage high current power supply with low output ripple and fast transient response are mandatory. Switch mode power supplies have come in to wide spread use in the last decade. An essential feature of efficient electronic power processing is the use of semiconductors in a power switching mode (to achieve low losses) to control the transfer of energy from source to load through the use of pulse width modulated techniques. Inductive and capacitive energy storage elements are used to smooth the flow of energy while keeping losses to a low level. As the frequency of switching increases, the size of the magnetic and capacitive elements decreases in a direct proportion. Because of their superior performance (i.e. high efficiency, small size and weight and relatively low cost), they are replacing conventional linear (dissipative as they operate in linear or

conduction mode) power supplies even at very low power levels.

The switching techniques of switch mode power supplies are of many types. Recently delta modulation has been successfully used for controlling inverters and rectifiers. This thesis has been an effort to investigate the possibility of using delta modulated switching in switch mode dc-dc power supplies. With this in mind extensive theoretical and practical work has been done to implement DM switching for a BUCK type switch mode power supply. The work included a review of SMPS and analysis of DM technique to investigate the possible way of implementing the technique in practice. It has been observed that output of delta modulated switching converter can be controlled in four ways. These are

- 1) By controlling the frequency of reference signal of the modulator
- 2) By variation of slope of the estimated wave of the modulator
- 3) By variation of window width of the modulator and
- 4) By variation of magnitude of reference signal.

These observations were made from the spectral analysis of the modulated wave of the simulated converter waveforms. Of the four parameters mentioned, the slope and window variation are significant in changing the output pulse numbers and harmonic contents rather than changing output dc voltage widely. The

frequency control of the input reference signal was quite dominant in changing the magnitude of the output dc voltage. With these observations, it was decided to place a delta modulator in the SMPS BUCK topology to maintain constant dc for 25 percent load and input voltage variations.

A practical modulator was designed and incorporated into a BUCK type SMPS (also designed and fabricated during this thesis work) to verify the simulated results. Results of practical modulator output waveforms, SMPS, filter and modulator as voltage regulator and high frequency switcher was observed. However, the result was not comprehensive and conclusive. It has been proved that delta modulator can be easily used as switch mode power supplies switching converter. It remains to be investigated by future researcher to highlight the merits and demerits of dm as SMPS controller.

Conventional approach has been made to design the SMPS and its filter and controller. But it has been felt that modern modelling, analysis and design of these should be undertaken. Future research may include modern modelling and solution techniques together with more appropriate circuit components to implement and justify the merits and demerits of delta modulated switch mode power supply. Initially it was observed that delta modulators are simple and easy to implement. The circuit diagrams presented in this thesis may appear to

contradict this when compared to present state of the art commercial SMPS. However, it should be noted that commercial SMPS use almost custom made integrated circuits to fabricate the SMPS and hence their circuits may look favorable than what is presented in this thesis. It can be claimed that DM SMPS controllers if fabricated in one single chip will also look simple in configuration.

One important point can be mentioned at this point is that design and construction of switch mode power supply is a combination of theory and practice. In the design construction phase practical results such as filter and loop frequency responses are of paramount importance. This research shows that design procedures without experimentation would fail at some point. Several aspects of switching regulators were not incorporated or implemented during this thesis work. One of these are the protection component of the regulator and the other is a reliability and redundancy study of the power supply. In future similar works such implementation and study should be undertaken to complete the analysis design point.

#### REFERENCES :

1. Cuk Slobodan, "BASICS OF SWITCHED-MODE POWER CONVERSION: TOPOLOGIES, MAGNETICS, AND CONTROL", California Institute of Technology, Pasadena, California, pp.265-281.
2. Rashid Muhammad H., "POWER ELECTRONICS - Circuits, Devices, and Applications", Purdue University at Fort Wayne, pp.317-387
3. G.S. Bhuja and G.B. Indri, "Optimal pulse width modulation for feeding ac motors", IEEE trans on IA, vol IA-13, Jan/Feb, 1977, pp. 38-44.
4. F.G. Turnbull, "Selected harmonic reduction in static dc-ac inverters", IEEE trans on Conrame and Elechm., vol 83, July 1964, pp. 374-378.
5. H.S. Patwl and R.G. Hoft, "Generalized techniques of harmonic elimination and voltage control in thyristor inverters", part I - Harmonic elimination", IEEE trans on IA, vol IA-9, May/June 1973, pp 310-317.
6. De Jager, F, "Delta modulation - a new method of pcm transmission using the 1 unit code" Philips research report, no.7, Dec/1952, pp.442-466.

7. Vande weg, N, "Quantization noise of a single integration delta modulation system with an N-digit code " Philips research report, no.7, Oct/1953, pp.367-385.
8. Schindler H.R, "Delta modulation" - IEEE Spectrum, Oct/1970, pp.69-78.
9. Greefkes, J.A and Dejager, F., "Continuous delta modulation" Philips Research report, no.23, Oct/1968, pp.233-246.
10. Goodman D.J., "The application of delta modulation, analog to pcm encoding" Bell systems Technical Journal, vol.48, Feb 1969, pp.321-342.
11. Steele, R and Thomas M.W.S, "Two transistor delta modulator.", Electronic Engineering, no.40, 1968, pp.513-516.
12. Steele, R., "Pulse delta modulators-inferior performance but simpler circuitry,", Electronic Engineering, no.42, 1970, pp.75-79.
13. Nielson, P.T, "On the stability of double integrator delta modulation", IEEE trans. on Communication Tech., June, 1971, pp.364-366.

14. Johnson, F.B, " Calculating delta modulator performance",  
IEEE trans. on AU, AU-16, 1968, pp.121-129.
15. Slepian, D., "On delta modulation.", Bell System  
Technical Journal., vol' 51, Dec./1971, no.10, pp.2101-  
2137.
16. Jayant N.S and Noll.P, "Digital coding of wave forms",  
Prentice-Hall Inc., 1984, pp.399-415.
17. Abate, J.E., "Linear and adaptive delta modulation."  
Proc. of IEEE, vol.55, no.3, March/1967, pp.298-307.
18. Cartmate, A.A, and Steele. R, "Calculating the  
performance of syllabically companded delta-sigma  
modulators.", Proc. of IEEE, 1970, pp.1915-1921.
19. Sharma, P.D, " Characteristics of asynchronous delta  
modulation and binary slope quantized pcm system.",  
Electronic engineering, JANUARY/1968, PP.32-37.
20. Das J. and Sharma,"Some asynchronous pulse modulation  
systems", Electronic letters, vol. 3, no. 6, June/1967,  
pp.75-79.

21. Sharma, P.D, "Signal characteristics of rectangular-wave modulation", Electronic Engineering, vol.40, Feb/1968, pp.103-107.
22. Steele, R., "Peak signal to noise ratio formulas for multistage delta modulation with RC - shaped Gaussian input signals", The Bell system Technical Journal., vol.61 no.3, March/1982, pp.348-7-362.
23. Chatterjee, P.K and Rao, V.R., :Digital computer simulation results of multistage delta modulation systems." Proc. of IEE, vol.120, no.11, Nov/1973, pp.1379-1382.
24. Jayant, N.S, "Multistage delta modulation of speechsignal", Proc. of IEE, Sept./1971, pp.1382.
25. MALVINO, "Electronic Principles", third edition, p.p. 602.
26. Albert Paul Malvino, Ph.D, Electronic Principles, Third edition, p.p. 600 - 602.



# APPENDIX

PROGRAM IN MATLAB LANGUAGE FOR CALCULATING SWITCHING  
POINTS AND SIMULATING WAVEFORMS AND FOURIER TRANSFORMS

```

tm=1./fm;
t=0:tm/511:tm;
wm=2.*pi*fm;
w=ga(t,0,tm/2.) - ga(t,tm/2.,tm);
Np=512;
ll=500;
t1(1)=0.0;
for i=2:ll;
    l=i;
    anum=2.*dv;
    den(i) = s+((-1.)^(i-1)*vm*wm*cos(wm*t1(i-1)));
    t1(i)=t1(i-1)+anum/den(i);
    if(t1(i) >= pi/wm)
        t1(i)=pi/wm;
        break
    end
end
wsum1=0.0;
for i=1:l/2;
    w1=ga(t,t1(2*i-1),t1(2*i));
    w2=ga(t,t1(2*i-1)+tm/2,t1(2*i)+tm/2);
    ww=w1+w2;
    wsum1=wsum1+ww;
end
clear w1;
clear w2;
clear ww;
inpwm=w.*wsum1;
smps=w.*inpwm;
zsum1=0.0;
for i=1:l-1;
    pm1=(-1)^(i+1)*ga(t,t1(i),t1(i+1));
    pm2=-(-1)^(i+1)*ga(t,t1(i)+tm/2,t1(i+1)+tm/2);
    pm = pm1+pm2;
    zsum1=zsum1+pm;
end
pwm=zsum1;
clear pm1;
clear pm2;
clear pm;
clear zsum1;
q2=(dv+vm*sin(wm*t1(2)))/t1(2);
qsum1=q2*t.*ga(t,t1(1),t1(2));

```

```

for i=2:l-1;
    q=s*(t-t1(i));
    y=(-1)^(i+1)*q+(-1)^i*dv+vm*sin(wm*t1(i)).*ga(t,t1(i),t1(i+1));
    qsum1=qsum1+y;
end
clear q2;
clear q;
clear y;
q3=(dv+vm*sin(wm*t1(2)))/t1(2);
qsum2=q3*(t-tm/2.).*ga(t,(t1(1)+tm/2.),(t1(2)+tm/2.));
for i=2:l-1;
    qq=s*(t-(t1(i)+tm/2.));
    y1=(-1)^(i+1)*qq+(-1)^i*dv+vm*sin(wm*(t1(i))));
    y2=ga(t,(t1(i)+tm/2.),(t1(i+1)+tm/2.));
    yy=y1.*y2;
    qsum2=qsum2+yy;
end
qsum=qsum1-qsum2;
clear qq;
clear y1;
clear y2;
clear yy;
clear qsum1;
clear qsum2;
axis([0 tm -2 2])
subplot(222),plot(t,smps,'-')
xlabel('Time in Sec.')
ylabel('Magnitude in p.u.')
subplot(223),plot(t,pwm,'-')
xlabel('Time in Sec.')
ylabel('Magnitude in p.u.')
fs=(Np-1)/tm;
f=(fs/Np)*(0:(Np/2)-1);
y=fft(smps,Np);
pYY=(y.*conj(y))/(Np/2);
spec=sqrt(pYY/(Np/2));
spec(1)=spec(1)/2.;
axis([0 45000 0 1.25])
subplot(224),plot(f,spec(1:Np/2));
xlabel('Frequency in Hz. '),ylabel('Magnitude in p.u.')
axis([0 tm -15 15])
y1=vm*sin(wm*t);
y2=+dv+vm*sin(wm*t);
y3=-dv+vm*sin(wm*t);
subplot(221),plot(t,y1,'-',t,y2,'-',t,y3,'-',t,qsum,'-');
xlabel('Time in Sec. '), ylabel('Magnitude in p.u. ');

```

